

High Temperature H<sub>2</sub>S Adsorption using Copper-Titanate Nanoparticles

by

Farzad Yazdanbakhsh

A thesis submitted in partial fulfillment of the requirements for the degree of

Doctor of Philosophy

in

Chemical Engineering

Department of Chemical and Materials Engineering  
University of Alberta

© Farzad Yazdanbakhsh, 2015

## Abstract

Direct desulfurization of syngas is an important measure to further increase the efficiency of IGCC systems. Solid-phase, metal oxide adsorbents which sequester the sulfur by converting  $\text{H}_2\text{S}$  to a metal sulfide are the only desulfurization technology capable of withstanding the combustion temperatures present at the outlet of the gasifier. Copper oxide is of particular interest due to its favourable thermodynamics across a wide range of temperatures. Cu-ETS-2 is a copper exchanged form of the sodium titanate ETS-2 and functions analogously to CuO for the conversion of  $\text{H}_2\text{S}$  into CuS at temperatures ranging from ambient to 950 °C.

The results of this study show that Cu-ETS-2 is capable of removing  $\text{H}_2\text{S}$  from  $\text{H}_2\text{S}/\text{He}$  mixture to concentrations below a mass spectrometer's detection limit at temperatures as high as 950°C. Temperature is, however, only one of the challenges facing a direct-desulfurization adsorbent; high concentrations of  $\text{H}_2$  and water vapour are present in the syngas stream which can influence the oxidation state of the metal and the efficiency of  $\text{H}_2\text{S}$  removal. In an attempt to prevent reduction of CuO, Chromium was successfully used to stabilize the oxidation state of copper oxide and maintain constant adsorption capacity throughout the whole temperature range.

While several studies have examined the effect hydrogen in the feed, there are few studies exploring the influence of water vapour on the efficiency of  $\text{H}_2\text{S}$  removal and none that explore the effect of water vapour at elevated temperatures. This study can be considered the only study to investigate the influence of water vapour on the desulfurization of a dilute  $\text{H}_2\text{S}$  stream at temperatures between 350 and 950 °C using copper oxide-based adsorbents. The findings demonstrate that the presence of water vapor promotes production of  $\text{H}_2$ , resulting in faster reduction of CuO to  $\text{Cu}_2\text{O}$  and elemental copper, leading to less adsorption capacity.

In the final chapter, the ability of the adsorbent for regeneration and use as a multi-cycle adsorbent was investigated. The results indicate that the adsorbent is capable of regeneration

for at least four times with no sign of reduction in capacity. The results also indicate that the exothermic nature of oxidation reaction results in temperatures up to  $\sim 1700^{\circ}\text{C}$  causing the partial melting of the quartz glass tube. However the adsorbent can withstand such high temperatures and does not lose adsorption capacity after the first oxidation step. This phenomenon is due to having nanotitanate ETS-2 as the support in the adsorbent.

## **Preface**

Some of the research conducted for this thesis forms part of an international research collaboration, led by Professor Steven Kuznicki at the University of Alberta, with Dr. Stefan Baumann being the lead collaborator at the Forschungszentrum Jülich in Germany. The results of the experiments presented in chapters 2 and 3 were done in the “Institute of Energy and Climate Research-2 (IEK-2)” at the Forschungszentrum Jülich under supervision of Dr. Michael Müller.

The technical apparatus referred to in chapter 2-5 was designed by the thesis autor (Farzad Yazdanbakhsh), with the assistance of Dr. Marc Bläsing in Forschungszentrum Jülich and Dr. Jim Sawada at the University of Alberta. The data analysis and conclusion are Farzad Yazdanbakhsh’s work, as well as the literature review in chapters 2-5.

Chapter 2 of this thesis has been published as F. Yazdanbakhsh, M. Bläsing, J. Sawada, S. Rezaei, M. Müller, S. Baumann and S. m. Kuznicki “Copper Exchanged Nanotitanate for High Temperature H<sub>2</sub>S adsorption” Journal of Industrial and Engineering Chemistry Research, 2014, 53, 11734-11739. In this paper, Farzad Yazdanbakhsh was responsible for the data collection and analysis as well as the manuscript composition. Dr. Marc Bläsing assisted with the data collection and Dr. Jim Sawada contributed to manuscript correction and preparation. Dr. Steven. M. Kuznicki was the supervisory author and was involved with concept formation and manuscript composition.

Chapter 3 of this thesis has been accepted for publication and at time of writing this thesis is in proof for publication as: F. Yazdanbakhsh, M. Alizadehgiashi, M. Bläsing, M. Müller, J. Sawada and S. m. Kuznicki “Cu-Cr-O Functionalized ETS-2 Nanoparticles for Hot Gas Desulfurization” in Journal of Nanoscience and Nanotechnology, 2015, 15. In this paper, Farzad

Yazdanbakhsh was responsible for the data collection and analysis as well as the manuscript composition. Dr. Jim Sawada assisted with the data collection and contributed to manuscript edits. Dr. Steven. M. Kuznicki was the supervisory author and was involved with concept formation and manuscript composition.

Chapter 4 of this thesis has been accepted for publication in the journal of Industrial and Engineering Chemistry Research as: F. Yazdanbakhsh, J. A. Sawada, M. Alizadehgiashi, M. Mohammadalipour, S.M. Kuznicki, “Effect of Moisture on High Temperature H<sub>2</sub>S Adsorption on Cu-ETS-2” Farzad Yazdanbakhsh was responsible for the data collection and analysis as well as the manuscript composition. Dr. Jim Sawada assisted with the data collection and contributed to manuscript edits together with M. Alizadehgiashi and Dr. Mehdi Mohammadalipour. Dr. Steven. M. Kuznicki was the supervisory author and was involved with concept formation and manuscript composition.

To my beloved parents, my brother and my sister

## **Acknowledgements**

First and foremost I am grateful to my supervisor Professor Steven. M. Kuznicki for his advice, patience, energy, guidance and above all, believing in me. Dr. Kuznicki not only showed me the right approach during my Ph.D. research, but he also taught me how to think creatively and look at problems from a different angle. I am very much grateful to his unconditional support and his vast knowledge to enrich my learning and professional development.

I am also thankful to Dr. James Sawada for helping me with every part of my research and for enriching this thesis through his fruitful comments and discussions. Since my first day in Dr. Kuznicki's group, he never stopped supporting me and gave me the energy to do my research in the best way I could.

I would like to send special thanks to Dr. Marc Bläsing at the Institute of Energy and Climate Research-2 (IEK-2) in Forschungszentrum Jülich, Germany for his support and motivation during my stay in Germany as a visiting researcher. Special thanks to Dr. Michael Müller, the head of Thermochemistry department in IEK-2 for having me in his group and his guidance during me stay in Germany and also Dr. Egbert Wessel for helping me with TEM, SEM and EDX analysis in IEK-2.

I want to extend my appreciation to Peng Li and Gayle Hatchard from the Nanofabrication and Characterization Facility (nanoFab) of the University of Alberta for collecting SEM and EDX data and Mrs. Diane Caird in the department of Earth and Atmospheric Sciences at the University of Alberta for doing the XRD analysis.

Finally I would like to thank my beloved parents for their precious love and support that giving me energy and inspiration.

## Table of Contents

<b>1- Introduction</b>	<b>1</b>
1-1 Hydrogen Sulfide and Power Generation.....	2
1-1-1 Water-Gas Shift Reaction.....	4
1-2 What Does Success Look Like?.....	5
1-3 Literature Review: Methods of H <sub>2</sub> S removal.....	5
1-3-1 Liquid Adsorption Processes.....	6
1-3-2 Dry Adsorption Processes .....	7
1-3-2-1 Chemical Processes .....	7
1-3-2-2 Physical Processes .....	14
1-4 Motivation for the research .....	18
1-5 References .....	19
<b>2- Copper Exchanged Nanotitanate for High Temperature H<sub>2</sub>S Adsorption</b>	<b>24</b>
2-1 Abstract .....	25
2-2 Introduction .....	25
2-3 Materials Preparation .....	28
2-4 Characterization .....	28
2-5 Experimental Setup .....	28
2-6 Results and Discussion .....	28
2-7 Conclusion .....	37
2-8 Acknowledgement .....	37
2-9 References .....	38
<b>3- Cu-Cr-O Functionalized ETS-2 Nanoparticles for Hot Gas Desulfurization</b>	<b>41</b>
3-1 Abstract .....	42
3-2 Introduction .....	42
3-3 Adsorbent Preparation .....	45

3-4 Characterization .....	46
3-5 Experimental Setup .....	47
3-6 Results and Discussion .....	47
3-6-1 Spinel Cu-Cr-O .....	48
3-6-2 CuCr-ETS-2 .....	50
3-7 Conclusion .....	55
3-8 Acknowledgement .....	56
3-9 References .....	56
<b>4- Effect of Moisture on High Temperature H<sub>2</sub>S Adsorption on Cu-ETS-2</b>	<b>60</b>
4-1 Abstract .....	61
4-2 Introduction .....	61
4-3 Materials Preparation .....	63
4-4 Characterization .....	64
4-5 Humidification and Reactor Configuration .....	65
4-6 Results and Discussion .....	66
4-7 Conclusion .....	75
4-8 Acknowledgement .....	75
4-9 References .....	76
<b>5- Cu-ETS-2 Regeneration</b>	<b>79</b>
5-1 Introduction .....	80
5-1-1 Thermodynamics .....	82
5-2 Materials Preparation .....	83
5-3 Characterization .....	83
5-4 Experimental Setup .....	84
5-5 Results and Discussion .....	84
5-5-1 Thermodynamic Simulation .....	90
5-5-2 Adiabatic Reaction Temperature .....	92
5-5-3 SEM/ EDX analysis.....	93

5-5-4 H <sub>2</sub> S Thermal Dissociation and Adsorption Capacity .....	99
5-6 Conclusions .....	102
5-7 References .....	103
<b>6- Conclusion and Future Work</b> .....	<b>104</b>
6-1 General conclusion .....	105
6-2 Recommendation for future work .....	106

## List of Tables

Table 1-1 Detailed information of commercial active iron oxide sorbents .....	9
Table 2-1 Point-specific EDX analysis of Cu-ETS-2 for 3 randomly selected points on the sample (values are in atomic %) .....	30
Table 2-2 Equilibrium concentration of hydrogen in decomposition of hydrogen sulfide under 1 atm (calculated) .....	35
Table 5-1 EDX analysis results for the selected points on Figure 11-A - All data are in Wt% .....	97
Table 5-2 – EDX analysis results for the selected points on Figure 12-A - All data are in Wt%.....	97

## List of Figures

Figure 1-1 schematic flow diagram of an IGCC plant .....	3
Figure 1-2 – SEM image of activated carbon fibers .....	13
Figure 1-3 - structure of Clinoptilolite, a naturally occurring zeolite .....	14
Figure 1-4 – The structure of titanosilicate ETS-10 .....	16
Figure 1-5 – SEM images of ETS-2 particles.....	17
Figure 1-6 - XRD pattern for ETS-2.....	17
Figure 1-7 – EDX analysis for ETS-2.....	18
Figure 2-1 a) TEM and b) SEM images of nanotitanate ETS-2 showing the particle size and cluster structure .....	30
Figure 2-2 XRD patterns of ETS-2 and Cu-ETS-2 .....	31
Figure 2-3. Breakthrough curve for H <sub>2</sub> S adsorption by Cu-ETS-2 at 550 °C .....	31
Figure 2-4. Breakthrough curves for Cu-ETS-2.....	32
Figure 2-5 Breakthrough capacities of Cu-ETS-2 at different temperatures .....	33
Figure 2-6. XRD patterns of Cu-ETS-2 after H <sub>2</sub> S adsorption at 350°C, 550°C and 750 °C.....	34
Figure 2-7. SEM images of Cu-ETS-2 after adsorption at: a) 350 °C, b) 550 °C, c) 750 °C and d) 950 °C .....	36
Figure 3-1 SEM (a) and TEM (b) images of nanotitanate ETS-2 .....	47

Figure 3-2 SEM images of CuCr -ETS-2 before adsorption .....	48
Figure 3-3 Breakthrough curves for H <sub>2</sub> S adsorption on Cu-Cr-O adsorbent from a 500 ppmv mixture of H <sub>2</sub> S and He with a flow rate of 500 ml/min at different temperatures.....	49
Figure 3-4: Breakthrough capacities of Cu-Cr-O at different temperatures as measured in 1ppmv H <sub>2</sub> S in the exit gas .....	50
Figure 3-5: Breakthrough curves for CuCr-ETS-2 from a 500 ppmv mixture of H <sub>2</sub> S and He with a flow rate of 500 ml/min at different temperatures...	51
Figure 3-6: Breakthrough capacities of CuCr-ETS-2 at different temperatures ranging from 350 to 1100°C .....	52
Figure 3-7. SEM images of CuCr-ETS-2 at: a) 350 °C, b) 550 °C, c) 750 °C and d) 950 °C .....	54
Figure 3- 8 SEM image of CuCr-ETS-2 at 1100 °C .....	54
Figure 3-9: XRD patterns of CuCr-ETS-2 after adsorption at different temperatures .....	55
Figure 4-1 Schematic of the humidification and reactor system.....	66
Figure 4-2 (a) TEM and (b) SEM images of ETS-2 together with (c) SEM image of Cu-ETS-2 showing the particles cluster size and morphology...	67
Figure 4-3 Comparison between H <sub>2</sub> S breakthrough curves for dry and humid stream at (a) 350 °C, (b) 550 °C and (c) 750 °C .....	69
Figure 4-4 XRD pattern of Cu-ETS-2 after H <sub>2</sub> S adsorption at (a) 550°C and (b) 750°C for dry and humid streams.....	71
Figure 4-5 Standardized and baseline-corrected H <sub>2</sub> signal as a function of temperature for humid and dry 500 ppm H <sub>2</sub> S in He .....	73

Figure 5-1 Phase diagram of Cu-S-O system at 727°C .....	82
Figure 5-2 Schematic diagram of the experimental setup .....	84
Figure 5-3 Typical adsorption breakthrough curves for multiple adsorption cycles on Cu-ETS-2. (the presented data are for experiments at 550 °C) .....	86
Figure 5-4 Breakthrough times (in minutes) for different adsorption cycles at different temperatures.....	87
Figure 5-5 Change in SO <sub>2</sub> concentration in the exit at (A) 350 and (B) 950 °C .....	88
Figure 5-6 XRD analysis of the adsorbent after 4 adsorption and 3 oxidation cycles .....	89
Figure 5- 7 changes in solid phases versus the amount of oxygen entering the system for oxidation process at 350°C .....	90
Figure 5-8 - change in solid phases versus the amount of oxygen entering the system for oxidation process at 950°C.....	91
Figure 5-9 - change in gas phases versus the amount of oxygen entering the system for oxidation process at 950°C .....	91
Figure 5-10 Temperature profile in Cu <sub>2</sub> S – O <sub>2</sub> system versus the amount of oxygen fed into the system for Cu-ETS-2 oxidation at 350°C assuming an adiabatic system .....	92
Figure 5-11 Scanning electron micrographs of Cu-ETS-2 after: (A) Adsorption and previously regeneration at 350°C, (B) Only 1 adsorption at 350°C and (C) Only 1 adsorption at 950°C .....	95
Figure 5-12 Scanning Electron Micrographs of Cu-ETS-2 after adsorption and previously oxidation at 950°C .....	96
Figure 5-13 Needle like phases observed in a previous study after adsorption of H <sub>2</sub> S on Cu-Cr-ETS-2 at 1100°C .....	97
Figure 5-14 – Needle like structures formed at CuCr-ETS-2 experiments at 1100°C .....	99

Figure 5-15 – EDX analysis for Cu-Cr-ETS2 at 1100°C ..... 99

## Chapter 1

# Introduction

## 1-1 Hydrogen Sulfide and Power Generation

Hydrogen Sulfide ( $H_2S$ ) is a colorless, highly flammable and extremely toxic gas with the characteristic odor of rotten eggs. The odor is so intense that the threshold for humans is as low as 0.1 ppmv<sup>1</sup>. Just five minutes exposure to  $H_2S$  with 1000 ppmv concentration is fatal to humans<sup>2</sup>. In nature it can be found in hot springs, volcanic gases, crude oil and natural gas. It can also be naturally produced as a result of bacteria digestion of organic matter and human or animal waste under anaerobic conditions.

$H_2S$  can also be released into the atmosphere due to human activities. Burning coal can be one of the major sources. Depending on the origin, coal can have between 0.1 to 6 wt% sulfur content, which is released in the form of  $H_2S$  during coal gasification and production of syngas for power generation<sup>3</sup>. Later, syngas should be free of  $H_2S$  in order to prevent serious corrosion of gas turbines and pipelines.

$H_2S$  can also be found in natural gas. Natural gas is considered “sour” if it contains more than 5.7 milligrams per normal cubic meter. According to the Clean Air Act (1989), pipeline and sales standard levels of  $H_2S$  should be no more than 4 ppmv.

### Necessity of $H_2S$ removal

In many different areas, hydrogen sulfide is an undesired and harmful gas and needs to be removed. Among these areas, coal gasification process and the water-gas shift reaction can be named.

### Coal gasification process

Nowadays, the main usage of coal is in electricity generation. More than half of the electricity in the U.S. is generated from coal<sup>4</sup>. As long as we rely on fossil fuels, coal will play a more important role due to its low price.

The Integrated Gasification Combined Cycle (IGCC) is considered to be the most efficient and environmentally acceptable technology for power generation from coal. This advanced process is one of the cleanest and most efficient available

technologies for coal-based power generation, with emissions comparable to natural gas-based power plants<sup>5</sup>. IGCC is a process in which syngas is produced by gasification of coal and it is later used as a fuel for the gas turbine and electricity generation. Figure 1-1 shows a schematic flow diagram of an IGCC plant.

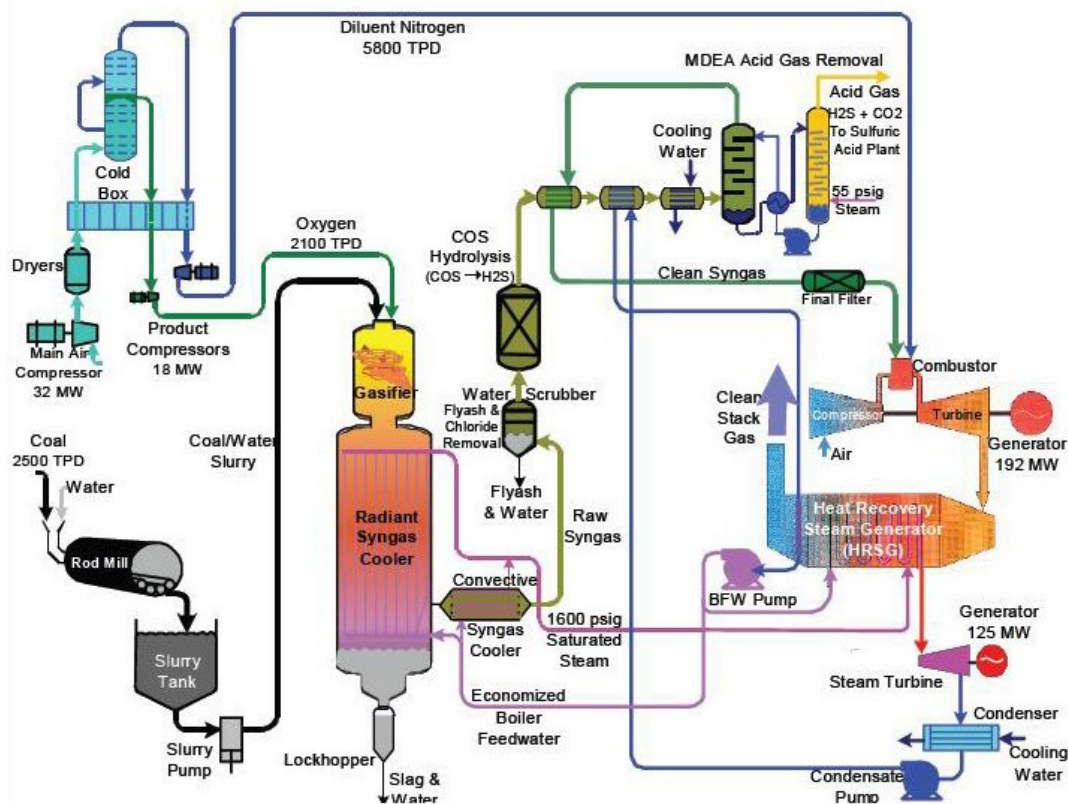


Figure 1-1 Schematic flow diagram of an IGCC plant<sup>6</sup>

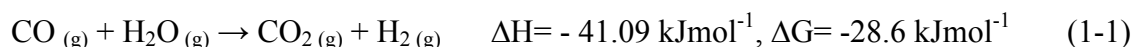
As the figure shows, the carbon source is crushed and mixed with water to form a slurry and is pumped into the gasifier together with oxygen. The gasifier is operated under pressure and gasification takes place rapidly at temperatures as high as 1200°C. The generated gas is mainly composed of H<sub>2</sub>, CO, CO<sub>2</sub> and H<sub>2</sub>O. The sulfur in coal is mostly converted to H<sub>2</sub>S and small amounts of COS. The raw fuel gas leaves the gasifier together with molten ash and a small amount of unburned carbon. The gas-molten solid mixture enters a radiant syngas cooler (RSC) and convective syngas cooler (CSC) to cool down the gas to about 150°C (27 bars) by generating additional steam. The gas stream is further cooled down through a gas scrubber and

a low temperature gas cooling section to reduce the raw fuel gas temperature to 40°C, prior to entering the sulfur removal unit.

Removing pollutants from fuel gas is required for effectively using this technology not only to protect equipment from corrosion, but also to meet the environmental legislation for sulfur emissions<sup>7</sup>. At the moment, H<sub>2</sub>S adsorption at most gasification plants is done using MDEA (Methyl diethanolamine) solutions. The disadvantage of this method for using in IGCC process and also water-gas shift reaction is that hot coal gas (Generally, 500°C or above<sup>10</sup>) must be cooled down for desulfurization by MDEA solution and then preheated to high temperature before being fed into gas turbine. As a result, the thermal efficiency of the system is significantly reduced. Due to this reason, it is important to perform the desulfurization process at high temperatures.

### 1-1-1 Water-gas shift reaction

There has been a huge demand for hydrogen in recent years due to its widely use in chemical and petroleum industries and also as a new source of energy in proton exchange membrane fuel cells. One way to produce hydrogen is through gasification of fossil fuels or biomass and then, adding steam to convert carbon monoxide to a mixture of carbon dioxide and hydrogen by the so-called water-gas shift reaction (WGS) at temperatures around 350°C<sup>8</sup> before feeding the gas to the gas turbine.



To obtain pure hydrogen, further separation processes such as physical or chemical sorption or membrane separation is needed to be done afterwards.

In order to increase hydrogen production while reducing carbon monoxide content, it is necessary to run reaction (1-1) at low temperatures. However, in order to obtain high reaction rates, higher temperatures are required. The high temperature reaction is performed at 320-350°C using Fe-Cr oxides catalyst, while the low-temperature shift reaction is conducted at 200-250°C and a Cu/ZnO/Al<sub>2</sub>O<sub>3</sub> catalyst is commonly used<sup>9</sup>.

Both of the above-mentioned catalysts can react with  $\text{H}_2\text{S}$  and as a result, the catalysts become inactive. In order to prevent inactivation, the gas stream should be free of  $\text{H}_2\text{S}$  prior to water gas shift unit.

Among the several desulfurization methods, adsorption of metal oxides has shown great potential to be used as an efficient high temperature desulfurization process.

### **1-2 What does success look like?**

In order to enable direct desulfurization of the syngas stream (prior to the WGS beds) the desulfurization system needs to accept syngas at temperatures between  $400\text{-}700^\circ\text{C}$  depending on the process design, having a  $\text{H}_2$  concentration ranging from 15 to 30 mole%, a water loading of 7-20 mole% and, ideally be regenerable for many cycles<sup>11</sup>. The desulfurization capacity should also be maximized to minimize the size of the reactor needed for desulfurization.

### **1-3- Literature review: Methods of $\text{H}_2\text{S}$ removal**

Prior to the early 1990's sulfur recovery and acid gas flaring were the most commonly used and most economic methods of handling the acid gas streams<sup>12</sup>. Gas streams containing less than 10 tons of sulfur a day used to be flared because at this amount, running a sulfur recovery unit was not economically reasonable.

As a result of public concern over human health and negative environmental impacts, flaring  $\text{H}_2\text{S}$ -containing gases was restricted. On the other hand, a weak sulfur market resulted in sulfur recovery units being uneconomical<sup>13</sup>. As a result, technologies for  $\text{H}_2\text{S}$  conversion, long term storage of sulfur or  $\text{H}_2\text{S}$  have gained more attention in recent years.

There are several commercial treatment techniques that are commonly used to remove  $\text{H}_2\text{S}$ , such as absorption in liquids (alkaloamines, ammonia solution...), biological processes, the Claus process, adsorption on activated carbon and metal oxides, and also separation by molecular sieves.

Almost all the H<sub>2</sub>S removal processes can be categorized into liquid absorption processes and dry processes.

### 1-3-1 Liquid adsorption processes

#### Alkanolamines

H<sub>2</sub>S is slightly soluble in water and once it is dissolved, makes the solution acidic:



In order to increase the amount of dissolved H<sub>2</sub>S, a chemical should be added to the solution that can consume either H<sup>+</sup> or HS<sup>-</sup>. The easiest choice would be a source of alkalinity that can consume H<sup>+</sup> in the solution and increases the amount of H<sub>2</sub>S absorbed.

The most commonly used sources of alkalinity for H<sub>2</sub>S absorption are alkanolamines (monoethanolamine (MEA), diethanolamine, triethanolamine), among which, (MEA) is more often used. It reacts with H<sub>2</sub>S to form amine sulfide and hydrosulfide<sup>14</sup>:



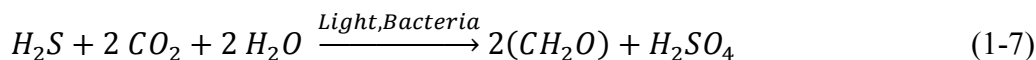
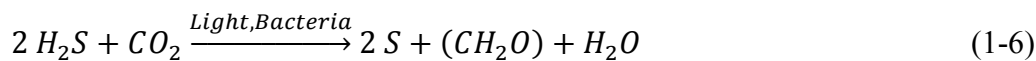
#### Biological processes

Biological processes have also been used for reduction of H<sub>2</sub>S from gas streams. In these processes H<sub>2</sub>S is converted to sulfuric acid under aerobic conditions:



In this process, the gas stream is passed through a packed bed biofilter where H<sub>2</sub>S is absorbed into a liquid film and oxidized by bacteria. In such processes, it is possible to reach 99% or even higher conversions for gas streams with up to 1000 ppm H<sub>2</sub>S concentrations<sup>15</sup>.

In some cases, H<sub>2</sub>S removal is done under anaerobic, inorganic acid gas bioconversion through the photosynthetic van Niel reaction<sup>16</sup>:



In this process, photoautotrophic bacteria provide nearly 100% H<sub>2</sub>S removal.

The main problem with biological processes is that they are not flexible and rapid enough on a large scale and much work related to the application of these processes for treatment of H<sub>2</sub>S still needs to be done<sup>17</sup>.

### 1-3-2 Dry adsorption processes

These processes involve using a dry adsorbent in a reactor that facilitates the flow of the gas stream through the adsorbent. The adsorbent will eventually become saturated with the contaminant and becomes inactive. In order to prevent the interruption in the adsorption process, there are usually two reactors operating in parallel so one vessel can be in service while the other one is offline for adsorbent change or adsorbent regeneration.

Generally, dry adsorption processes are divided into two categories: chemical and physical adsorption.

#### 1-3-2-1 Chemical processes

Chemical adsorption processes are based on the reaction of an adsorbent with a target molecule to form a new compound.

- **The Claus process**

The Claus process is a technology that is able to remove H<sub>2</sub>S from a gas stream and recover sulfur in elemental form<sup>18</sup>. It was first developed over 100 years ago and is suitable for gases with high H<sub>2</sub>S concentrations (above 20% v/v), on a large scale<sup>18</sup>.

The process consists of two steps; thermal and catalytic. During the thermal step, H<sub>2</sub>S reacts in a substoichiometric combustion above 850°C and at the downstream process gas cooler, elemental sulfur is formed.



In the catalytic step, the process continues with activated Al<sub>2</sub>O<sub>3</sub> or TiO<sub>2</sub> in order to boost the sulfur yield.

A single Claus reactor can usually achieve H<sub>2</sub>S conversions of up to 70%. In industry, several stages are usually used to achieve conversions of about 95-97%. The problem with the Claus process is that the exit gas still contains up to 2-3% of H<sub>2</sub>S together with other gases such as COS, CS<sub>2</sub> and CO<sub>2</sub>. These concentrations are still above the current allowable standards and further treatments are required on the gas stream before its release in the atmosphere<sup>19</sup>.

- **Adsorption on metal oxides**

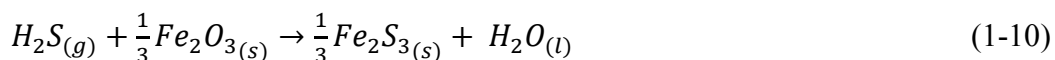
For small scale desulfurization processes of less than 10 tons of sulfur per day, adsorption by metal oxides is an effective and economical method of removing H<sub>2</sub>S from gas streams. Metal oxide sorbents work by reacting with H<sub>2</sub>S to form metal sulfides. Metal sulfides can later be converted back into metal oxide during an oxidation (regeneration) process by exposing to air or oxygen.

Oxides of many metals such as Zn, Cu, Fe, Co, W, Mo, Ca, Ba, and Sr have been reported to be efficient adsorbents even at high temperatures<sup>20</sup>.

One of the first metal oxides to be used as a sulfur removing agent was iron oxide. It was first used in the 19<sup>th</sup> century<sup>21</sup>. Once iron oxide is exposed to H<sub>2</sub>S, iron sulfide is formed and after the adsorbent become inactive, it can be regenerated by air to oxidize the iron sulfide and generate elemental sulfur. After several regeneration cycles, the reactor will be clogged by sulfur and has to be shut down for sulfur removal. Ferric oxide based sorbent, CG-4 has even been used in small scale natural

gas processing plants in Canada. The adsorbent is reported to have sulfur adsorption capacity of 150 mg sulfur per gram of adsorbent<sup>12</sup>. However, the adsorbent is designed for low temperature processes and due to having porosity in its structure; it is prone to pore blockage and severe loss of adsorption capacity when used in humid gas streams. One of the significant drawbacks of the sorbent is that it is just regenerable for just 2 or 3 cycles.

The reaction of H<sub>2</sub>S with iron oxide is as follows<sup>22</sup>:



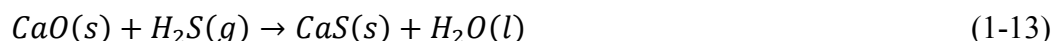
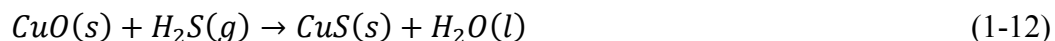
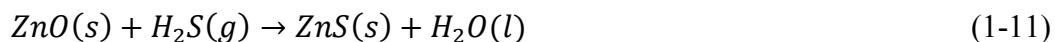
One of the problems with using iron oxide as a high temperature H<sub>2</sub>S adsorbent is that the adsorption reaction is best carried out at room temperature. If performed at higher temperatures, iron oxide will become dehydrated and results in considerable reduction in the rate of reaction<sup>22</sup>.

Active iron oxide adsorbents are usually sold under several trademarks related to the different support media, such as Iron sponge, Sulfa Treat, Sulfur-Rite, Media-G2, and CG-4. Detailed information of these adsorbents is presented in table 2-1.

Table 1-1 – detailed information of commercial active iron oxide sorbents

Adsorbent	Operating Temperature	Ability to regenerate	Cons / Pros	Manufacturers
Iron sponge	20-23 °C	Max 2-3 times	High labor cost	Connely GMP, Physichem, Verac
Sulfa Treat	20-23 °C	No	Easy to handle	Sulfatreat
Sulfur Rite	20-23 °C	No	Prepackaged- forms iron pyrite	US Filter, Merichem
Media G-2	20-23 °C	Up to 15 times	Requires multiple regenerations for high efficiency	ADI international
CG-4	20-23 °C	Max 2-3 times	High sulfur loading- easy to handle	CLEAN Catalysis and Purification Tech.

Zinc, copper and calcium oxides are also good H<sub>2</sub>S adsorbents. They have spontaneous reactions with H<sub>2</sub>S at room temperature. The reactions are as follows:



Calcium oxide is believed to be a better choice for H<sub>2</sub>S adsorption at high temperatures (250-500°C) and zinc oxide appears to have better adsorption capacity at temperatures lower than 100°C<sup>23</sup>.

Rare metal elements include 15 lanthanides together with Sc and Y. Among them, lanthanum and cerium(III) oxides have shown great H<sub>2</sub>S adsorption capacity especially in realistic reformat gas compositions, such as steam reforming, autothermal reforming, or partial oxidation of heavy oils, diesel, jet fuels or coal gasification<sup>24</sup>.

Li et al.<sup>25</sup> investigated the catalytic oxidation of H<sub>2</sub>S to elemental sulfur on four rare earth orthovanadates (Ce, Y, La and Sm) and three magnesium vanadates (MgV<sub>2</sub>O<sub>6</sub>, Mg<sub>2</sub>V<sub>2</sub>O<sub>7</sub> and Mg<sub>3</sub>V<sub>2</sub>O<sub>8</sub>). For the rare earth orthovanadates, it was found that sulfur yield increased in the order LaVO<sub>4</sub> < SmVO<sub>4</sub> < YVO<sub>4</sub> < CeVO<sub>4</sub>.

Flytzani- Stephanopoulos et al.<sup>26</sup> developed adsorbents based on cerium and lanthanum oxide surfaces and capable of reversible adsorption of H<sub>2</sub>S for several cycles at temperatures up to 800°C. They reported a very fast adsorption and desorption process together with the ability to remove H<sub>2</sub>S to a sub-ppm level at very short (millisecond) contact time. According to these authors any type of sulfur-free gas, including water vapor, can be used to regenerate the adsorbent.

In order to improve the adsorptive performance of metal oxides, strategies such as doping with other metals have also been used. As an example, zinc ferrite was used as an adsorbent for H<sub>2</sub>S in coal gases at 538°C<sup>27</sup>. Mixed oxides of copper together with Cr, Ce, Al, Mg, Mn and Ti have also been investigated and CuCr<sub>2</sub>O<sub>4</sub> (CuO-

$\text{Cr}_2\text{O}_3$ ) and  $\text{CuCeO}_2$  were found to be the most efficient adsorbents at high temperatures<sup>28</sup>.

Hee Kwon et al.<sup>7</sup> used a mixture of zinc oxide, titanium oxide, nickel oxide and cobalt oxide together with an inorganic binder bentonite to prepare Zn-Ti based adsorbents for  $\text{H}_2\text{S}$  removal. Adsorbents showed very good sulfur removing capacity even after 15 cycles of regeneration, while conventional Zn-Ti sorbents deactivate much earlier. Nickel and cobalt worked as the active sites for desulfurization reaction and they also helped to stabilize the structure of the adsorbent.

In 1997, Li et al.<sup>25</sup> compared ZnO based adsorbents with copper oxides and realized that CuO can be used at much higher temperatures than ZnO based adsorbents. They also reported reduction of  $\text{H}_2\text{S}$  from several thousand ppm to sub-ppm levels using CuO and  $\text{Cu}_2\text{O}$  sorbents. The disadvantage of their sorbent was that it reduced to elemental copper by  $\text{H}_2$  and CO present in the gas stream.

Li<sup>25</sup> also tested a CuO-CeO<sub>2</sub> adsorbent and reported that  $\text{H}_2\text{S}$  levels were reduced to concentrations as low as 5-10 ppm from a gas stream containing several thousand ppm at temperatures between 650-850°C.

Increasing the surface area of the adsorbent, results in an increase in the number of active sites. In order to enhance the utilization of active chemicals (metals/metal oxides) and their  $\text{H}_2\text{S}$  breakthrough capacities, increasing the number of active sites is required. This can be achieved by substituting the active compound on the surface of different supports such as  $\text{Al}_2\text{O}_3$ ,  $\text{TiO}_2$ ,  $\text{SiO}_2$  and zeolites. As a result, the surface area and the number of active sites are increased and the structural stability is also improved.

Lew et al.<sup>29</sup> studied the adsorption of  $\text{H}_2\text{S}$  on pure zinc oxide and zinc titanates. The authors concluded that zinc titanate reduces more slowly to volatile zinc; therefore, it can be used at higher temperatures. Ko et al.<sup>30</sup> compared the  $\text{H}_2\text{S}$  adsorption capacity of Mn, Fe, Cu, Co, Ce and Zn when substituted on  $\text{Al}_2\text{O}_3$  in syngas at 500-700°C. They reported 100% utilization for copper and manganese. Another study<sup>31</sup>

showed that when Cu, Mo and Mn are supported on SP-115 zeolite, the mechanical strength of the adsorbent is considerably increased.

Kyotani et al.<sup>32</sup> investigated H<sub>2</sub>S adsorption of Cu supported on natural zeolites (Mordenite and Clinoptilolite) and SiO<sub>2</sub>. They also compared the results with adsorption on pure copper oxide. The conclusion was that the breakthrough capacity is almost the same at 600°C for Cu on SiO<sub>2</sub> (15wt% Cu) and zeolite (20 wt% Cu) as for pure copper oxide.

The study also revealed the weaknesses of using pure copper oxide. It was observed that it has the lowest reactivity for sulfidation due to formation of dense copper sulfate on the adsorbent.

- **Adsorption on carbon-based materials**

When molecules are adsorbed on the carbon surface, they are bound by Van der Waals forces that work mostly in small pores. Moreover, the surface of activated carbons promotes catalytic/ oxidative reactions due to the basic and acidic functional groups, resulting in the adsorption and catalysis for H<sub>2</sub>S oxidation<sup>33</sup>.

The wide application of activated carbons is mainly due to their large surface area exceeding 1000 m<sup>2</sup>/g, high pore volume, high density of carbon atoms in graphite layers and surface hydrophobicity.

Carbonaceous materials are usually made from different organic sources including peat, wood, coconut shells, and polymers. In order to activate the carbonaceous materials by physical activation, they are carbonized at temperatures ranging from 700-1000°C and then exposed to steam or carbon dioxide at temperatures ranging from 800-1000°C. During the chemical activation process, different chemicals such as phosphoric acid, zinc chloride or potassium hydroxide are mixed with the material and then carbonized under various temperatures. Sometimes, in order to improve the performance of the sorbents, carbons are impregnated with chemicals such as KI, KMnO<sub>4</sub>, KOH or NaOH. Using different activation processes gives rise

to activated carbons with different features, including surface area, porosity and surface chemistry<sup>34</sup>.

Activated carbon sorbents can effectively remove H<sub>2</sub>S from gas streams. Carbons impregnated with caustics can lead to fast and complete dissociation of H<sub>2</sub>S in the basic environment and lead to its oxidation to elemental sulfur. A combination of porosity and surface chemistry results in the oxidation of H<sub>2</sub>S mainly to sulfuric acid which can later be removed by water washing<sup>35,36</sup>.

Bandosz et al.<sup>37</sup> investigated the use of activated carbon as an H<sub>2</sub>S removing agent. Results of the experiments showed that the surface functional groups (containing oxygen and phosphorous) and the porosity of carbon significantly contribute to the process of H<sub>2</sub>S removal. They also discovered that functional groups present on the carbon surface act as a catalyst for H<sub>2</sub>S oxidation.

Activated carbon fibers have special advantages compared to the usual activated carbons: (i) narrow pore size distribution, (ii) larger surface area and, (iii) faster adsorption kinetics. Moreover, their adsorption capacity for sulfur can be increased by the formation of suitable nitrogen-based surface groups through reaction with ammonia gas at high temperature<sup>39</sup>. Figure 1-2 shows a scanning electron microscopy image of activated carbon fibers. As can be seen, activated carbon fibers consist of long thin sheets of carbon. A single ACF filament is a thin tube with a diameter of 5-8 micrometers.

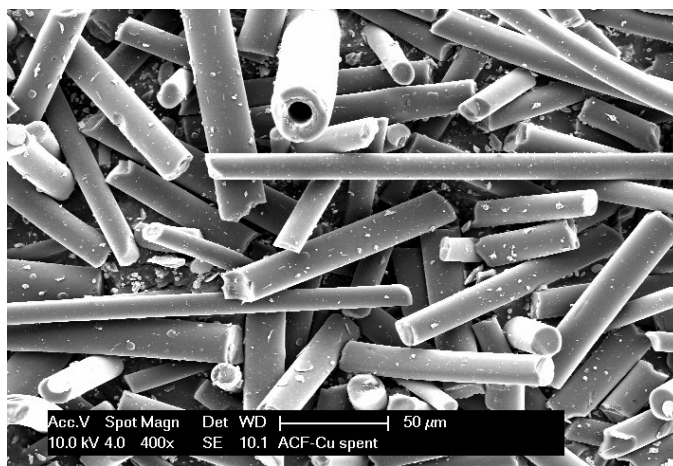


Figure 1-2 – SEM image of activated carbon fibers (38)

### 1-3-2-2 Physical processes

- **Classical molecular sieves**

Another approach to H<sub>2</sub>S removal is physisorption of H<sub>2</sub>S onto a solid surface. Zeolites or molecular sieves are naturally occurring or synthetic silicates with a highly uniform pore size and large surface area, making them ideal for adsorption applications. They are commonly used in chemical industries as H<sub>2</sub>S adsorbents due to the fact that polar compounds such as water, H<sub>2</sub>S, SO<sub>2</sub> and NH<sub>3</sub>, are strongly adsorbed.

Zeolites have three dimensional frameworks that bring about their unique characteristics. They have crystalline, microporous hydrated aluminum silicate structures of (SiO<sub>4</sub>)<sup>4-</sup> and (AlO<sub>4</sub>)<sup>5-</sup> linked together and forming pores with diameters ranging from 2.5 to 10Å. All AlO<sub>4</sub> units in the framework have a negative charge which is balanced by non-framework cations like Na<sup>+</sup>, K<sup>+</sup> or Ca<sup>+</sup>. These cations can be replaced by other cations through ion exchange. Figure 1-3 shows the structure of a zeolite framework:

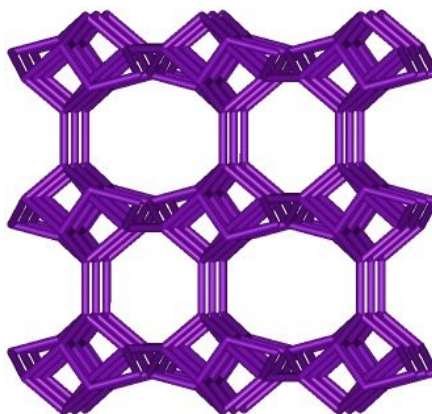


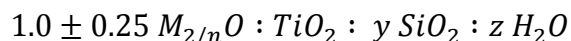
Figure 1-3 - structure of Clinoptilolite, a naturally occurring zeolite<sup>40</sup>

Since zeolites have high surface area and unique porous structure, molecules like H<sub>2</sub>S can be adsorbed into their framework, resulting in the removal of the target compound from a gas stream. One disadvantage of using zeolites is pore blockage due to the presence of water in gas streams. Water can occupy the adsorption sites and inhibit H<sub>2</sub>S from adsorbing. The presence of a very high amount of water can

flood the zeolite structure but even at low levels (50 ppm), the capacity for H<sub>2</sub>S can be reduced to nearly zero. Normally, water is considered a poison for aluminosilicate zeolites when the application is gas adsorption.

### **Mixed coordination molecular sieves, ETS-4 and ETS-10**

Mixed octahedral/ tetrahedral titanium silicate molecular sieves consist of three dimensional frameworks of interconnecting channels. In 1973 a natural molecular sieve called Zorite with a titanosilicate framework was discovered in trace amounts on the Siberian Tundra<sup>41</sup>. A synthetic form of Zorite were later developed under the commercial name of ETS-4 and patented at 1989<sup>42</sup>. They can be identified by the following molecular ratio of the oxides:



M is at least one cation having a balance of n, y ranges from 1.0 to 10.0 and z is between 0 and 100. M is typically a mixture of alkali metal cations like sodium and potassium. Later, another titanosilicate structure (ETS-10) with nearly the same molecular ratio of the above mentioned oxides was also developed and patented by Kuznicki<sup>41</sup>. The structure of ETS-10 comprises corner-sharing SiO<sub>4</sub> tetrahedra and TiO<sub>6</sub> octahedra linked through bridging oxygen atoms resulting in a 12-membered ring structure. Figure 1-4 shows a high-resolution transmission electron micrograph of ETS-10 together with a computer simulation of the structure<sup>43</sup>.

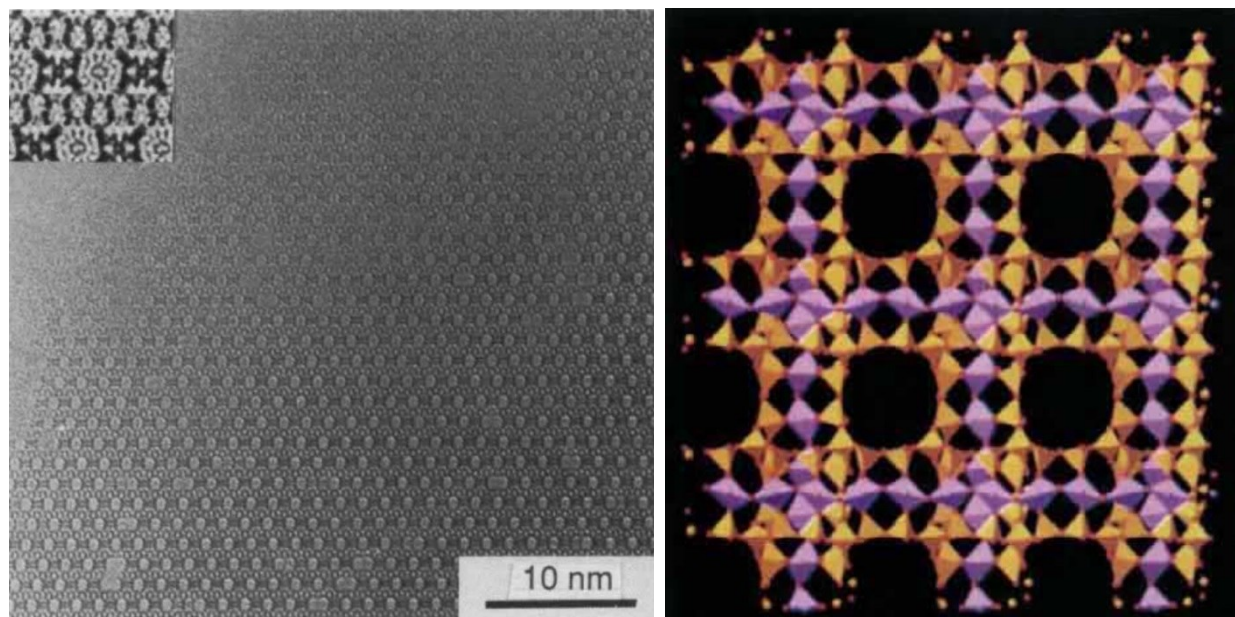


Figure 1-4 – The structure of titanosilicate ETS-10

ETS-4 and ETS-10 have been used in different applications ranging from catalysis to adsorption and ion exchange.

### **Sodium nanotitanate, ETS-2**

ETS-2 is a sodium nanotitanate structure which was developed by Kuznicki in 1989<sup>41</sup>. ETS-2 has a fundamental difference with ETS-4 and ETS-10. It doesn't have a porous structure. ETS-2 is a form of sodium titanate which by addition of silica during synthesis becomes a highly efficient ion exchanger. ETS-2 has a semi-crystalline framework with a high surface area due to its small particle size. Since ETS-2 does not have a porous structure, it does not suffer from pore blockage or capillary condensation. Another advantage of ETS-2 is that it has a huge affinity towards divalent atoms like copper. As a result, it is easy to substitute copper on top of ETS-2 through an ion exchange process. Once copper is exchanged onto the surface, it can be formed into copper oxide by heating the adsorbent to high temperatures (up to 500°C) in an atmospheric environment.

SEM analysis of ETS-2 reveals that the particles tend to form clusters, typically a few micrometers in size while each particle is 5-10 nanometers. XRD pattern of ETS-2 also shows that it is almost an amorphous material with some degree of

crystallinity (~20%) due to anatase and rutile  $\text{TiO}_2$ . Figures 1-5 and 1-6 show SEM images of ETS-2 particles and their XRD spectrum, respectively.

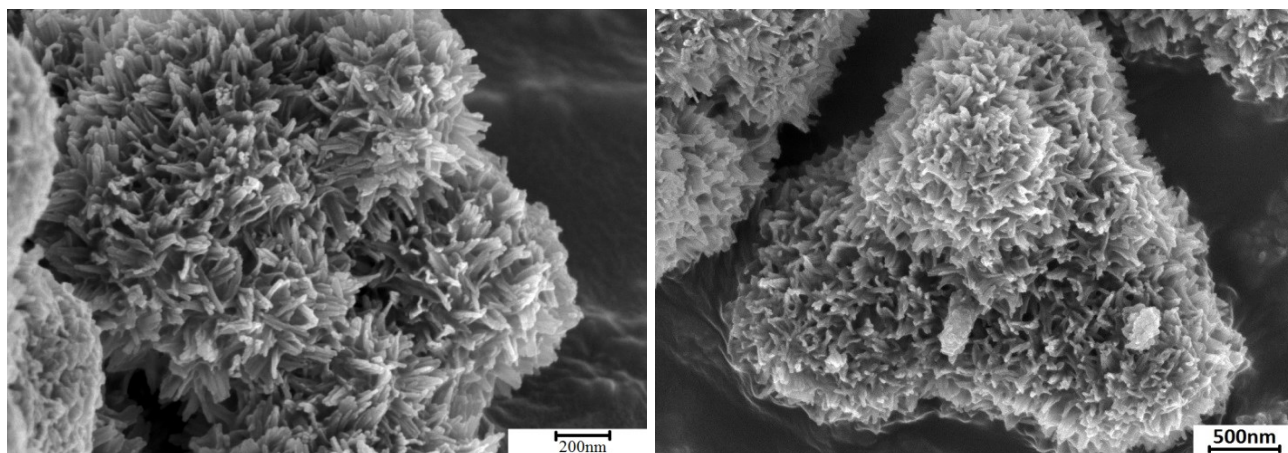


Figure 1-5 – SEM images of ETS-2 particles

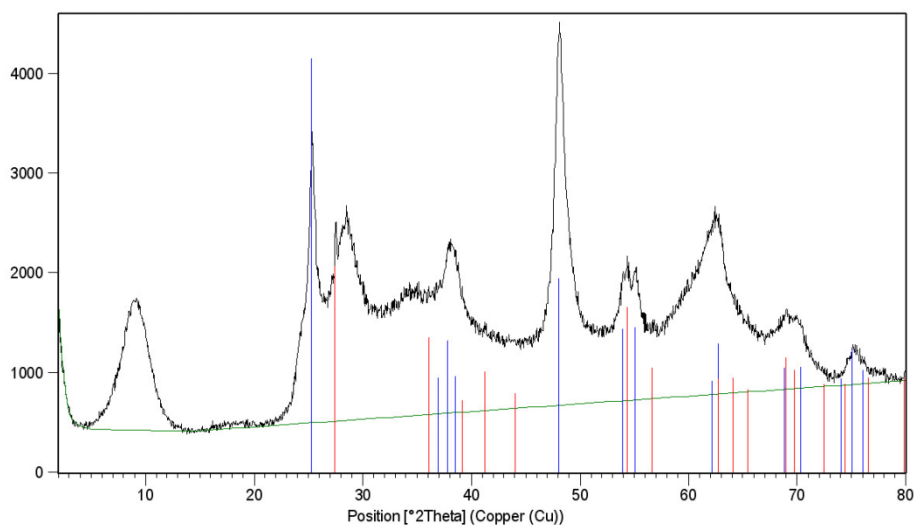


Figure 1-6 - XRD pattern for ETS-2

EDX analysis of the particles also verifies the presence of Ti, Si, O and Na elements in the ETS-2 structure as shown in Figure 1-7.

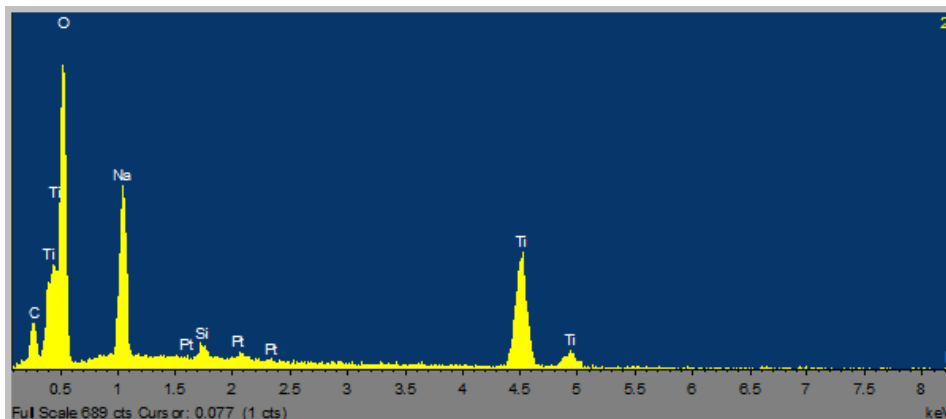


Figure 1-7 – EDX analysis for ETS-2

#### 1-4 motivation for the research

Several chemical and physical separation methods are commonly used in industries for this purpose such as reaction with alkaloamines, biological processes, Claus process, adsorption on metal oxides, activated carbons, zeolites and molecular sieves. The disadvantage of these techniques for using in the IGCC process and also the water-gas shift reaction is that hot coal gas (generally, 500°C or above<sup>10</sup>) must be cooled down to around 40°C for desulfurization and then preheated to high temperature before being fed into gas turbine. As a result, the thermal efficiency of the system is significantly reduced. Due to this reason, it is economically important to perform the desulfurization process at high temperatures. Among the several desulfurization methods, adsorption of metal oxides has shown great potential to be used as an efficient high temperature desulfurization process.

---

**1-5- References**

- (1) Health and Safety Fact Sheet, Hydrogen Sulfide. [http://cupe.ca/health-and-safety/Hydrogen\\_Sulfide](http://cupe.ca/health-and-safety/Hydrogen_Sulfide) (Accessed November 1, 2011)
- (2) Patnaik, P., "A Comprehensive Guide to the Hazardous Properties of Chemical Substances," 2nd ed., John Wiley, New York (1999), pp. 505-536.
- (3) Stirling, D. Sulfur Problem - Cleaning up Industrial Feedstocks, 2000.
- (4) U.S. DOE Topical Report # 21, Clean Coal Technology: Coproduction of Power, Fuels, and Chemicals, p., September 2001.
- (5) Chauk SS, Agnihotri R, Jadhav RA, Misro SK, Fan L-S: Kinetics of high-pressure removal of hydrogen sulfide using calcium oxide powder. *AIChE Journal* 2000;46:1157.
- (6) <http://energy.gov/fe/how-coal-gasification-power-plants-work>
- (7) Hee Kwon J, Tae Jin L, Si Ok R, Jae Chang K: A study of Zn - Ti-based H<sub>2</sub>S removal sorbents promoted with cobalt oxides. *Industrial and Engineering Chemistry Research* 2001;40:3547.
- (8) R. Kam, J. Scott, R. Amal, C. Selomulya, Pyrophoricity and stability of copper and platinum based water-gas shift catalysts during oxidative shut-down/start-up operation, *Chem Eng Sci*, 65 (24) (2010), pp. 6461-6470
- (9) N.A. Koryabkina, A.A. Phatak, W.F. Ruettinger, R.J. Farrauto, F.H. Ribeiro, J. *Catal.* 217 (2003) 233.
- (10) Ko T-H, Chu H, Chaung L-K: The sorption of hydrogen sulfide from hot syngas by metal oxides over supports. *Chemosphere* 2005;58:467.
- (11) Prakash, A., On the effects of syngas composition and water-gas-shift reaction rate on FT synthesis over iron based catalyst in a slurry reactor. *Chem. Eng. Commun.* **1994**, 128, (1), 143-158.

(12) Bachu, S., and W. D. Gunter, "Overview of Acid-Gas Injection Operations in Western Canada", Proceedings of 7th International Conference on Green House Gas Control Technologies (2005).

(13) Wang, H., D. Fang, and K.T. Chuang, "A Sulfur Removal and Disposal Process through H<sub>2</sub>S Adsorption and Regeneration: Ammonia Leaching Regeneration," Process Safety and Environment Protection, 8, 296-302 (2008).

(14) Wang, L. K., "Advanced Air and Noise Pollution Control," Humana Press, New York (2004), pp. 367-420.

(15) Sublette, K. L., and N. D. Sylvester, "Oxidation of Hydrogen Sulfide: Desulfurization of Natural Gas," Biotechnology and Bioengineering, 29, 595- 600 (1987).

(18) Sardesai, P., "Exploring the Gas Anaerobic Bioremoval of H<sub>2</sub>S for Coal Gasification Fuel Cell Feed Streams," Fuel Processing Technology, 87, 319-324 (2006).

(17) Jensen AB, Webb C: Treatment of H<sub>2</sub>S-containing gases: a review of microbiological alternatives. Enzyme and Microbial Technology 1995;17:2.

(18) Wang, H., D. Fang, and K.T. Chuang, "A Sulfur Removal and Disposal Process through H<sub>2</sub>S Adsorption and Regeneration: Ammonia Leaching Regeneration," Process Safety and Environment Protection, 8, 296-302 (2008).

(19) Eow JS: Recovery of sulfur from sour acid gas: A review of the technology. Environmental Progress 2002, 21:143.

(20) Westmoreland, P. R.; Harrison, D. P. Evaluation of candidate solids for high-temperature desulfurization of low-Btu gases. Environ. Sci. Technol. 1976, 10, 659.

(21) Crynes, B. L., "Chemical Reactions as a Means of Separation: Sulfur Removal," Marcel Dekker, New York (1977), pp. 212-223.

- (22) Miura, K., "Simultaneous Removal of COS and H<sub>2</sub>S from Coke and Oven Gas at Low Temperature by Use of an Iron Oxide," *Industrial and Engineering Chemistry Research*, 31, 415-419 (1992).
- (23) Xue, M., R. Chitrakar, K. Sakane, and K. Ooi, "Screening of Adsorbents for Removal of H<sub>2</sub>S at Room Temperature," *Green Chemistry*, 5, 529-534 (2003).
- (24) Li Z, Flytzani-Stephanopoulos M: Cu-Cr-O and Cu-Ce-O Regenerable Oxide Sorbents for Hot Gas Desulfurization. *Industrial & Engineering Chemistry Research* 1997;36:187-196.
- (25) Li K-T, Chi Z-H: Selective oxidation of hydrogen sulfide on rare earth orthovanadates and magnesium vanadates. *Applied Catalysis A: General* 2001;206:197.
- (26) Flytzani-Stephanopoulos M, Sakbodin M, Wang Z: Regenerative adsorption and removal of H<sub>2</sub>S from hot fuel gas streams by rare earth oxides. *Science* 2006;312:1508.
- (27) Ayala, R. E.; Marsh, D. W. Characterization and Long-Range Reactivity of Zinc Ferrite in High-Temperature Desulfurization Processes. *Industrial and Engineering Chemistry Research* 1991, 30, 55-60.
- (28) Abbasian, J.; Hill, A. H.; Wangerow, J. R.; Flytzani-Stephanopoulos, M.; Bo, L.; Patel, C.; Chang, D. Development of novel copper-based sorbents for hot-gas cleanup. Final technical report, September 1, 1991-August 31, 1992
- (29) Lew, S.; Sarofim, A. F.; Flytzani-Stephanopoulos, M. Sulfidation of zinc titanate and zinc oxide solids. *Ind Eng Chem Res* 1992, 31, 1890-1899.
- (30) Ko, T.; Chu, H.; Chaung, L. The sorption of hydrogen sulfide from hot syngas by metal oxides over supports. *Chemosphere* 2005, 58, 467-474.
- (31) Gasper-Galvin, L.; Atimtay, A. T.; Gupta, R. P. Zeolite-supported metal oxide sorbents for hot-gas desulfurization. *Ind Eng Chem Res* 1998, 37, 4157-4166.

- (32) Kyotani, T.; Kawashima, H.; Tomita, A.; Palmer, A.; Furimsky, E. Removal of H<sub>2</sub>S from Hot Gas in the Presence of Cu-Containing Sorbents. *Fuel* 1989, 68, 74-80.
- (33) Bagreev A, Bandosz TJ: A role of sodium hydroxide in the process of hydrogen sulfide adsorption/oxidation on caustic-impregnated activated carbons. *Industrial and Engineering Chemistry Research* 2002;41:672
- (34) Bagreev A, Adib F, Bandosz TJ: pH of activated carbon surface as an indication of its suitability for H<sub>2</sub>S removal from moist air streams. *Carbon* 2001;39:1897.
- (35) Turk A, Sakalis E, Rago O, Karamitsos H. Activated carbon systems for removal of light gases. *Ann NY Acad Sci* 1992;661:221-7.
- (36) A, Mahmood K, Mozaffari J. Activated carbon for air purification in New York City's sewage treatment plants. *Water Sci Techn* 1993;27:121-6.
- (37) Bandosz TJ: Effect of pore structure and surface chemistry of virgin activated carbons on removal of hydrogen sulfide. *Carbon* 1999;37:483.
- (38) Davini P: Flue gas desulphurization by activated carbon fibers obtained from polyacrylonitrile by-product. *Carbon* 2003;41:277.
- (39) Li, Huixing, Selective catalytic oxidation of hydrogen sulfide from syngas, M.Sc thesis, university of Pittsburg, June 2008
- (40) <http://www.bza.org/zeolites.html>
- (41) Mer'kov, A.N.; Bussen, I.V.; Goiko, E.A.; Kul'chitskaya, E.A.; Men'shikov, Yu.P.; Nedorezova, A.P. Raite and zorite-new minerals from the Lovozero Tundra. *Zapiski Vsesoyuznogo Mineralogicheskogo Obshchestva*, 1973, 102, 54-62 (in Russian).
- (42) Kuznicki, S. M. *Large-Pored Crystalline Titanium Molecular Sieve Zeolites*; Patent US 4,853,202, 1989

---

(43) Anderson, M.W.; Terasaki, O. Structure of the microporous titanosilicate ETS-10, *Nature*, 367, 347-351, 1994

## Chapter 2

# Copper Exchanged Nanotitanate for High Temperature H<sub>2</sub>S Adsorption

This work was performed while the author was visiting Forschungszentrum Jülich, Institute of Energy and Climate Research, Jülich, Germany and working under supervision of *Dr. Michael Müller*, during May-July 2013

This chapter has been published in *Industrial and Engineering Chemistry Research*, 2014, 53, 11734-11739

**2-1- Abstract:**

The H<sub>2</sub>S breakthrough capacity of copper-exchanged Engelhard TitanoSilicate-2 (ETS-2) was measured at temperatures up to 950 °C and it was found that the adsorbent efficiency remains unchanged across the entire temperature range. Below 750 °C, the adsorption capacity at breakthrough is 0.7 moles of H<sub>2</sub>S per mole of copper while above 750 °C the capacity of the adsorbent is halved. The change in H<sub>2</sub>S capacity is due to Cu<sup>2+</sup> reduction by the H<sub>2</sub> which is formed through the thermal dissociation of H<sub>2</sub>S. The adsorbent shows good potential for use over a wide range of operating temperatures in H<sub>2</sub>S scrubbing processes.

**Keywords:** H<sub>2</sub>S, ETS-2, High temperature, Desulfurization, Copper oxide, Adsorption

**2-2. Introduction**

Hydrogen sulfide (H<sub>2</sub>S) is a highly odorous and toxic gas, which can be found in the majority of coal gasification plants, petrochemical industries and wastewater treatment plants.<sup>1</sup> H<sub>2</sub>S is known to severely poison catalytic systems. It takes ppm quantities of sulfur contaminants to reduce the lifetime of a supported metal catalyst to a few months or even a few weeks.<sup>2</sup>

Depending on the origin, coal can have between 0.1- 6 wt% sulfur content, which is released in the form of H<sub>2</sub>S during coal gasification processes and production of syngas for power generation using IGCC process.<sup>3, 4</sup> In IGCC syngas is produced by gasification of coal and it is later used as a fuel for the gas turbine and electricity generation. Syngas is also used to produce hydrogen in a process called water-gas shift reaction at temperatures between 250°C and 350 °C. However, to prevent serious poisoning of the water-gas shift catalyst and corrosion of the pipelines and equipment in IGCC, syngas should be free of H<sub>2</sub>S.<sup>5</sup>

Several commercial treatment techniques are commonly used to remove H<sub>2</sub>S, such as absorption in liquids (alkaloamines, ammonia solution, and alkaline salt solution), biological processes,<sup>6</sup> adsorption on activated carbon<sup>7</sup> and metal oxides,<sup>8</sup>

and separation by molecular sieves.<sup>9</sup> The disadvantage of most of these processes is the low operating temperatures which necessitates the cooling down and subsequent reheating of the hot gas produced from coal gasification. The system efficiency increases when high temperature desulfurization is used.<sup>10,11</sup>

Among different methods for H<sub>2</sub>S removal, adsorption on metal oxides has shown good potential for use at temperatures as high as 1500 °C. Oxides of many metals such as Fe, Cu, Zn, Co, W, Mo, Ca, Ba, and Sr are reported to be efficient adsorbents at high temperatures.<sup>12</sup>

Iron oxide is one of the first metal oxides to be used for H<sub>2</sub>S removal since 19<sup>th</sup> century.<sup>13</sup> Iron oxide when exposed to H<sub>2</sub>S forms iron sulfide which can be regenerated by air; the resulting SO<sub>2</sub> can be used in the Claus process to produce elemental sulfur.<sup>14</sup> After several regeneration cycles, the reactor will clog and has to be shut down for sulfur removal. Another disadvantage of using iron oxide adsorbents is that they are not capable of removing H<sub>2</sub>S to an absolute concentration below few hundreds parts per million and therefore, they have to be used in combination with another adsorbent to reach a level of less than 10 ppm.<sup>15</sup>

Copper oxides have also been reported to reduce H<sub>2</sub>S from several thousand ppm to sub ppm levels. However the disadvantage of copper oxide is that in the presence of a reducing agent (like H<sub>2</sub> and CO) in the gas stream Cu<sup>2+</sup> reduces to metallic copper lowering the sulfidation efficiency.<sup>16,17</sup>

In order to improve the adsorptive performance of metal oxides, strategies such as doping with other metals have been used. Recently a Ca-Ba -based sorbent was used to reach H<sub>2</sub>S concentration below 0.5 ppm at 800-900 °C.<sup>18</sup> Zinc ferrite was used as an adsorbent for H<sub>2</sub>S in coal gases at 538 °C.<sup>19</sup>

Mixed oxides of copper together with Cr, Ce, Al, Mg, Mn and Ti have also been investigated with CuCr<sub>2</sub>O<sub>4</sub> (CuO-Cr<sub>2</sub>O<sub>3</sub>) and CuCeO<sub>2</sub> found to be the most efficient adsorbents at temperatures as high as 850 °C.<sup>20</sup>

Li et al.<sup>21</sup> tested an CuO-CeO<sub>2</sub> adsorbent and reported an H<sub>2</sub>S reduction down to 5-10 ppm from a gas stream containing several thousand ppm at temperatures between 650-850 °C.

In order to enhance the utilization of the adsorbents and their H<sub>2</sub>S breakthrough capacities, the number of active sites has to increase. This can be achieved by substituting the metal oxide on the surface of different supports such as Al<sub>2</sub>O<sub>3</sub>, TiO<sub>2</sub>, SiO<sub>2</sub> and zeolites. Ko et al.<sup>10</sup> compared the H<sub>2</sub>S adsorption capacity of Mn, Fe, Cu, Co, Ce and Zn when supported on Al<sub>2</sub>O<sub>3</sub> in syngas at 500-700 °C. They reported 100% utilization for Mn-Al<sub>2</sub>O<sub>3</sub>. A result of substitution is the increased mechanical strength of the adsorbent, as reported by Gasper-Galvin et al.<sup>22</sup> when Cu, Mo and Mn were supported on SP-115 zeolite.

In this paper improvements were made to the support material using a high surface area nanotitanate Engelhard TitanoSilicate-2 (ETS-2) as the support and copper oxide as the active species. ETS-2 was first introduced by Kuznicki<sup>23</sup> and is a high surface area sodium nano-titanate with superior ion exchange capabilities formed by the alkaline digestion of TiO<sub>2</sub>. The caustic digestion converts the surface of the TiO<sub>2</sub> particles into sodium titanate, which is an effective ion-exchanger; particularly for transition metals.<sup>24</sup> The material has no measurable microporosity which makes it immune to pore blockage or capillary condensation.<sup>23,24</sup> Having no measurable microporosity, its surface area can be as high as 250 m<sup>2</sup>/g due to the nano-scale platelets. ETS-2 particles are on the order of 50 - 100 nanometers long. The core of these particles is presumed to be TiO<sub>2</sub> while the surface titania species carry a net negative charge which is offset by sodium ions.

ETS-2 has been demonstrated to be an effective support for transition metals and for removing trace levels of H<sub>2</sub>S at ambient temperature. In our previous study,<sup>24</sup> copper was exchanged onto the surface of ETS-2 and the H<sub>2</sub>S removal efficiency was measured at ambient temperature using a dynamic breakthrough system. Samples were pre-conditioned at various temperatures before testing and it was determined that at pre-treatment temperatures beyond 500 °C, the material underwent a structural change and lost the majority of its H<sub>2</sub>S capacity. The adsorption capacity of the samples, however, was always measured at ambient temperature. In the present study, the adsorption capacity of Cu-ETS-2 was measured at temperatures between 250 and 950 °C to understand whether the structural changes that occur as the adsorbent is heated beyond 500 °C limit the H<sub>2</sub>S

capacity of the adsorbent. Another goal was to understand the stability and the performance of Cu-ETS-2 as high temperature H<sub>2</sub>S adsorbent in a non-reductive environment at temperatures ranging from 250 to 950 °C.

### 2.3 Materials preparation

ETS-2 was hydrothermally synthesized according to a procedure published elsewhere<sup>23</sup> and was used as-made. ETS-2 is typically synthesized by addition of sources of titanium, silica, alkalinity and water. Solid TiO<sub>2</sub> is used as the source of titanium and sodium silicate (29% SiO<sub>2</sub>, 9% NaOH) as the source of silica.

Cu-ETS-2 was prepared by mixing the as-made ETS-2 with a copper nitrate solution. The weight proportion of adsorbent to copper salt and water was 1:2:100. The copper salt was first dissolved in water and ETS-2 was added afterwards. The amount of water used in our preparation is higher than the amount cited by Rezaei et al.<sup>24</sup> so that the suspension could be more easily stirred. The mixture was kept mixing at 80 °C for approximately 1 day. In the next step, the ion-exchanged sample was filtered and washed extensively with deionized water and dried in a vacuum oven at 60°C overnight. Prior to sulfidation experiments, a 10 g sample of the adsorbent was activated by heating to 500 °C under a static airflow in a furnace at 10 °C/min with an isothermal dwell of 2 hours.

### 2-4 Characterization

The crystal structure of the powders was analyzed by powder X-ray diffraction (XRD) using a BRUKER D4 Endeavor diffractometer (Bruker-AXS, Karlsruhe, Germany). The measurements were carried out with Cu K<sub>a</sub> radiation, a step size of 0.05° and a step time of 5 s. The acceleration voltage was 40 kV and the emission current was 40 mA. The computer program HighScore Plus (PANalytical, 2004) was used for phase identification of the samples.

The microstructure of the adsorbents was investigated by Scanning Electron Microscopy (SEM) using a Zeiss Ultra 55 device (Carl Zeiss NTS GmbH, Oberkochen, Germany).

High resolution TEM images were collected using Zeiss Libra (Fa. Carl Zeiss Microscopy, Oberkochen, Germany) 200 Cs (200 KeV) combined with an objective Cs corrector. The elemental analysis was carried out by energy-dispersive X-ray spectroscopy (EDX) using an INCA energy-dispersive X-ray analysis system (Oxford Instruments, Uedem, Germany). Point specific elemental analysis by the EDX detector attached to the SEM instrument was used to estimate the amount of copper atoms exchanged on the surface of ETS-2. Three separate spots (measuring a few hundred nm in size) were analyzed. Data was collected for the elements Na, Ti, Si, Cu, and O and the copper loading was calculated as the weight fraction of this combination of elements. The measured copper loading was identical within the sensitivity of the instrument for all spots measured.

For the mass spectrometry measurements a standard ABB Extrel mass spectrometer (Questor QGP) capable of detecting down to 100 ppb concentrations was used.

### **2-5 Experimental setup**

The experimental setup consists of a gas mixing unit, an electrical heated tube reactor furnace and mass spectrometer. To ensure the temperature uniformity, the furnace has 3 temperature zones with a total length of 600 mm. 1g of adsorbent was packed between plugs of quartz wool inside a heat resistant alumina tube with internal diameter of 6 mm. The tube was then placed inside the furnace and was fed by a continuous flow of 500 mL/min of He/ H<sub>2</sub>S mixture. The H<sub>2</sub>S concentration in the feed gas stream was 500 ppmv. The flow rates were controlled by electronic mass flow controllers.

The mass spectrometer was used to determine the H<sub>2</sub>S concentration at the exit of the adsorbent bed. The H<sub>2</sub>S concentration was monitored continuously during the experiment at 1 minute intervals. The breakthrough point was determined when the H<sub>2</sub>S concentration exceeded 5 ppmv and the adsorption experiments were stopped at exit concentration of 50 ppmv.

### **2-6. Results and discussion**

Figure 2-1 presents the electron microscopy graphs of ETS-2. It shows that the particles tend to form clusters. SEM analysis presented in Figure 2-1 a) shows that each cluster is almost 1 micron in size. TEM analysis presented in Fig. 1 b) shows each particle is typically between 50-100 nm long and almost 20 nm wide.

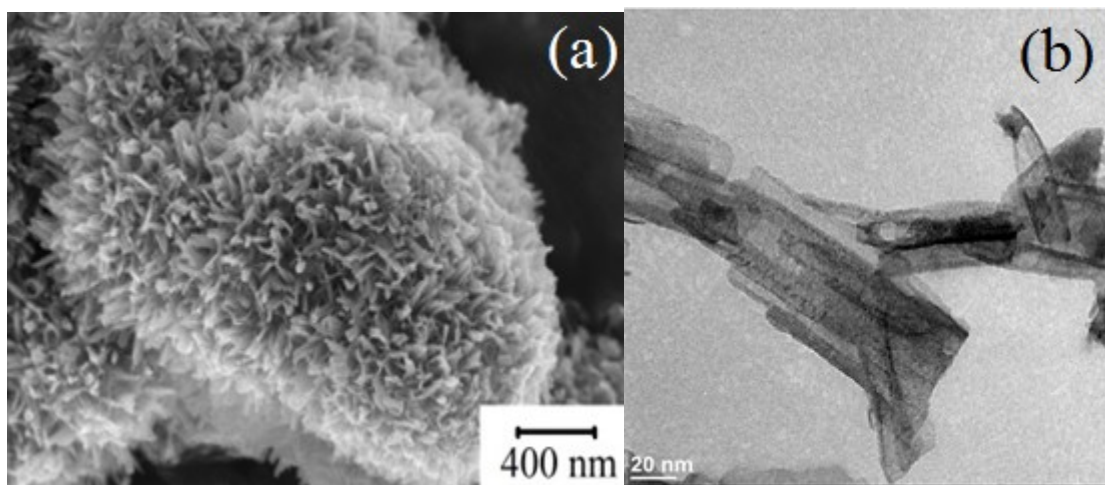


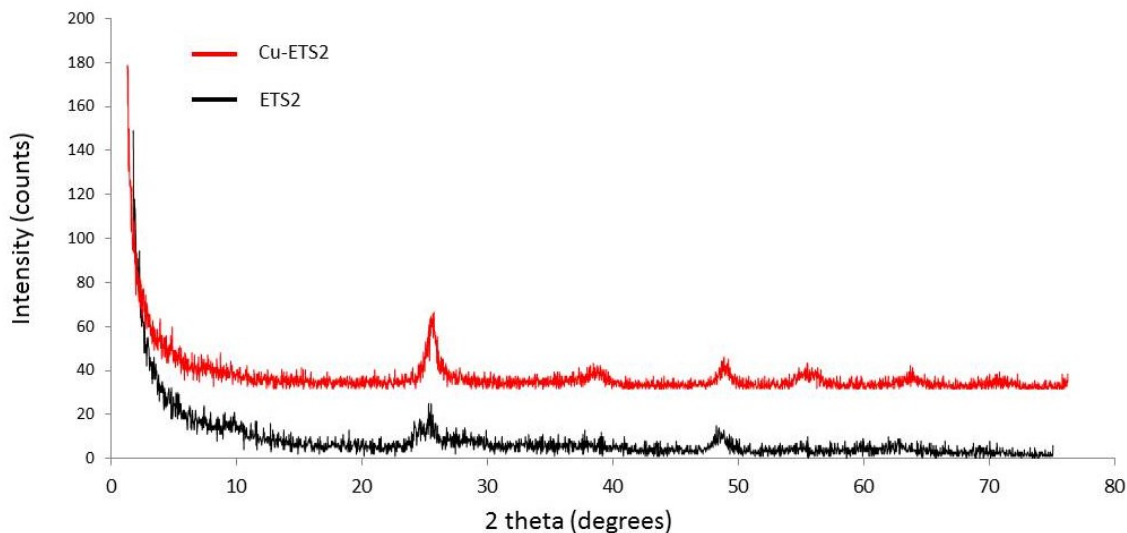
**Figure 2-1.** a) TEM and b) SEM images of nanotitanate ETS-2 showing the particle size and cluster structure.

The results of point specific EDX analysis (Table 1) indicated presence of about 7.5 atomic% (equivalent to 17 wt%) of copper on the sample.

**Table 2-1.** Point-specific EDX analysis of Cu-ETS-2 for 3 randomly selected points on the sample (values are in atomic%)

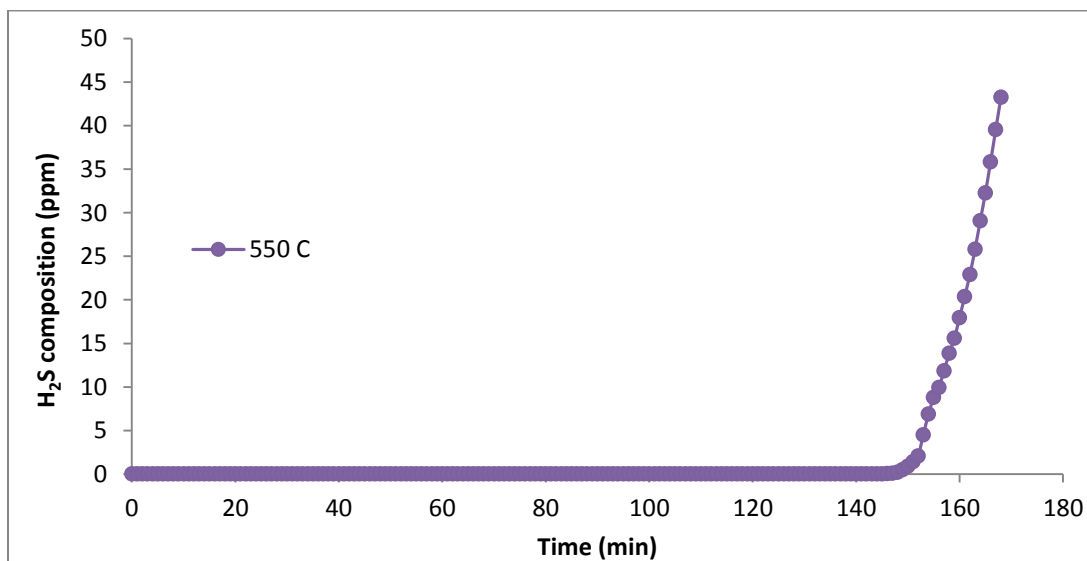
Elements Point number	Si	Ti	Cu	O
1	1.7	26.6	7.5	64.2
2	2.2	26.1	7.5	64.2
3	2	26.4	7.5	64.2

Figure 2-2 shows the XRD patterns of ETS-2 and Cu-ETS-2. ETS-2 pattern consists of broad peaks, which are characteristic of nano-scale particles of anatase.<sup>25</sup> The presence of these reflections is to be expected as only the surface of the particles have been converted to sodium titanate and the bulk of the particle is TiO<sub>2</sub>.



**Figure 2-2.** XRD patterns of ETS-2 and Cu-ETS-2.

The adsorbent was tested for H<sub>2</sub>S capacity at temperatures between 250 °C to 950 °C at 100 °C intervals. Figure 2-3 shows a typical adsorption breakthrough curve for Cu-ETS-2 at 550 °C. The inlet concentration of 500 ppmv H<sub>2</sub>S is effectively removed by the adsorbent as the concentration of H<sub>2</sub>S in the outlet is maintained below the detection limit of the instrument (100 ppbv) for a significant period of time. As time passes, the H<sub>2</sub>S concentration rises above baseline and the curve inflects as H<sub>2</sub>S “breaks through”.



**Figure 2-3.** Breakthrough curve for H<sub>2</sub>S adsorption by Cu-ETS-2 at 550 °C.

The concentration rises rapidly after breakthrough as a result of the adsorbent becoming saturated and having fewer sites with which to react with H<sub>2</sub>S. The capacity of the adsorbent is calculated by multiplying the mass flow rate of H<sub>2</sub>S into the bed by the time it takes for the outlet to show a concentration of 5 ppmv H<sub>2</sub>S. Figure 2-4 shows the breakthrough curves for different adsorption experiments carried out at varying temperatures to understand how this variable affects the capacity of the adsorbent.

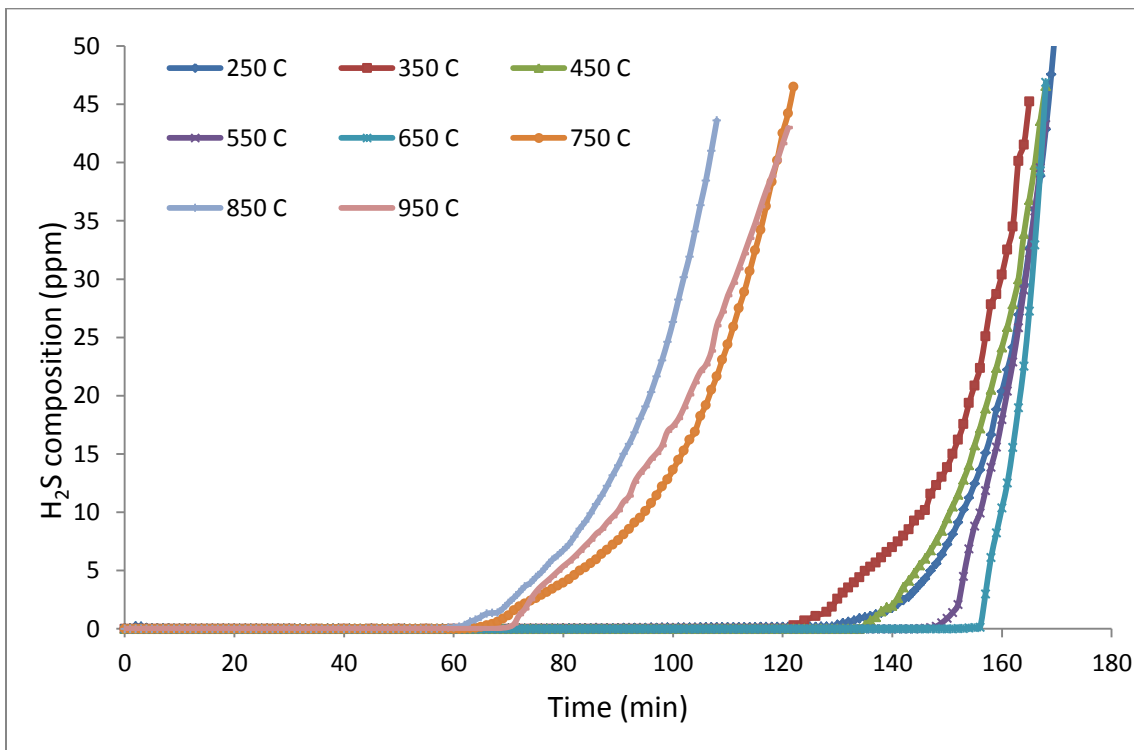


**Figure 2- 4.** Breakthrough curves for Cu-ETS-2.

The capacity of the adsorbent for H<sub>2</sub>S at different temperatures is presented in Figure 2-5. The H<sub>2</sub>S adsorption capacity is largely equivalent between 250 °C to 650 °C. As the temperature is increased to 750 °C, the adsorption capacity undergoes a step change and the adsorbent loses about half of its capacity. The capacity stays at nearly the same level up to 950 °C.

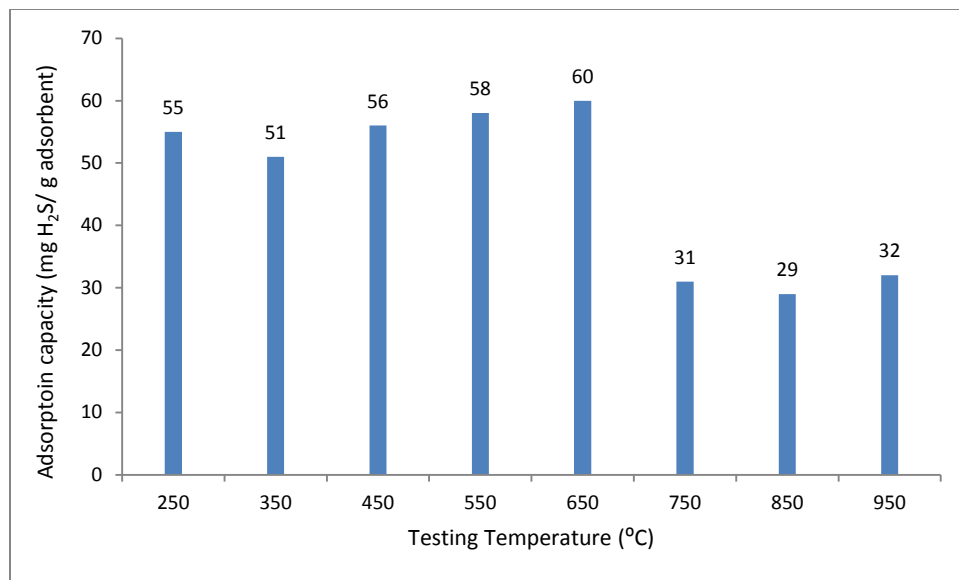


**Figure 2- 5.** Breakthrough capacities of Cu-ETS-2 at different temperatures.

In order to understand the reason for the sudden change, the adsorbent was characterized by XRD analysis after adsorption. The results are presented in Figure 2-6.

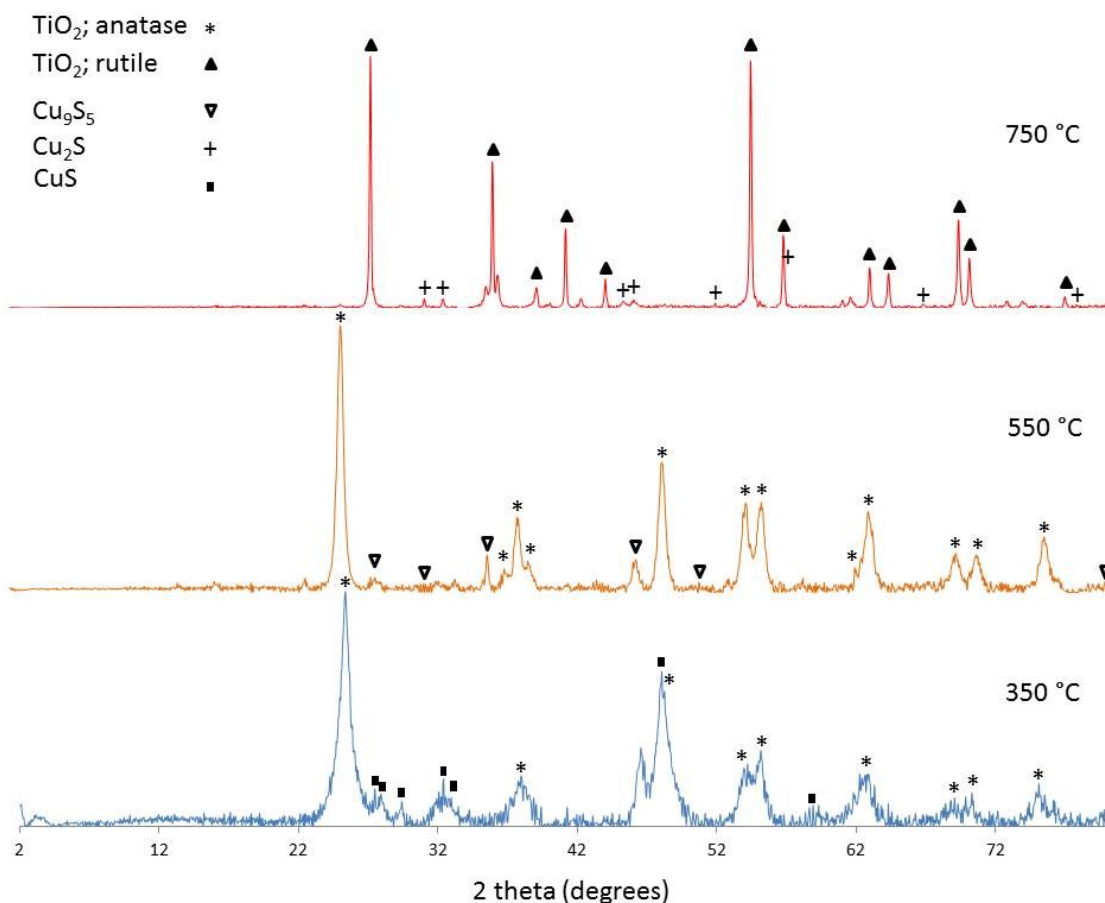


**Figure 2-6.** XRD patterns of Cu-ETS-2 after H<sub>2</sub>S adsorption at 350 °C, 550 °C and 750 °C.

The analysis results show that titania in the adsorbent becomes more crystalline at higher temperatures as evidenced by the growing intensity of the peaks and the sharpness of the reflections. At 350 and 550°C, TiO<sub>2</sub> is present in the form of tetragonal anatase while at 750 °C TiO<sub>2</sub> peaks are sharper still, and indicate a phase transformation to rutile.

The XRD results indicate the presence of predominantly CuS crystals at 350 °C and Cu<sub>2</sub>S at 750 °C. At 550 °C, new crystal morphology is also observed which indicates copper to sulfur ratios between 9:5 and 2:1 called digenite. According to literature,<sup>26</sup> digenite can be formed during copper sulfidations from temperatures as low as 80 °C (low digenite) up to 775 °C (high digenite). In our study digenite is presumed to have formed due to partial reduction of Cu<sup>2+</sup> at the same temperature range.

The change in copper sulfide species seen in the XRD patterns can be explained by a change in the oxidation state of copper and change in the adsorption mechanism due to the presence of hydrogen introduced by thermal dissociation of H<sub>2</sub>S. It has been established that at higher temperatures, H<sub>2</sub>S is dissociated into hydrogen and sulfur as indicated by reaction (1)<sup>27</sup>:



where S<sub>x</sub> indicates different allotropes of sulfur. On the basis of thermodynamic data, Barin and Knacke<sup>28</sup> suggested that at temperatures above 627 °C the reaction (1) can be written as:



According to Table 2, at temperatures up to 627°C, just a small amount of H<sub>2</sub>S is dissociated to form H<sub>2</sub>. In this region CuO is the predominant active species and adsorption is governed by the following reaction:



**Table 2-2.** Equilibrium concentration of hydrogen in decomposition of hydrogen sulfide under 1 atm (calculated) (27).

Temperature, °C	Equilibrium concentration, mol%
127	1.3×10 <sup>-3</sup>
227	6.1×10 <sup>-3</sup>
327	2.0×10 <sup>-2</sup>
427	4.8×10 <sup>-2</sup>
627	1.9
927	13.1
1127	25.6

As the temperature increases, the amount of hydrogen generated increases significantly (estimated to be 7 mol%) which, with an incoming stream of 500 ppmv H<sub>2</sub>S, must be enough to effectively reduce CuO to Cu as per equation (4)<sup>29</sup>:



Once in its metallic form, the copper sulfidation reaction proceeds as per equation (5):



The copper to sulfur stoichiometry in Equation (5) is half that compared to Equation (3). Thus, while the metal utilization may remain unchanged, the amount of sulfur that will be adsorbed scales with the oxidation state of the metal.

The observation that the adsorption capacity of Cu-ETS-2 does not change dramatically as a function of temperature is likely the result of a shift in the adsorption mechanism. The XRD patterns suggest a continual sintering process, evidenced by the increasing intensity of the titania peaks (Figure 2-6) compared to the starting material which might be expected to have a negative effect on the adsorption capacity.

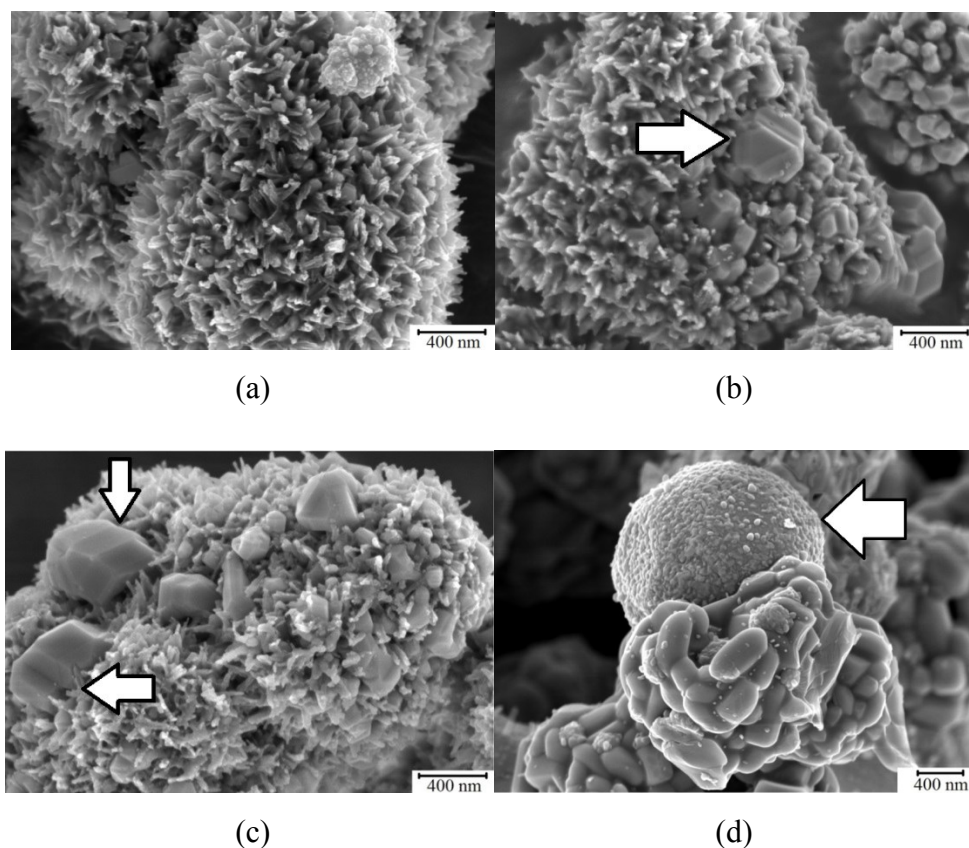


**Figure 2-7.** SEM images of Cu-ETS-2 after adsorption at: a) 350 °C, b) 550 °C, c) 750 °C and d) 950 °C.

The SEM images in Figure 2-7, however, clearly show a growth in the size of the copper sulfide crystals as the sulfiding temperature is increased. The growth of these crystals as a function of temperature suggests that the copper sulfide crystals behave as an active adsorption site. While Cu-ETS-2 may progressively sinter, which could lead to a loss of copper adsorption sites, the loss of these sites is compensated for by the growth of the copper sulfide crystals. The two effects apparently counter each other and provide for a relatively constant adsorption capacity under our test conditions.

### **2-7. Conclusions**

Cu-ETS-2 is found to be an efficient H<sub>2</sub>S adsorbent at temperatures suitable for direct desulfurization of gas streams. Under our test conditions, the H<sub>2</sub>S capacity for Cu-ETS-2 remains unchanged up to 650 °C after which a change in the oxidation state of copper causes a reduction in capacity. At breakthrough, 99% of the H<sub>2</sub>S has been removed and almost 0.7 moles of H<sub>2</sub>S per Cu is adsorbed below 750 °C, while above this temperature close to 0.35 mole H<sub>2</sub>S is adsorbed per mole Cu. The reduction in H<sub>2</sub>S adsorption capacity is due to the reduction of Cu<sup>2+</sup> in the presence of H<sub>2</sub> generated from thermally dissociated H<sub>2</sub>S.

### **2-8 Acknowledgments**

We thank Albana Zeko for her helpful comments on the manuscript, Dr. Egbert Wessel, Dr. D. Grüner, and Mr. M. Ziegner from Forschungszentrum Jülich GmbH for help in TEM, SEM, EDX, and XRD analyses. Financial support from the Initiative and Networking Fund of the Helmholtz Association (HGF) through the Helmholtz-Alberta Initiative is kindly acknowledged.

**2-9 References**

- (1) Gupta, R. P.; Turk, B. S.; Portzer, J. W.; Cicero, B. C. Desulfurization of Syngas in a Transport Reactor. *Environ. Prog.* **2001**, *20*, 187.
- (2) Bartholomew, C. H.; Agrawal, P. K.; Katzer, J. R. Sulfur Poisoning of Metals. *Adv. Catal.* **1982**, *31*, 135-242.
- (3) Stirling, D.; Clark, J. H.; Braithwaite, M. J. *Sulfur Problem - Cleaning up Industrial Feedstocks*; The Royal Chemical Society: Cambridge, 2000.
- (4) Bläsing, M., Müller, M. Release of Alkali Metal, Sulphur, and Chlorine Species from High Temperature Gasification of High- And Low-Rank Coals. *Fuel Process. Technol.* **2013**, *106*, 289.
- (5) Koryabkina, N. A.; Phatak, A. A.; Ruettinger, W. F.; Farrauto, R. J.; Ribeiro, F. H. Determination of Kinetic Parameters for the Water-Gas Shift Reaction on Copper Catalysts under Realistic Conditions for Fuel Cell Applications. *J. Catal.* **2003**, *217*, 233.
- (6) Jensen, A. B.; Webb, C. Treatment of H<sub>2</sub>S-Containing Gases: A Review of Microbiological Alternatives. *Enzyme Microb. Technol.* **1995**, *17*, 2.
- (7) Klein, J.; Henning, K. D. Catalytic Oxidation of Hydrogen Sulfide on Activated Carbons. *Fuel* **1984**, *63*, 1064.
- (8) Elseviers, W. F.; Verelst, H. Transition Metal Oxides for Hot Gas Desulphurization. *Fuel* **1999**, *78*, 601.
- (9) Melo, D. M. A.; De Souza, J. R.; Melo, M. A. F.; Martinelli, A. E.; Cachima, G. H. B.; Cunha, J. D. Evaluation of the Zinox and Zeolite Materials as Adsorbents to Remove H<sub>2</sub>S from Natural Gas. *Colloids Surf., A*: **2006**, *272*, 32.
- (10) Ko T. H.; Chu, H.; Chaung, L. K. The Sorption of Hydrogen Sulfide from Hot Syngas by Metal Oxides over Supports. *Chemosphere* **2005**, *58*, 467.

- (11) Müller, M. Integration of Hot Gas Cleaning at Temperatures above the Ash Melting Point in IGCC. *Fuel* **2013**, *108*, 37.
- (12) Westmoreland, P. R.; Harrison, D. P. Evaluation of Candidate Solids for High-Temperature Desulfurization of Low-Btu Gases. *Environ. Sci. Technol.* **1976**, *10*, 659.
- (13) Crynes, B. L. *Chemical Reactions as a Means of Separation: Sulfur Removal*; Marcel Dekker: New York, 1977.
- (14) Gollmer, H. A. in *Chemistry of Coal Utilization*; Lowry, H.H., Eds.; John Wiley & Sons: New York, 1945; pp947-1007.
- (15) Swisher, J. H.; Swerdtfeger, K.; Review of Metals and Binary Oxides as Sorbents for Removing Sulfur from Coal-Derived Gases. *JMEPEG* **1992**, *1*, 399.
- (16) Kyotani, T.; Kawashima, H.; Tomita, A. High Temperature Desulfurization with Copper-Containing Sorbents. *Environ. Sci. Technol.* **1989**, *23* (2), 218-223.
- (17) Patrick, V.; Gavalas, G. R. Structure and Reduction of Mixed Copper-Aluminum Oxide. *J. Am. Ceram. Soc.* **1990**, *73* (2), 358-369
- (18) Stemmler, M.; Tamburro, A.; Müller, M. Laboratory Investigations on Chemical Hot Gas Cleaning of Inorganic Trace Elements for the “UNIQUE” Process. *Fuel* **2013**, *108*, 31.
- (19) Ayala, R. E.; Marsh, D. W. Characterization and Long-Range Reactivity of Zinc Ferrite in High-Temperature Desulfurization Processes. *Ind. Eng. Chem. Res.* **1991**, *30*, 55.
- (20) Abbasian, J.; Hill, A. H.; Wangerow, J. R.; Flytzani-Stephanopoulos, M.; Bo, L.; Patel, C.; Chang, D. Development of Novel Copper-Based Sorbents for Hot-Gas Cleanup. *IGT-Final technical report to CRSC; IGT project No. 40330*, **1992**.
- (21) Li, Z.; Flytzani-Stephanopoulos, M. Cu-Cr-O and Cu-Ce-O Regenerable Oxide Sorbents for Hot Gas Desulfurization. *Ind. Eng. Chem. Res.* **1997**, *36*, 187.

- (22) Gasper-Galvin, L.; Atimtay, A. T.; Gupta, R. P. Zeolite-Supported Metal Oxide Sorbents for Hot-Gas Desulfurization. *Ind. Eng. Chem. Res.* **1998**, *37*, 4157.
- (23) Kuznicki, S. M. *Large-Pored Crystalline Titanium Molecular Sieve Zeolites*; Patent US 4,853,202, 1989.
- (24) Rezaei, S.; Tavana, A.; Sawada, J.; Junaid, A.; Kuznicki, S. M. Novel Copper-Exchanged Titanosilicate Adsorbent for Low Temperature H<sub>2</sub>S Removal. *Ind. Eng. Chem. Res.* **2012**, *51*, 12430.
- (25) Yogamalar, R.; Srinivasan, R.; Vinu, A.; Ariga, K. X-ray Peak Broadening analysis in ZnO Nanoparticles. *Solid state Commun.* **2009**, *149*, 1919–1923.
- (26) Donnay, G.; Donnay, J. D. H.; Kullerud, G. Crystal Structure of Digenite, Cu<sub>9</sub>S<sub>5</sub>. *Am. Mineral.* **1958**, *43*, 228-242.
- (27) Fukuda, K.; Dokiya, M.; Kameyana, T.; Kotera, Y. Catalytic Decomposition of Hydrogen Sulfide. *Ind. Eng. Chem. Res.* **1978**, *17*, 243-248.
- (28) Barin, I.; Knacke, O. *Thermochemical Properties of Inorganic Substances*; Springer-Verlag: Berlin, 1973.
- (29) Patrick, V.; Gavalas, G. R.; Flytzani-Stephanopoulos, M.; Jothimurugesan, K. High Temperature Sulfidation-Regeneration of CuO-Al<sub>2</sub>O<sub>3</sub> Sorbents. *Ind. Eng. Chem. Res.* **1989**, *28*, 931-940.

## Chapter 3

# Cu-Cr-O Functionalized ETS-2 Nanoparticles for Hot Gas Desulfurization

This work was performed while the author was visiting Forschungszentrum Jülich, Institute of Energy and Climate Research, Jülich, Germany and working under supervision of *Dr. Michael Müller*, during May-July 2013

This chapter has been published in *Journal of Nanoscience and Nanotechnology*, 2015, 15, xx-xx

### 3-1 Abstract

Engelhard Titanium Silicate -2 (ETS-2), a sodium nanotitanate, was surface functionalized by ion exchanging the solid with copper and chromium ions. The ability of this bi-metallic adsorbent to remove H<sub>2</sub>S at elevated temperatures was assessed using a dynamic breakthrough system and contrasted against an analogous mixed metal oxide, Cu-Cr-O. Unlike Cu-Cr-O, the H<sub>2</sub>S capacity for CuCr-ETS-2 remains unchanged from 350°C up to 950 °C. Using ETS-2 as a support for the metals increased the adsorbents surface area and improved its sulfur capacity from 35 mg H<sub>2</sub>S/g for Cu-Cr-O to 61 mg H<sub>2</sub>S/g adsorbent for CuCr-ETS-2. The consistent presence of Cu<sub>9</sub>S<sub>5</sub> on the sulfided adsorbents suggests that chromium effectively stabilizes the copper against reduction to metallic copper up to temperatures as high as 950 °C.

**Keywords:** H<sub>2</sub>S, ETS-2, CuCr<sub>2</sub>O<sub>4</sub>, High temperature, Desulfurization, Adsorption

### 3-2. Introduction

Coal constitutes the largest portion of the world's fossil fuel resources and, each year, provides around one third of world's electricity requirement.<sup>1</sup> One of the challenges in the energy conversion industry is to extract energy from coal with the minimum environmental impact. Sulfur is a key contaminant that must be removed in order to facilitate more efficient conversion processes.<sup>2,3</sup> IGCC or Integrated Gasification Combined Cycle is a clean and efficient process to lower the environmental impact of using coal for the purpose of power generation.<sup>4</sup> In an IGCC system, carbonaceous feedstock is gasified to produce syngas.<sup>5</sup> Depending on the origin, coal may contain different amounts of sulfur components, which is released in the form of H<sub>2</sub>S during gasification.<sup>6,7</sup> The H<sub>2</sub> content of the syngas is increased through water-gas shift reaction at temperatures ranging from 200 °C up to 450 °C depending on the catalyst.<sup>8-10</sup> The longevity of different catalysts in this reaction is limited by their sensitivity to sulfur poisoning. As a result, production of H<sub>2</sub>S free syngas is of high importance.<sup>11,12</sup>

Different treatment techniques are used for H<sub>2</sub>S removal, among which are adsorption by activated carbon, incineration or catalytic combustion, condensation, chemical oxidation and wet absorption.<sup>13,14</sup> The disadvantage of most of these processes is that they operate at, or near ambient temperature, which necessitates cooling down the hot gas produced from coal gasification and subsequently reheating it prior to the water-gas shift process.<sup>1,13,15</sup>

Activated carbon has low capacity for high temperature H<sub>2</sub>S adsorption from gas streams, but using it as a support with certain metal oxides has increased the capacity in hot gas cleanup in an IGCC system. The breakthrough time, when zinc impregnated carbon is used, approached that of the best metal oxides. In addition, it is cheaper and unlike CuO and ZnO it retains its activity in temperatures lower than 550°C.<sup>13,16,17</sup>

Metal oxide-based H<sub>2</sub>S adsorbents such as oxides of iron, copper, zinc, manganese, cerium, calcium and tin have been studied for high temperature applications.<sup>18-21</sup> Among different metal oxides, zinc oxide was believed to possess the best qualities like high diffusion rate and high H<sub>2</sub>S adsorption. Copper oxides have attracted much attention to substitute zinc oxide adsorbents because they have lower vapor pressure, making them non-volatile at high temperatures, and also possess the highest sulfidation equilibrium constant.<sup>22</sup> In the presence of a reducing agent like H<sub>2</sub>, however, CuO reduces to Cu<sub>2</sub>O and eventually to elemental copper, which increases the solid diffusion resistance due to sintering and sulfide formation of onion-like dense layers.<sup>23,24</sup>

To avoid formation of onion-like sulfide structures different studies sought to disperse the metals on a support material such as alumina (Al<sub>2</sub>O<sub>3</sub>), titania (TiO<sub>2</sub>), silica (SiO<sub>2</sub>), and chromia (Cr<sub>2</sub>O<sub>3</sub>). Kyotani et al.<sup>25</sup> studied different copper oxides and showed that impregnation of CuO on zeolite and on SiO<sub>2</sub> led to adsorbents having higher copper utilization compared to when CuO was used as a pure metal oxide. At sulfidation temperatures between 500–700°C Ko et al.<sup>24</sup> studied metal oxides including Zn, Cu, Fe, Mn, Co and Ce supported on  $\gamma$ -Al<sub>2</sub>O<sub>3</sub> and investigated

their H<sub>2</sub>S removal performance. They achieved an adsorption capacity as high as 29 mg sulfur/g adsorbent and the results showed Mn and Cu had the best performance.

In recent years, several studies exploring mixed metal oxides have showed superior properties in comparison to single metal oxides. Studies of different copper oxides such as Cr<sub>2</sub>O<sub>3</sub>-Al<sub>2</sub>O<sub>3</sub>, MgO- Al<sub>2</sub>O<sub>3</sub>, TiO<sub>2</sub>- Al<sub>2</sub>O<sub>3</sub> and CuFe<sub>2</sub>O<sub>4</sub> or CuAl<sub>2</sub>O<sub>4</sub> have shown that the reduction of CuO at high temperatures was slower in comparison to pure CuO in metal oxide compounds.<sup>26, 27</sup> Other oxides, such as MgO, TiO<sub>2</sub>, and CeO<sub>2</sub> do not form compounds or oxide solid solutions with CuO due to immiscibility of certain metal oxides at high temperatures. Instead, they might be used as dispersants of copper.<sup>27, 28</sup> Abbasian et al.<sup>29</sup> evaluated several copper-based mixed compounds and showed that the H<sub>2</sub>S removal capacity of Cu-Cr-O with surface area of 3 m<sup>2</sup>/g exceeds that of elemental copper at temperatures around 650 °C.<sup>29</sup> The work to date suggests that mixed copper and chromium oxides possess the highest thermodynamic stability and the slowest reduction rate of all oxide compounds of copper. Binary oxides of CuO-Cr<sub>2</sub>O<sub>3</sub> and Cu-CeO<sub>2</sub> have also been studied. The presence of stable CuCr<sub>2</sub>O<sub>4</sub> in CuO-Cr<sub>2</sub>O<sub>3</sub> solids is believed to preserve copper in Cu<sup>2+</sup> or Cu<sup>+</sup> oxidation form. Preserving the oxidation state of copper is important for H<sub>2</sub>S removal because if the copper oxide reduces to elemental copper the H<sub>2</sub>S adsorption will decrease, as sulfidation equilibrium constant for copper oxide is ten orders of magnitude higher than that of metallic copper.<sup>22, 27</sup>

In this paper, a high surface area nanotitanate, Engelhard Titanium Silicate -2 (ETS-2) was used as a metal support to create an analogous metal titanate comparable to the bi-metal oxide Cu-Cr-O. ETS-2 was first introduced by Kuznicki<sup>30</sup> and is a high surface area (up to 300 m<sup>2</sup>/g), non-porous sodium nanotitanate formed by the alkaline digestion of titania. The caustic treatment converts the surface of the titania nanoparticles to sodium titanate which is a powerful ion exchanger, particularly for transition metals.<sup>31,32</sup> The core of the ETS-2 particles is presumed to be TiO<sub>2</sub> while the surface titania species carry a net negative charge which is offset by sodium ions. The surface area of ETS-2 is derived entirely from the scale of its nano-platelets. ETS-2 particles are on the order of 50-100

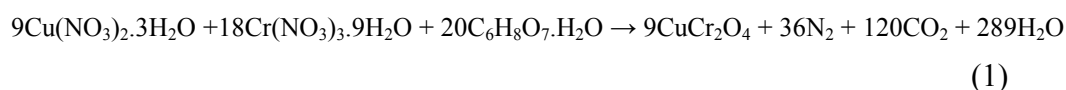
nanometers long and almost 20 nm wide. The lack of microporosity makes ETS-2 non-susceptible to pore blockage or capillary condensation.<sup>33,34</sup> Cu-exchanged ETS-2 has been demonstrated to be effective at removing trace levels of H<sub>2</sub>S at ambient temperature.<sup>31</sup>

### 3.3 Adsorbent preparation

Two adsorbents were prepared: ETS-2 functionalized with copper and chrome, and the copper/chrome oxide CuCr<sub>2</sub>O<sub>4</sub>. Both adsorbents were tested for H<sub>2</sub>S removal from an inert gas stream at temperatures ranging from 350 to 1100 °C.

ETS-2 was synthesized according to the literature.<sup>30, 31</sup> It was hydrothermally synthesized from a mixture of titanium and silica, a source of alkalinity and water. Solid TiO<sub>2</sub> was used as the source of titanium while sodium silicate (29% SiO<sub>2</sub>, 9% NaOH) was the source of silica.

Copper (II) nitrate trihydrate (Cu(NO<sub>3</sub>)<sub>2</sub>·3H<sub>2</sub>O), chromium(III) nitrate nonahydrate, (Cr(NO<sub>3</sub>)<sub>3</sub>·9H<sub>2</sub>O) and citric acid were all purchased from Sigma-Aldrich and used as received. Spinel copper chromite (CuCr<sub>2</sub>O<sub>4</sub>) was synthesized according to literature.<sup>35-37</sup> Target masses of Cu(NO<sub>3</sub>)<sub>2</sub>·3H<sub>2</sub>O and Cr(NO<sub>3</sub>)<sub>3</sub>·9H<sub>2</sub>O were dissolved in distilled water to achieve a stoichiometric ratio of Cu:Cr = 1:2:



Citric acid was added as an 18:5 molar ratio to nitrate ions. The temperature was kept at 50 °C while stirring vigorously. Then the temperature was increased and further kept at 80 °C until a transparent and viscous gel was attained. The remaining viscous gel was heated up to 130 °C for 3 hours until a foamy dark powder was formed. The powder was activated in air at 10 °C/min to 650 °C and held isothermally for two hours.

To introduce copper and chromium to ETS-2, the same synthesis procedure was followed. As the viscous gel was formed, ETS-2 was added to the gel and the

mixture was kept under mixing overnight at 80 °C. During this time the desired ions substitute on the surface of ETS-2 through ion-exchange process. The ion-exchanged ETS-2 was then filtered out of the mixture washed by deionized water and dried overnight in a vacuum oven at 60 °C. The adsorbent was later heated in a furnace under air atmosphere to 500 °C at a rate of 10 °C/min. The sample was maintained at 500 °C for 2 hours.

### **3-4 Characterization**

The crystal structure of the powders was analyzed by powder X-Ray Diffraction (XRD) using a BRUKER D4 Endeavor Diffractometer (Bruker-AXS, Karlsruhe, Germany). The measurements were carried out with Cu K<sub>a</sub> radiation with a step size of 0.01° and time interval of 0.5 s. The acceleration voltage and emission current were equal to 40 kV and 40 mA, respectively. The computer program HighScore Plus (PANalytical, 2004) was used to evaluate the composition of the sample.

The microstructure of the adsorbents was investigated by Scanning Electron Microscopy (SEM) using a Zeiss Ultra 55 device (Carl Zeiss NTS GmbH, Oberkochen, Germany).

High-resolution Transmission Electron Microscope (TEM) images were collected using Zeiss Liba (Fa. Carl Zeiss Microscopy, Oberkochen, Germany) 200 Cs (200 KeV) combined with an objective Cs corrector.

The elemental analysis was carried out by Energy-Dispersive X-ray spectroscopy (EDX) using an INCA energy-dispersive X-ray analysis system (Oxford Instruments, Uedem, Germany).

For the mass spectrometry measurements a standard ABB Extrel mass spectrometer (Questor QGP) capable of detecting down to 100 ppb concentrations was used.

### **3-5 Experimental Setup**

The adsorption test system consists of a gas blending unit, an electrically heated tube reactor furnace and a mass spectrometer. 1 g of the adsorbent was packed between plugs of quartz wool inside a heat resistant alumina tube with an internal diameter of 6 mm. The tube was then placed inside a high temperature furnace and was fed by a continuous flow of 500 ml/min of He/H<sub>2</sub>S mixture. The H<sub>2</sub>S concentration in the feed gas stream was 500 ppmv. The flow rates were controlled by electronic mass flow controllers.

Exit H<sub>2</sub>S concentration was monitored continuously during the experiment at 1 minute intervals. The breakthrough point was determined when the H<sub>2</sub>S concentration exceeded 1 ppmv and the adsorption experiments were stopped at exit concentration of 30 ppmv. Adsorption experiments were performed at different temperatures starting from 350 °C up to 1100 °C.

### 3-6. Results and Discussion

SEM analysis of ETS-2 revealed that the needle-like titania nanocrystals tend to form clusters, typically few micrometers in size. Figure 3-1 shows the clusters of titanate particles that are about 1 micron in size together with TEM image showing each particle is typically between 50-100 nm long and almost 20 nm wide.

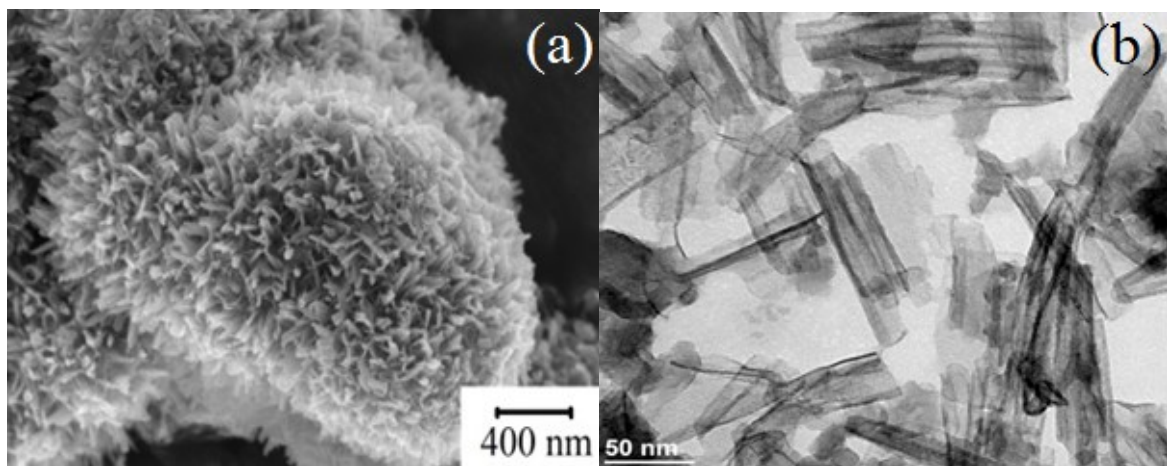


**Figure 3-1.** SEM (a) and TEM (b) images of nanotitanate ETS-2.

SEM images of CuCr-ETS-2 in Figure 3-2 show no dramatic change in the morphology of the nanotitanate particles after the ion exchange and activation process.

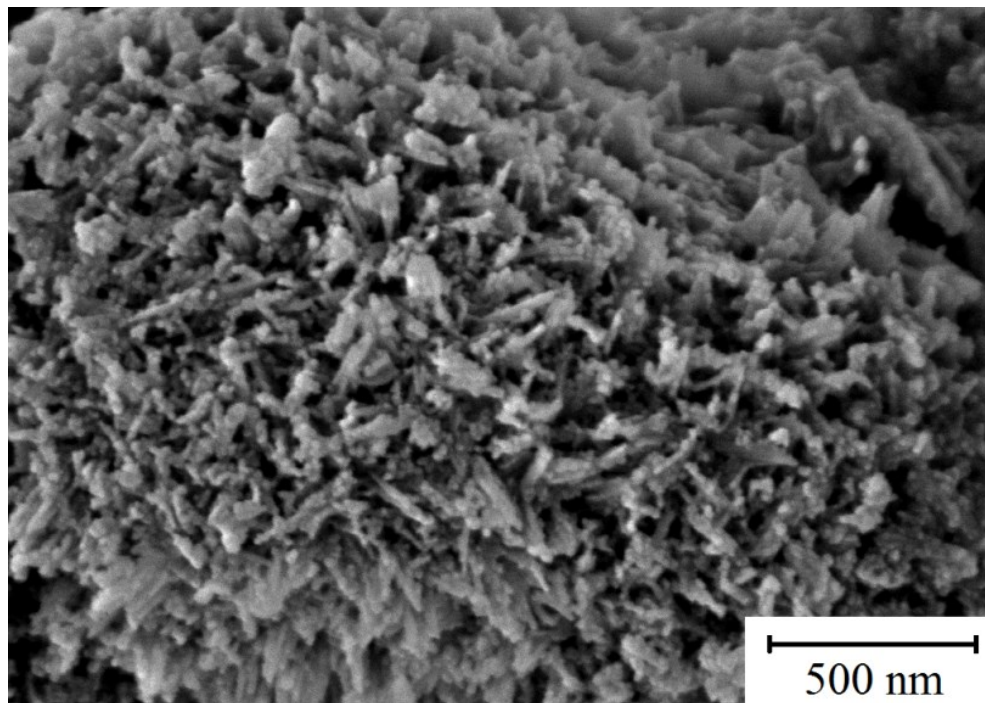


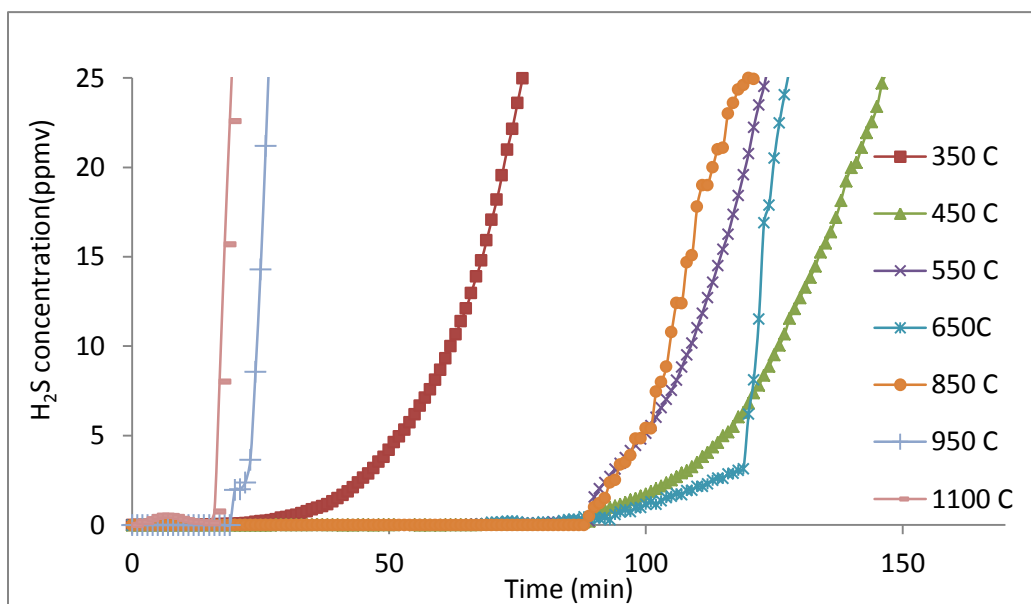
**Figure 3-2.** SEM images of CuCr-ETS-2 before adsorption.

EDX analysis was performed on CuCr-ETS-2 before adsorption to observe the elements on the adsorbent. The result demonstrates the existence of five elements; titanium, chromium, copper, silicon and oxygen.  $\text{TiO}_2$  and  $\text{SiO}_2$  are base components of ETS-2 while chromium and copper are ion exchanged on the surface.

### 3-6-1 Spinel Cu-Cr-O

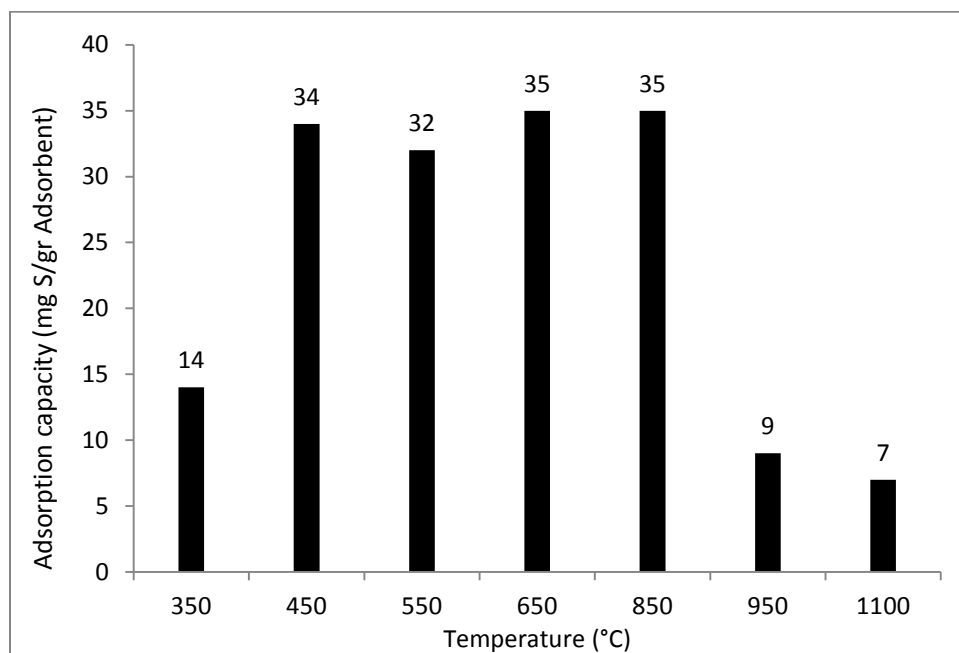
Single adsorption experiments were performed on the adsorbent at temperatures as low as 350 °C up to 1100 °C with 100 °C intervals. In a typical adsorption experiment, the  $\text{H}_2\text{S}$  concentration in the exit gas stream is almost zero until a certain time, after which it starts to rise and then increases rapidly. The time of the abrupt change of slope in the  $\text{H}_2\text{S}$  concentration is called the breakthrough time.

Figure 3-3 shows the breakthrough curves for the adsorbent at different temperatures. The results are presented in terms of ppmv of H<sub>2</sub>S in the exit stream versus time. The further the profile is shifted to the right, the higher the capacity of the adsorbent. It can be seen that for temperatures from 450 °C to 850 °C the adsorbent was capable of removing the H<sub>2</sub>S from 500 ppmv (in the feed) to concentrations below the detection limit of approximately 100 ppbv for up to 90 minutes.



**Figure 3-3:** Breakthrough curves for H<sub>2</sub>S adsorption on Cu-Cr-O from a 500 ppmv mixture of H<sub>2</sub>S and He with a flow rate of 500 ml/min at different temperatures.

According to Figure 3-4, Cu-Cr-O is an effective H<sub>2</sub>S adsorbent at elevated temperatures. While different studies have studied the adsorbent for H<sub>2</sub>S removal at temperatures between 600°C to 800°C,<sup>22, 26, 29</sup> it has not been tested for lower temperatures. In our experiments, the adsorbent has higher capacity at temperatures ranging from 450 °C to 850 °C with a maximum capacity 35 mg H<sub>2</sub>S/mg adsorbent. Our results indicate at temperatures below 450 °C and above 850 °C the adsorption capacity is considerably lower.



**Figure 3-4:** Breakthrough capacities of Cu-Cr-O at different temperatures as measured in 1 ppmv H<sub>2</sub>S in the exit gas.

### 3-6-2 CuCr-ETS-2

The adsorption capacity and breakthrough times for CuCr-ETS-2 were obtained using the same test system and under the same conditions as described in the previous section. A stream of gas with 500 ppmv H<sub>2</sub>S content was used. Adsorption tests were conducted at temperatures from 350 °C to 1100 °C. The results are shown in Figure 3-5.

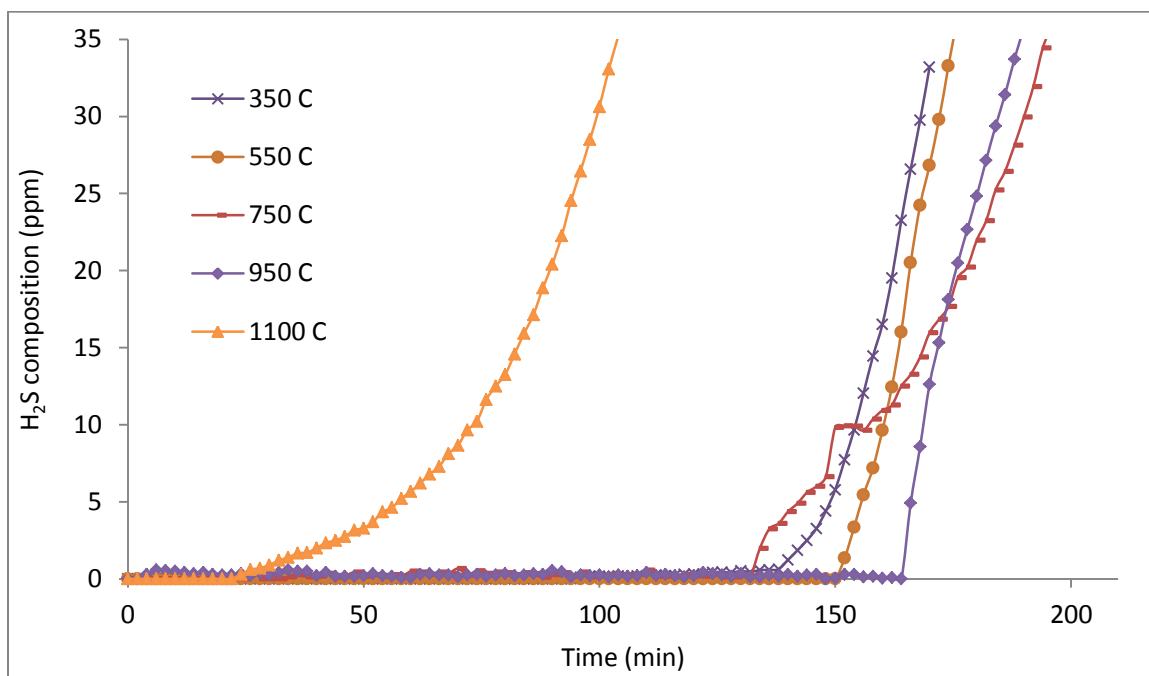


**Figure 3-5:** Breakthrough curves for CuCr-ETS-2 from a 500 ppmv mixture of H<sub>2</sub>S and He with a flow rate of 500 ml/min at different temperatures.

Unlike Cu-Cr-O, CuCr-ETS-2 maintains the high adsorption capacity at temperatures as low as 350 °C up to 950 °C. This behavior makes CuCr-ETS-2 a good candidate for a wide range of desulfurization applications from low temperature water-gas shift to near combustion-temperature gas streams. A comparison between the two adsorbents shows an increase in the adsorption capacities from 35 mg H<sub>2</sub>S/g adsorbent for the Cu-Cr-O to about 60 mg/g adsorbent for Cu-Cr-ETS-2.

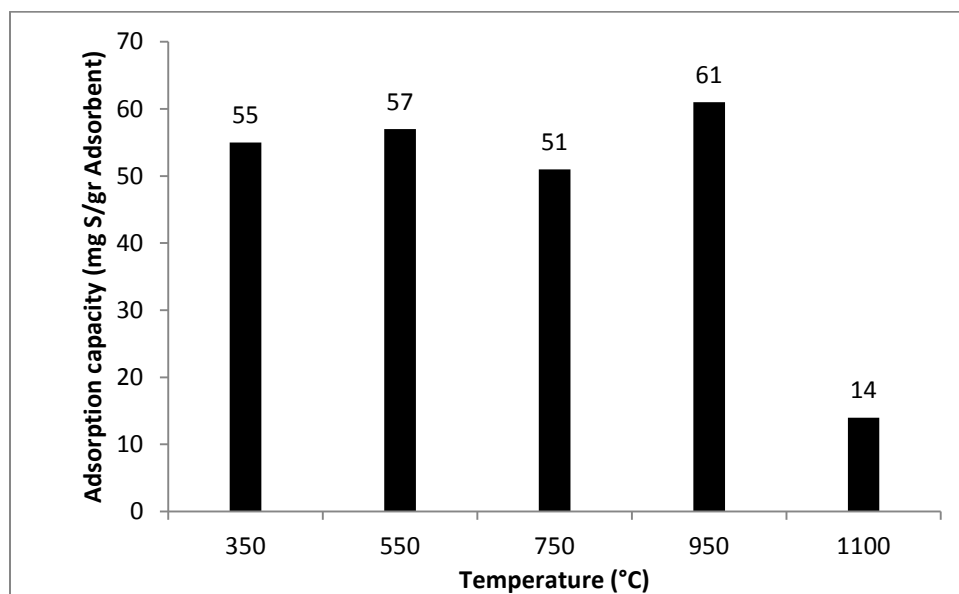
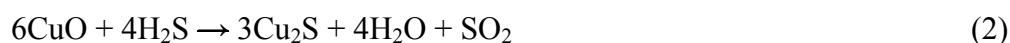


**Figure 3-6:** Breakthrough capacities of CuCr-ETS-2 at different temperatures.

The reaction of our adsorbent with H<sub>2</sub>S in an inert atmosphere should follow one of the following mechanisms. CuCr-ETS-2 may react directly with the H<sub>2</sub>S to form a copper sulfide and water. The stability of the measured adsorption capacity of CuCr-ETS-2 over a wide temperature range could be due to the ability of chromium to stabilize copper against complete reduction by H<sub>2</sub>, which is formed through the autothermal dissociation of H<sub>2</sub>S at high temperatures.<sup>38</sup>

It is also possible that the adsorbent undergoes a reaction with H<sub>2</sub>S given by reaction (2).<sup>39</sup>



The initial reaction in the sequence that combines to produce Eq. 2 has CuO reduced to Cu<sub>2</sub>O with the production of SO<sub>2</sub> and H<sub>2</sub>. The H<sub>2</sub> produced in this reaction could risk reducing the copper oxide to copper metal at elevated temperatures. The stability of CuCr-ETS-2's adsorption capacity suggests that the chromium in the adsorbent stabilizes the oxidation state of copper and prevents its reduction to metal. We have tested, under the same conditions, Cu-ETS-2 with no chromium and found that the capacity of the adsorbent is not stable across as wide a temperature range as when chromium is added.

According to Yasyerli and Flytzani<sup>22,38</sup> different copper sulfides will form during adsorption of H<sub>2</sub>S on Cu<sub>2</sub>O with copper to sulfur ratios between 1.8 (digenite) to 2 (chalcocite). XRD analysis of the adsorbent after adsorption shows formation of the same species. At lower temperatures (350 °C and 550 °C), Cu<sub>9</sub>S<sub>5</sub> (digenite) with a copper to sulfur ratio of 1.8 was the only detected copper sulfide species. As the temperature increases to 750 °C, Cu<sub>2</sub>S starts to form together with Cu<sub>9</sub>S<sub>5</sub> and at 950 °C and 1100 °C, Cu<sub>2</sub>S is the only detected copper sulfide species. XRD data, showing almost the same copper to sulfur ratio, are in good agreement with the calculated H<sub>2</sub>S adsorption capacity of the adsorbent (Figure 3-6), as the capacity does not significantly change at different temperatures. Having comparable adsorption capacities throughout the whole temperature range suggests the existence of the same reaction stoichiometry at different temperatures. The presence of chromium on the adsorbent is believed to be the reason, as it keeps copper in the Cu<sup>2+</sup> or Cu<sup>+</sup> oxidation state.<sup>22</sup> In our experiments, taking into account the copper to sulfur ratio indicated by XRD analysis, the oxidation state has been kept constant at +1 throughout the whole temperature range, in good agreement with Eq. (2).

Figure 3-7 shows the SEM micrographs of CuCr-ETS-2 after adsorption testing at 350, 550, 750, and 950 °C. As the images show, two visually different crystals have been formed on the surface of adsorbent. At lower temperatures (e.g. 550 °C) almost all the copper sulfide crystals are pseudo hexagonal, which according to XRD analysis are Cu<sub>9</sub>S<sub>5</sub> (digenite). At 750 °C, both pseudo hexagonal and card-like structures are observed. Card-like structures represent Cu<sub>2</sub>S (chalcocite). At 950 °C all the observed sulfides are card-like structures, which are Cu<sub>2</sub>S according to XRD analysis. Figure 3-8 shows that at 1100 °C the adsorbent undergoes widespread sintering which is believed to explain the dramatic loss in H<sub>2</sub>S capacity observed at this temperature.

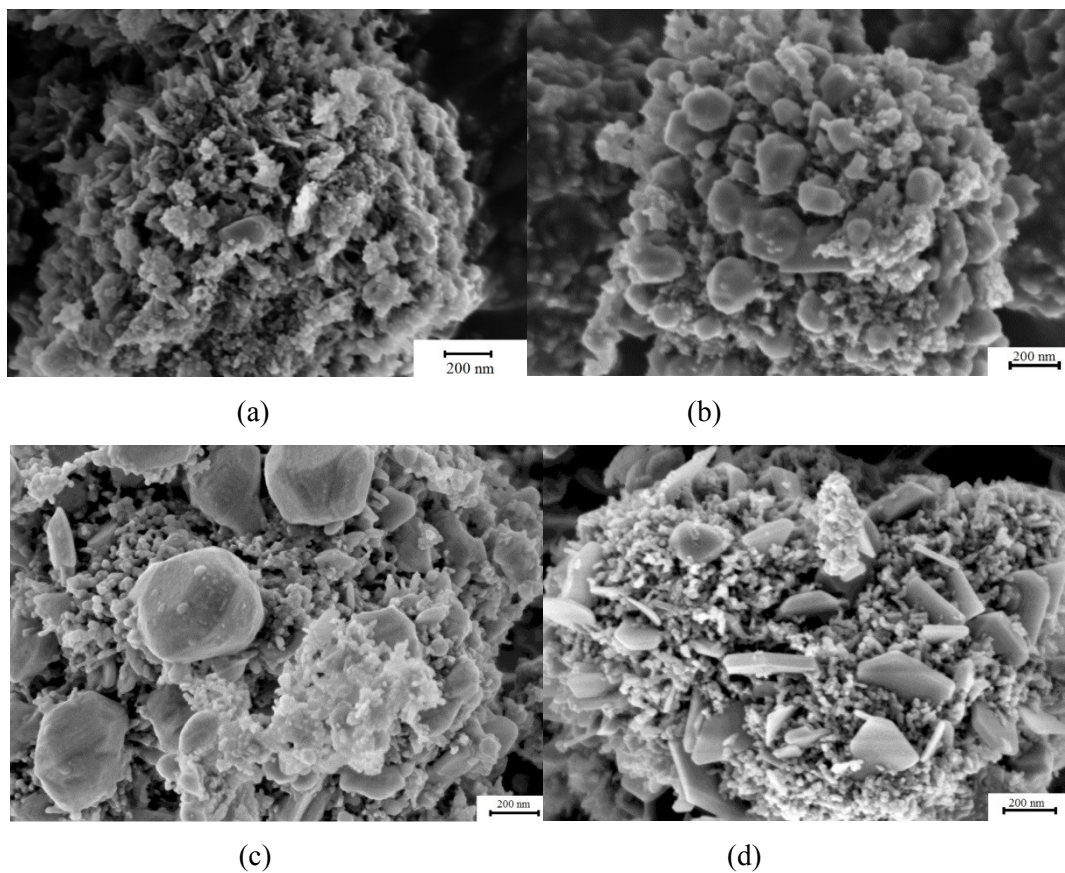


**Figure 3-7.** SEM images of CuCr-ETS-2 at: a) 350 °C, b) 550 °C, c) 750 °C and d) 950 °C.

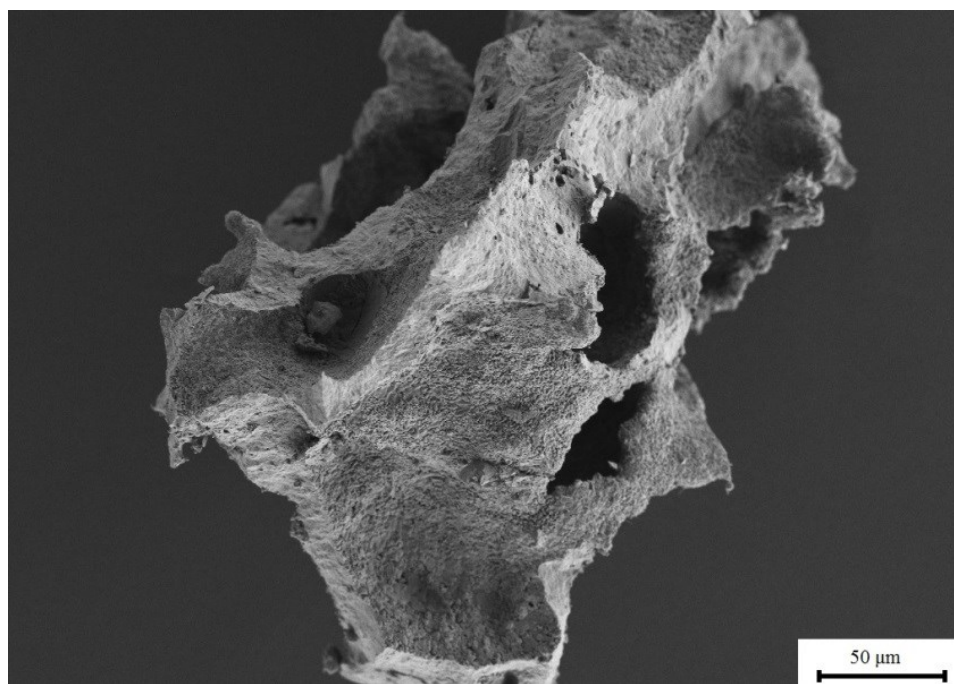


**Figure 3-8.** SEM image of CuCr-ETS-2 at 1100 °C.

XRD analysis (Figure 3-9) also reveals a morphology change in the titania as the temperature is increased. At lower temperatures, (350 °C), the dominant titania phase is anatase while at 750 °C peaks of rutile appear. At 950 °C rutile is the only form of  $\text{TiO}_2$  in the adsorbent. The change in morphology has no apparent effect on the sulfur capacity of the adsorbent.

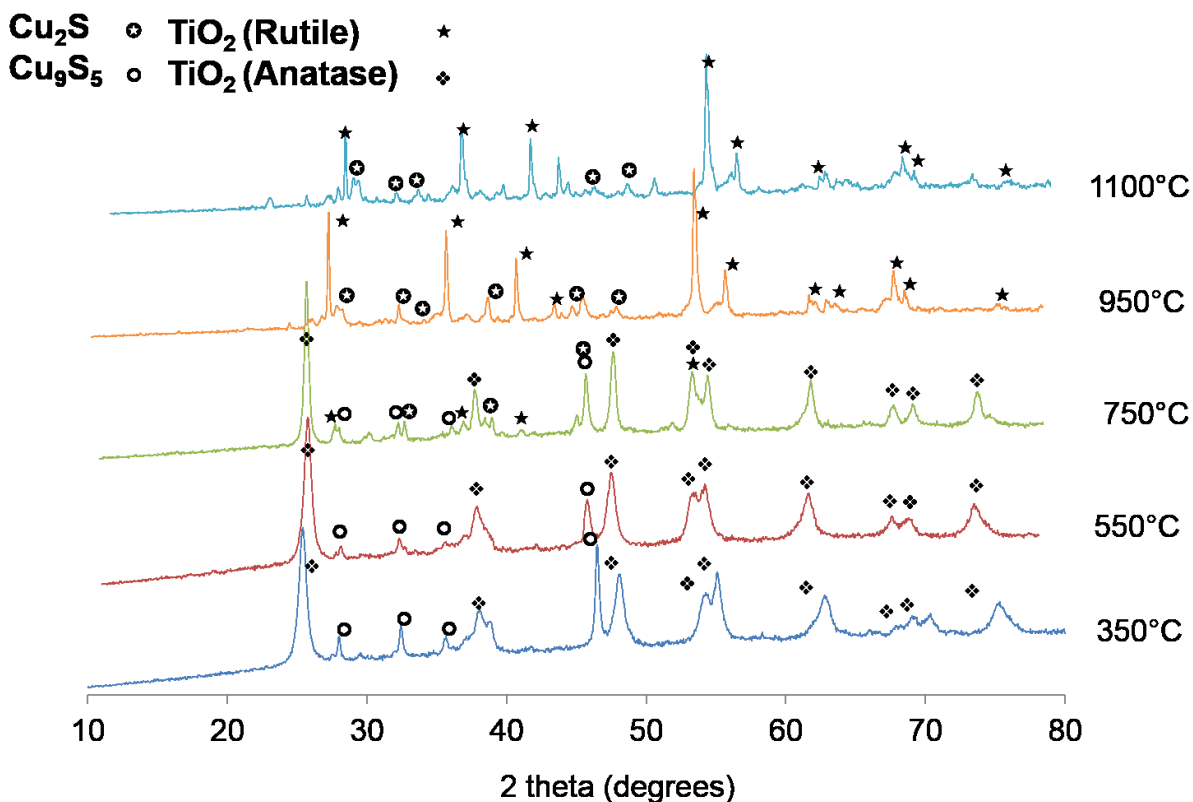


Figure 3-9: XRD patterns of CuCr-ETS-2 after adsorption at different temperatures.

### 3-7- Conclusions

$\text{H}_2\text{S}$  removal directly from a syngas stream is needed to maximize efficiency of IGCC systems and for any process using metal catalysts susceptible to sulfur poisoning. The Cu-Cr-O mixed-metal oxide adsorbent system was adapted by dispersing copper and chromium oxides on the surface of ETS-2 via ion exchange. The  $\text{H}_2\text{S}$  breakthrough testing showed that CuCr-ETS-2 has twice the sulfur capacity compared to Cu-Cr-O for temperatures between 450°C to 850°C. CuCr-ETS-2 also

has a wider temperature range and maintains its sulfur capacity between 350 and 950 °C making the same adsorbent equally good for both low and high temperature desulfurization. The presence of  $\text{Cu}_9\text{S}_5$  in the sulfided adsorbent strongly suggests that the chromium is able to stabilize oxidation state of copper at +1.

### 3-8 Acknowledgments

We thank Albana Zeko for her helpful comments on the manuscript, Dr. Egbert Wessel, Dr. D. Gruner, and Mr. M. Ziegner from Forschungszentrum Julich GMBH for help in TEM, SEM, EDX and XRD analyses. Financial support from the Canada research Chair in Molecular Sieve Nanomaterials, Helmholtz-Alberta Initiative and network fund of the Helmholtz Association (HGF) is kindly acknowledged.

### 3-9 References

- (1) M. Müller, *Fuel* 108, 37 (2013)
- (2) L. Fenouil, G. Towler and S. Lynn, *Ind. Eng. Chem. Res.* 33(2), 265 (1994)
- (3) N. A. Khan, H. Zubair and H. J. Sung, *Adv. Porous Mater.* 1(1), 91 (2013)
- (4) M. Müller, D. Pavone, M. Rieger and R. Abraham, 4th International Conference on Clean Coal Technologies, Dresden, Germany, May (2009)
- (5) J. W. Portzer, J. R. Albritton, C. C. Allen, R. P Gupta. *Fuel process. Technol.* 85(6), 621 (2004)
- (6) D. Stirling, J. H. Clark and M. J. Braithwaite, *Sulfur Problem - Cleaning up Industrial Feedstock*, The Royal Chemical Society, Cambridge, (2000)
- (7) M. Bläsing and M. Müller, *Fuel Process. Technol.* 106, 289 (2013)
- (8) D. S. Newsome, *Catal. Rev.* 21(2), 275 (1980)
- (9) C. Rhodes, G. J. Hutchings and A. M. Ward, *Catal. Today* 23(1), 43 (1995)

- (10) M. Stemmler and M. Müller, *Biomass. Bioenerg.* 35, S105 (2011)
- (11) P. Hou, D. Meeker and H. Wise, *J. Catal.* 80(2), 280 (1983)
- (12) G. Ma, Y.Hou, X. Han, and Z. Huang. *Energy Environm. Focus.* 3(1), 74 (2014)
- (13) M. P. Cal, B. W. Strickler and A. A. Lizzio, *Carbon* 38(13), 1757 (2000)
- (14) R. C Hansford, R. H. Hass and H. Hennig, U.S. Patent No. 4,088,743. 9 May (1978)
- (15) T. Ko, H. Chu and L. Chuang, *Chemosphere.* 58, 467 (2005)
- (16) J. J. Park, C. G. Park, S. Y Jung, S. C. Lee, D. Ragupathy and J. C. Kim, *Nanoelectron. Optoelectron.* 6(3), 306 (2011)
- (17) J.J. Park, S.Y. Jung, C.Y. Ryu, C.G. Park, J.N. Kim, and J.C. Kim. *J. Nanoelectron. Optoelectron.* 5(2), 222 (2010)
- (18) Y. Motoo and E. Furimsky, *Ind. Eng. Chem. Process. Des. Dev.* 24(4), 1165 (1985)
- (19) Y.Zeng, S. Zhang, F. R. Groves, and D. P. Harrison. *Chem. Eng. Sci.* 54(15), 3007 (1999)
- (20) S. K. Gangwal, in *Proceedings of the 3rd International Symposium and Exhibition: High-Temperature Gas Cleaning*, University of Karlsruhe, Karlsruhe, Germany (1996), p. 489.
- (21) J. S. Yong, S. C. Lee and J. C. Kim. *J. Nanoelectron. Optoelectron.* 7(5), 536 (2012)
- (22) L. Zhijiang and M. Flytzani-Stephanopoulos, *Ind. Eng. Chem. Res.* 36(1), 187 (1997)
- (23) M. Flytzani-Stephanopoulos, G. R. Gavalas, S. S. Tamhankar and P. K. Sharma, Final Report to DOE, DOE/MC/ 20417-1898, (1985)

- (24) G. Sick and K. Schwerdtfeger, *Metall. Trans. B.* 18(3), 603 (1987)
- (25) T. Kyotani, H. Kawashima, A. Tomita, A. Palmer and E. Furimsky, *Fuel.* 68(1), 74 (1989)
- (26) M. Flytzani-Stephanopoulos, G. R. Gavalas, and S. S. Tamhankar, U.S. Patent No. 4,729,889 (1988)
- (27) P. Valerle and G. Gavalas, *J. Am. Ceram. Soc.* 73(2), 358 (1990)
- (28) A. T. Atimtay and D. P. Harrison, eds. *Desulfurization of hot coal gas.* No. 42. Springer, (1998)
- (29) J. Abbasian, A. H. Hill, J. R. Wangerow, M. Flytzani-Stephanopoulos, L. Bo, C. Patel and D. Chang, IGT-Final Technical Report to CRSC; IGT Project No. 40330, (1992)
- (30) S. M. Kuznicki, Patent US4853202, (1989)
- (31) S. Rezaei, A. Tavana, J. A. Sawada, L. Wu, A.S. Junaid and S. M. Kuznicki, *Ind. Eng. Chem. Res.* 51(38), 12430 (2010)
- (32) M. Shi, C.C. Lin, L. Wu, C. Holt, D. Mitlin and S. M. Kuznicki. *J. Nanosci. Nanotechnol.* 10(12), 8448 (2010)
- (33) B. Tanchuk, J. A. Sawada and S. M. Kuznicki, *AIChE J.* 59(12), 4727 (2013)
- (34) A. Tavana, *Characterization of Copper Supported on Titanosilicates for Room Temperature H<sub>2</sub>S Adsorption.* MSc thesis, University of Alberta, Edmonton (2012)
- (35) Q. Geng, X. Zhao, X. Gao, S. Yang and G. Liu, *J. Sol-Gel. Sci. Techn.* 61(1), 281 (2012)
- (36) W. Li and H. Cheng, *J. Cent. South Univ. T.* 14, 291 (2007)
- (37) A. M. Kawamoto, L. C. Pardini and L.C. Rezende. *Aerosp. Sci. Technol.* 8, 591 (2004)

(38) K. Fukuda, M. Dokiya, T. Kameyana, Y. Kotera, *Ind. Eng. Chem. Res.* 17, 243 (1978)

(39) S. Yasyerli, G. Dogu and I. Ar, *Ind. Eng. Chem. Res.* 40(23), 5206 (2001)

## Chapter 4

# Effect of moisture on high temperature H<sub>2</sub>S adsorption on Cu-ETS-2

This chapter has been submitted for publication in *Journal of Nanoscience and Nanotechnology*

#### 4-1 Abstract

The removal of H<sub>2</sub>S at combustion temperatures can be accomplished using metal oxides which react and sequester H<sub>2</sub>S as a metal sulfide. Cu-ETS-2 is an ion-exchangeable titanate which has been modified to hold about 17 wt% copper supported on its surface. Cu-ETS-2 has previously been shown to be an effective adsorbent for removing hydrogen sulfide from dry, inert gas streams at temperatures as high as 950 °C. This study measured the influence of water vapor on the H<sub>2</sub>S adsorption capacity of Cu-ETS-2 using an inert stream containing 500 ppm H<sub>2</sub>S and 10 vol% H<sub>2</sub>O. The results demonstrate that the presence of water vapor reduces the capacity of the adsorbent at temperatures greater than 350 °C. The loss in capacity can be explained by an unexpected increase in the amount of H<sub>2</sub> present in the humid gas stream at elevated temperatures.

Keywords: H<sub>2</sub>S adsorption; Hydrogen sulfide; ETS-2; High temperature; Copper oxide; Desulfurization; Effect of water

#### 4-2. Introduction

Integrated gasification combined cycle (IGCC) power systems are appealing due to the potential to achieve higher efficiency and cleaner power from a variety of fuel sources, including coal. The synthesis gas produced from gasification contains CO, CO<sub>2</sub>, CH<sub>4</sub> and H<sub>2</sub> and, due to presence of sulfur in most coals, H<sub>2</sub>S is present in quantities ranging from 0.1 to 6 wt% <sup>1</sup>. The H<sub>2</sub>S generated during the gasification reaction needs to be removed from the syngas to prevent corrosion concerns with the system equipment and to protect catalysts downstream of the gasifier.

After exiting the gasifier, syngas typically undergoes a catalytic water-gas shift (WGS) reaction at temperatures between 250 and 450°C to generate additional hydrogen by using steam to convert CO to CO<sub>2</sub>. H<sub>2</sub>S can rapidly poison the WGS catalysts and thus must be removed to a level below at least 20 ppmv before being

introduced to the WGS process<sup>2</sup>. Several treatment options exist for removing H<sub>2</sub>S from syngas streams, including chemisorption on solid adsorbents, catalytic combustion, chemical oxidation, and absorption in liquids<sup>3, 4</sup>. Most of the techniques, however, are operated at temperatures lower than the gasifier temperature which requires the syngas to be cooled down prior to desulfurization and subsequently reheated before being introduced into the water-gas shift reaction<sup>3, 5</sup>. An ideal H<sub>2</sub>S adsorbent for an IGCC system would be able to desulfurize the syngas stream without requiring the gas to be cooled or dehumidified. As a result, adsorbents capable of adsorbing H<sub>2</sub>S at temperatures greater than 500°C have become of growing interest.

Different metal oxides have been used for the purpose of H<sub>2</sub>S removal from high temperature gas streams<sup>6-8</sup>. Among them, zinc oxide has been shown to have high hydrogen sulfide adsorption capacity and suitable diffusion rate<sup>9, 10</sup>, however ZnO sinters at temperatures around 700°C and thus has a limiting thermal stability. Copper oxide has appealing thermodynamics at higher adsorption temperatures and has been the subject of a number of investigations<sup>5, 11-13</sup>. However, the existence of hydrogen in the gasification stream leads to the rapid reduction of CuO to Cu<sub>2</sub>O and eventually to elemental copper; a sequence of events which increases the solid diffusion resistance due to sintering and the formation of onion-like, dense layers of copper<sup>14-16</sup>. Metallic copper has a sulfidation equilibrium constant 10 orders of magnitude lower than CuO or Cu<sub>2</sub>O<sup>17</sup> which renders it ineffective as an adsorbent.

Gasification streams also contain a significant amount of water ranging from 5 to 50 vol%<sup>18</sup>. One study showed, for H<sub>2</sub>S streams having a range of humidity, the presence of moisture in the gas stream can dramatically lower the adsorption capability of H<sub>2</sub>S for a Cu-impregnated activated carbon<sup>19</sup>. Huang et al attributed the loss in adsorption capacity partially to competitive adsorption from water on the surface of the carbon as well as to the reduction of Cu(II) to Cu(I) in the presence of water. The breakthrough measurements, however, were carried out at 303K and so the results of this study do not necessarily predict the behaviour of such systems at or near combustion temperatures.

Previous work by the authors examined copper-exchange ETS-2 (Cu-ETS-2) for high temperature (250°C -950°C) H<sub>2</sub>S removal<sup>20</sup>. ETS-2 was first reported by Kuznicki in 1989<sup>21</sup> and is prepared through the caustic digestion of TiO<sub>2</sub>, which converts the surface titania groups to sodium titanate. ETS-2 is non-porous yet, due to the size of the individual platelets, can have a BET surface area as high as 300m<sup>2</sup>/g. ETS-2 particles composed of a TiO<sub>2</sub> core covered with charged, titanate groups are on the order of 50-100 nm long and 20 nm wide<sup>22</sup>. Cu-ETS-2 is prepared through simple ion exchange of the substrate with an aqueous solution of a copper salt. The previous testing used a dry stream containing 500 ppm H<sub>2</sub>S in He. The results demonstrated that Cu- ETS-2 had a consistent sorption capacity of between 50 and 60 mg H<sub>2</sub>S/g<sub>(Cu-ETS-2)</sub> which was reduced by half at temperatures above 750 °C<sup>20</sup>.

In this work Cu-ETS-2 was challenged by blending 11 vol% water with the 500 ppm H<sub>2</sub>S (balance He) stream. The water loading was selected as typical of the syngas composition before the water gas shift reaction (WGSR)<sup>23</sup>. Breakthrough profiles for a number of gases were collected simultaneously at temperatures ranging from 250°C to 950°C to understand the difference, if any, in H<sub>2</sub>S adsorption capacity under dry and humid conditions. It was elected to explore pure Cu-ETS-2 as opposed to a bi- or tri-metallic form of the adsorbent to isolate the influence of steam on the reaction of H<sub>2</sub>S with copper oxide.

### 4-3 Materials preparation

ETS-2 was synthesized hydrothermally using an alkaline source, solid, nano-particulate TiO<sub>2</sub>, and sodium silicate (29% SiO<sub>2</sub>, 9%NaOH) as based on the previous methods reported in the literature<sup>20, 24</sup>. Copper-exchanged ETS-2 was similarly prepared as reported previously<sup>22</sup> by ion-exchanging of slurry of solid ETS-2 mixed with copper nitrate solution using the weight proportions of 1:2:100 for adsorbent to salt and water respectively. The slurry was stirred at 80 °C for approximately 24 hours. Afterwards the ion exchanged sample was filtered and washed with deionized water and dried in a vacuum oven overnight at 60 °C. Prior to the adsorption

experiments, the Cu-ETS-2 adsorbent was activated in air by heating it to 500 °C in a muffle furnace at 10 °C/min with an isothermal dwell of two hours.

#### 4-4 Characterization

Powder X-ray Diffraction (XRD) Analysis:

A BRUKER D4 Endeavor X-ray diffractometer (Bruker-AXS, Karlsruhe, Germany) was used to collect the powder X-ray diffraction patterns. The measurements were carried out using Cu K $\alpha$  radiation, a step size of 0.01° and a step time of 0.5 s. The acceleration voltage was 40 kV and the emission current was 40 mA. The computer program HighScore Plus (PANalytical, 2004) was used to evaluate the composition of the sample.

Scanning Electron Microscope (SEM):

Zeiss Ultra 55 device (Carl Zeiss NTS GmbH, Oberkochen, Germany) Scanning Electron Microscopy (SEM) has been used to study the microstructure of the adsorbents.

Transmission Electron Microscope (TEM):

Samples in powder form were dispersed in methanol in an ultrasonic bath for 10 min. One or two drops of each of these suspensions were then placed on a Carbon Type B, Au grid (300 mesh) and dried prior to analysis. The image was taken by a JEOL 2010 and JEOL 2100 with Lab6 filament transmission electron microscopes.

Mass Spectrometry:

The gas species present in the exhaust stream of the reactor were sampled using a Pfeiffer Omnistar GSD 320 with QMA 200 residual gas analyzer has been used. Fragments at  $m/z = 2, 34, 48,$  and  $64$  were tracked using a 500 ms sampling time and an electron multiplier voltage of 800 C to monitor the relative concentrations of H<sub>2</sub>, H<sub>2</sub>S and SO<sub>2</sub> in the exhaust stream.

#### 4-5 Humidification and Reactor Configuration

A Bronkhorst CEM (controlled evaporator mixer) system was used to humidify the H<sub>2</sub>S stream. The CEM system uses separate gas flow and a liquid flow controllers to meter specified amounts of each component into a heated evaporator-mixer that was maintained at 110 °C. The humid stream exiting the CEM was fed through a heat-traced tube (similarly maintained at 110 °C) to a quartz tube reactor placed in an electrically heated furnace. The CEM system can provide both dry and humidified gas and for the humidified experiments 500 sccm of gas was blended with 0.052 ml/min of liquid water to generate a stream that was 11 vol% steam. This water loading corresponds, roughly, to a gas stream at 50 °C and 100% relative humidity.

Figure 4-1 shows a schematic of the reactor system used in the experiments. For every run, 0.5 g of adsorbent was packed between two plugs of quartz wool in the center of an 8 mm (ID) quartz tube. The sample was first equilibrated under 500 sccm helium for 5 minutes before the three-way valve was switched to the start an equal flow of dilute H<sub>2</sub>S. The same sequence was used for the humidified experiments where both He and H<sub>2</sub>S/He mixtures were humidified to the same level. The gas stream exiting the adsorbent bed was passed through a condenser to knock out excess water before being sampled by the quartz capillary connected to the mass spectrometer to analyze the composition. The H<sub>2</sub>S concentration was determined at 3 second intervals and the breakthrough point was defined as when the concentration of H<sub>2</sub>S exceeded 1% of its maximum concentration. When the concentration of the gas approached the inlet gas concentration the experiments were stopped.

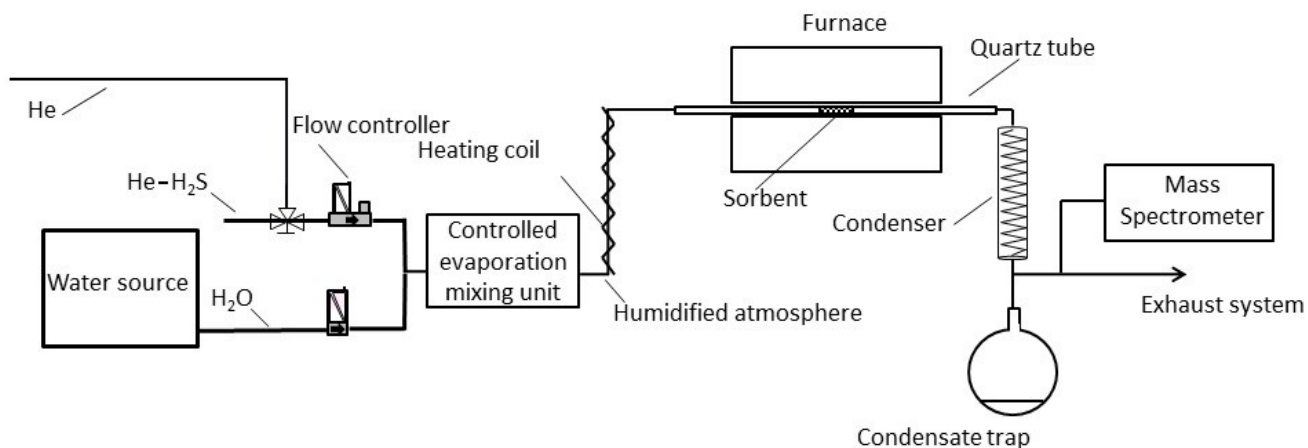
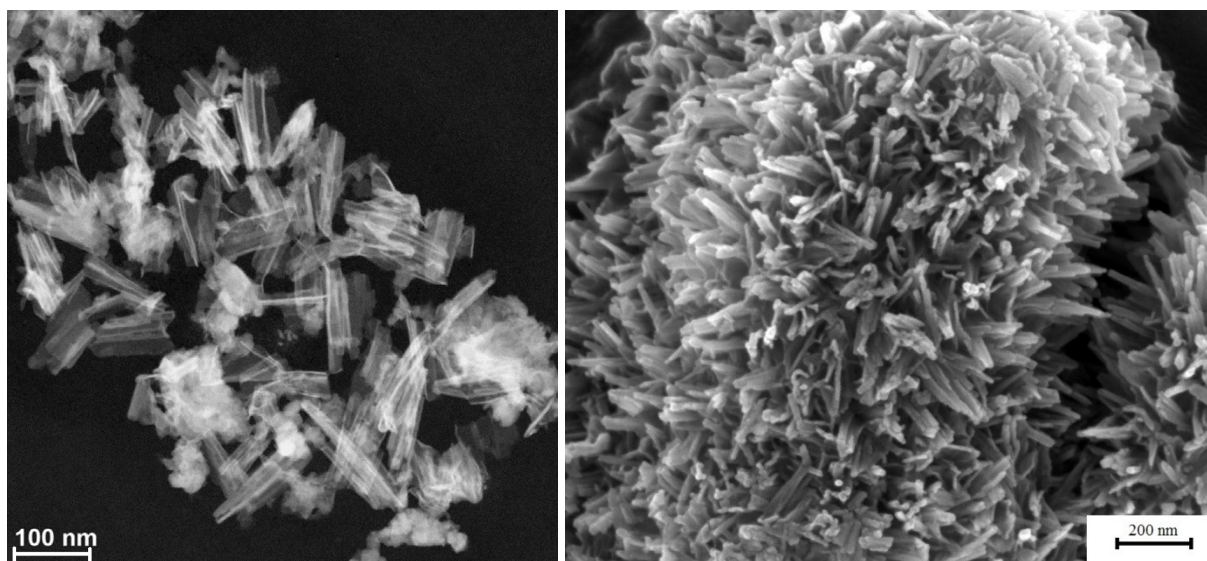
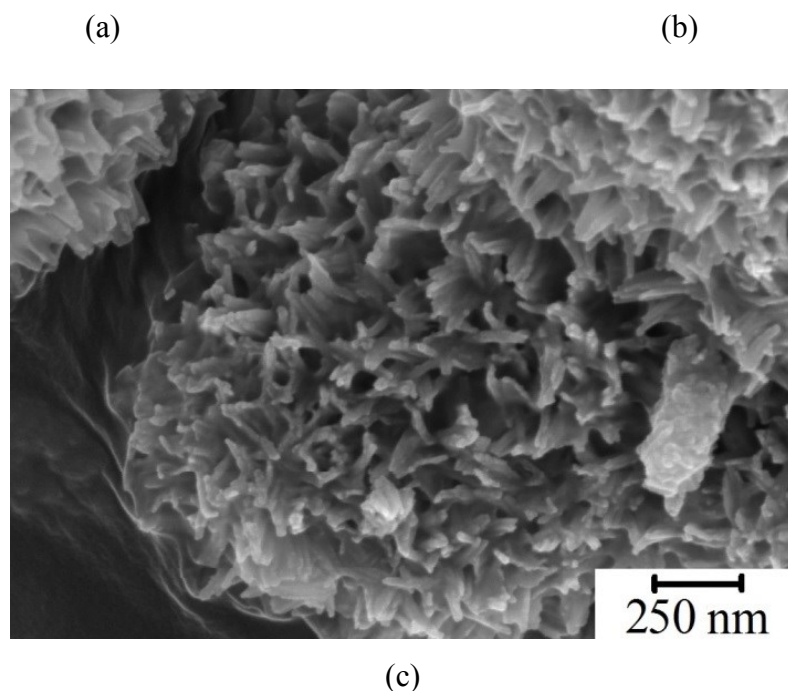


Figure 4-1. Schematic of the humidification and reactor system.

#### 4-6. Results and Discussions

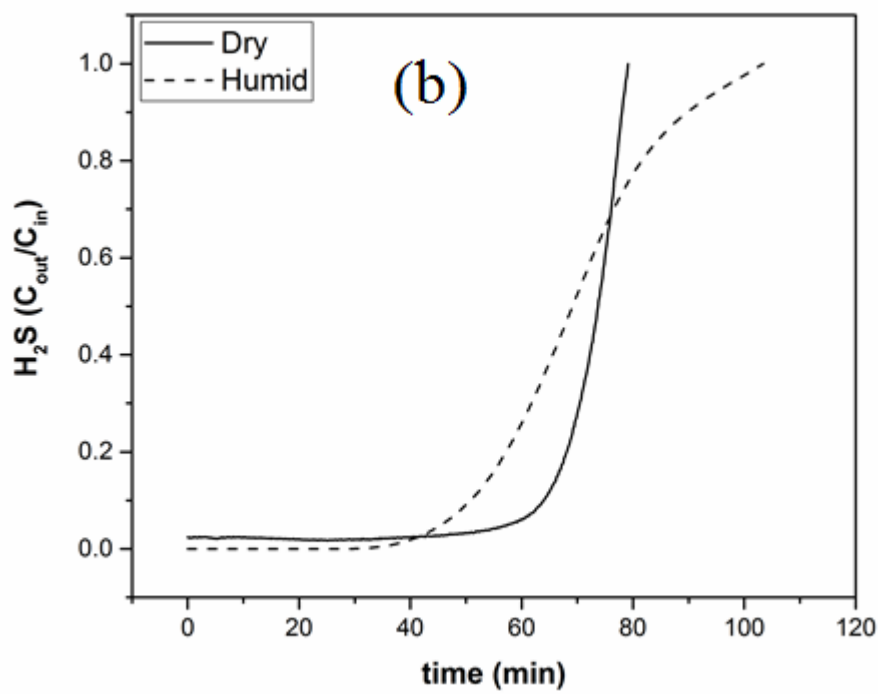
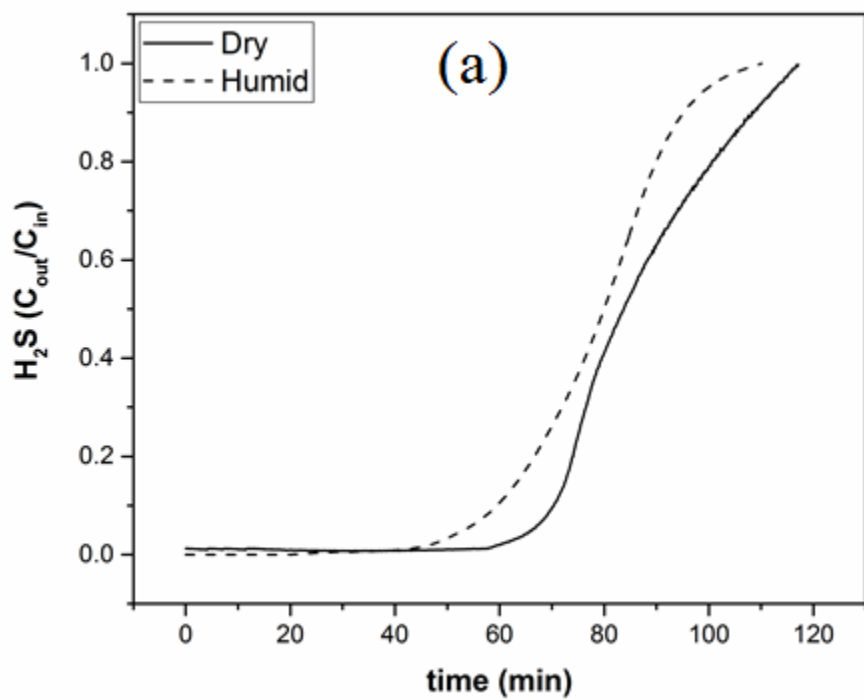
Figure 4-2 shows a transmission electron micrograph (TEM) of as-synthesized ETS-2 and scanning electron micrographs (SEM) of ETS-2 and Cu-ETS-2. As the TEM image in Figure 4-2a shows, each ETS-2 particle is typically 50 to 100nm in length and 20 nm wide. The SEM image in Figure 4-2b demonstrates that particles tend to form aggregates or clusters. As reported in a previous study, each cluster is, on average, about 1-2  $\mu\text{m}$  in diameter<sup>22</sup>. Figure 4-2c is an SEM image of the copper-exchanged ETS-2 and this image indicates that, after ion exchange with the copper solution, the morphology of the material does not change.





**Figure 4-2.** (a) TEM and (b) SEM images of ETS-2 together with (c) SEM image of Cu-ETS-2 showing the particles cluster size and morphology.

The adsorption experiments were performed both with and without the presence of water at intervals of 100 °C ranging from 250 °C to 950 °C. Fresh adsorbent was used for each experiment. Figure 4-3 shows typical H<sub>2</sub>S breakthrough curves for humid and dry streams at three different temperatures ranging from 350 °C to 750 °C.



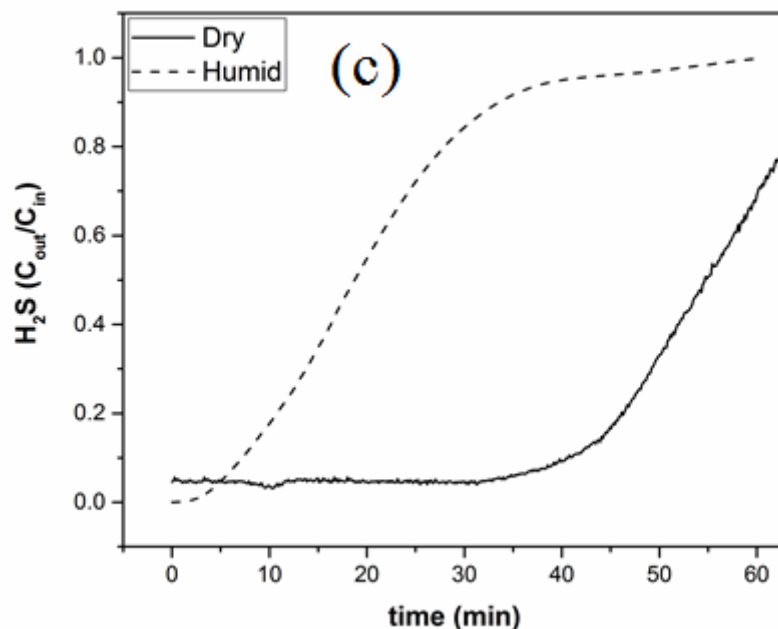
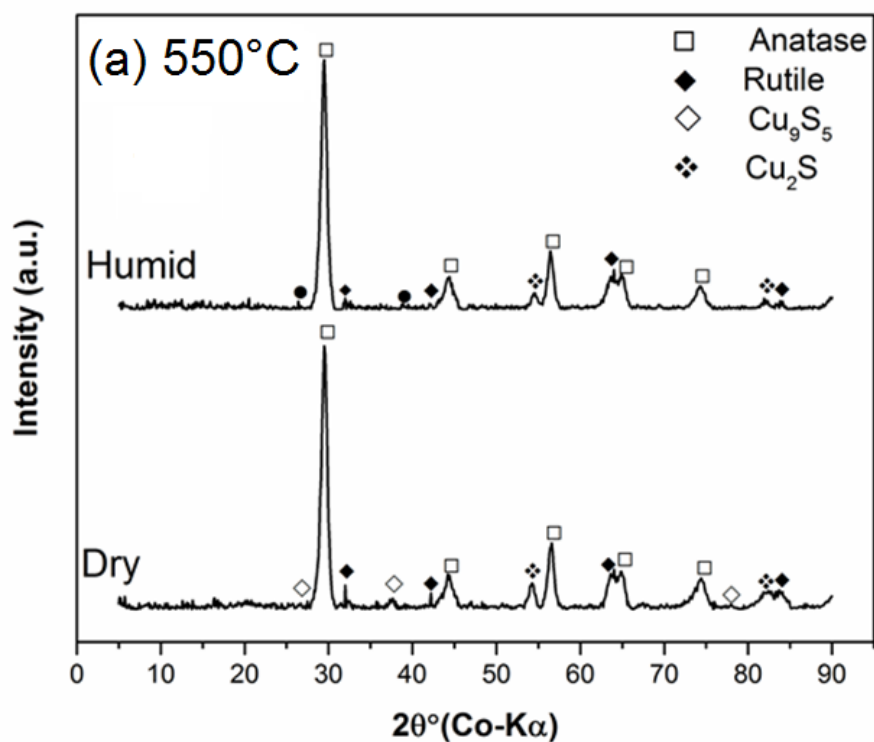


**Figure 4-3** – Comparison between H<sub>2</sub>S breakthrough curves for dry and humid stream at (a) 350 °C, (b) 550 °C and (c) 750 °C

The curves related to dry H<sub>2</sub>S adsorption in Figure 4-3 show a progressive reduction in breakthrough time and the roughly 50% reduction in capacity between 350 and 750 °C has been previously attributed to the thermal dissociation of H<sub>2</sub>S and the associated formation of H<sub>2</sub>, which promotes the reduction of CuO to Cu<sub>2</sub>O and elemental copper<sup>24</sup>. Under our dynamic adsorption conditions metallic copper is effectively non-adsorbing and thus does not contribute to the desulfurization capacity of the adsorbent<sup>25</sup>. Under *humid* conditions there is a measurable loss (compared to the dry experiments) in H<sub>2</sub>S capacity at 350 and 500 °C but at 750 °C the H<sub>2</sub>S capacity loss was, unexpectedly, almost absolute.

The samples exposed to humid H<sub>2</sub>S were measured using powder X-ray diffraction to determine whether the products of reaction are changing with the introduction of moisture. Figure 4-4 shows the diffraction patterns for samples of Cu-ETS-2 that had been exposed to dry and humid H<sub>2</sub>S at 550 and 750 °C. The measurable loss in H<sub>2</sub>S capacity seen in the breakthrough profiles at 550 °C is not

accompanied by any change in the crystalline phases present in the sample. At 750 °C, however, the XRD pattern for the sample exposed to humid H<sub>2</sub>S stream shows a significant amount of metallic copper present in the sample which is not present in the control sample exposed to dry H<sub>2</sub>S. The presence of a large amount of non-adsorbing, metallic copper in the sample exposed to the humid stream explains the abrupt loss in adsorption capacity for this sample. The presence of metallic copper in the sample can only be reasonably explained by the presence of a higher H<sub>2</sub> concentration in the feed stream.



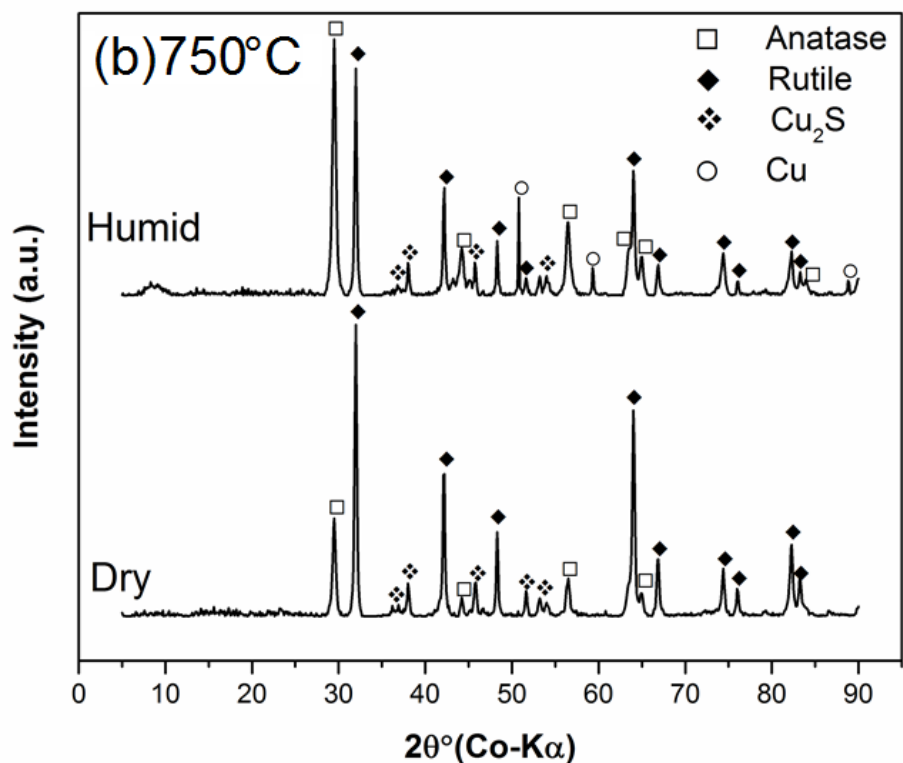


**Figure 4-4.** XRD pattern of Cu-ETS-2 after H<sub>2</sub>S adsorption at (a) 550°C and (b) 750°C for dry and humid streams

Only two reactions were identified that could generate H<sub>2</sub> using the feed gas specified. The endothermic, thermal decomposition of H<sub>2</sub>S is described by Equation 1.



The contribution of H<sub>2</sub> to the system through this reaction is obvious in the dry experiments as a coating of yellow solid builds up on the outlet of the reactor as it exits the furnace and is cooled on exhaust. The deposition of elemental sulfur is more pronounced at longer run times and at temperatures above 650 °C.

There was no evidence of elemental sulfur deposit anywhere in the exhaust system for the experiments run under humid conditions. The absence of this signature product was unexpected because elemental sulfur is not known to react with water. It was considered that the H<sub>2</sub>S may be reforming with the excess water vapor to generate H<sub>2</sub> via Equation 2.



Since both reactions are endothermic the reactor system was adapted to sample the gases at high temperature to prevent the reactants from recombining as the gas cools on exhaust. To study the high temperature gas phase species, the exhaust system shown in Figure 4-1 was removed and a longer, stainless steel capillary with a 5 micron ID was mounted to the mass spectrometer. The capillary was inserted directly into the quartz reactor tube so that the inlet to the capillary for the mass spectrometer was at the center of the furnace. In addition, the 60 cm long 10 mm OD quartz tube used for the adsorption reaction was replaced with 1.5 m of 0.25" OD, serpentine-folded quartz tubing. The additional length of tubing was selected to encourage the reactions to reach equilibrium by extending their residence time in the furnace. The inlet of the mass spectrometer was heated to 150 °C and the capillary was heated to 200 °C to ensure liquid water did not condense in the sampling system of the mass spectrometer.

The concentration of H<sub>2</sub> as a function of temperature was measured under both dry and humid conditions by ramping the furnace at 5 °C/min from 200 °C to 800 °C. The furnace was pre-heated to 200 °C to prevent water from condensing anywhere in the reactor system and the ramp program was started once stable baseline signals were achieved on the mass spectrometer. The difference in sensitivity and total system pressure between experiments was accounted for by dividing the H<sub>2</sub>S signal for the humid experiment by the H<sub>2</sub>S signal for the dry experiment. The H<sub>2</sub> signal for the humid experiment was then divided by this ratio. Both the humid and dry traces were then baseline corrected so that the signal at 200 °C was reduced to zero. The baseline correction is valid, and effectively cosmetic, because the amount of H<sub>2</sub>S converted at 200 °C is expected to be below the detection threshold of the instrument.

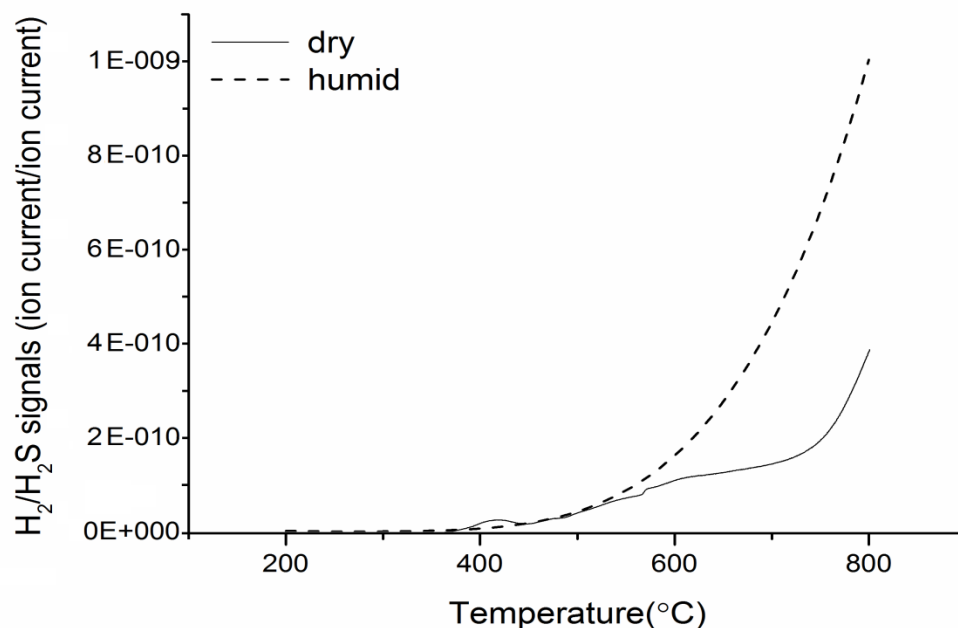


**Figure 4-5** Standardized and baseline-corrected H<sub>2</sub> signal as a function of temperature for humid and dry 500 ppm H<sub>2</sub>S in He

Figure 4-5 shows the H<sub>2</sub> signal from the mass spectrometer as a function of temperature for both the humid and dry gas experiments. The trend for the dry stream in shows a series of inflections; the first at about 400 °C and again at about 600 °C before the H<sub>2</sub> concentration trends steadily upward above 750 °C. This behavior is not characteristic of an endothermic reaction where a steady exponential trend is expected as a function of temperature. The lack of uniformity in the H<sub>2</sub> profile for the dry experiment could be due to a combination of instrument sensitivity and, potentially, adsorption/desorption effects on the stainless steel capillary. The trend for the humid experiment, however, is more uniform and shows the expected profile for an endothermic reaction. The cause of the difference in the uniformity of the trends is not entirely clear though the water vapor is expected to provide a passivating influence on the steel capillary.

The trends for the humid and dry streams diverge between 500 and 600 °C where the H<sub>2</sub> signal for the humid experiment consistently exceeds that of the dry experiment. At 800 °C the H<sub>2</sub> signal for the humid experiment is 2.5 times greater than that for the dry experiment. The mass spectrometry data can be considered, at

best, semi-quantitative due to the challenges associated with maintaining the high temperature equilibrium conditions for the gases sampled from the reactor. The trends seen in Figure 4-5 do, however, clearly indicate the presence of larger amounts of H<sub>2</sub> in the humid stream, particularly at the highest temperatures.

The breakthrough data in Figure 4-3 demonstrated that the presence of water vapor had no effect on the H<sub>2</sub>S capacity of Cu-ETS-2 at 350 °C, caused a modest reduction in capacity at temperatures around 550 °C, and caused a virtually complete reduction in capacity at 750 °C. The data in Figure 4-5 coupled with the XRD data in Figure 4-4 suggest the explanation for this trend lies in an increase in H<sub>2</sub> concentration and the associated reduction of copper oxide to copper metal brought about by the presence of a greater amount of H<sub>2</sub> in the feed stream.

The mechanism for the increase in H<sub>2</sub> concentration was probed by looking at the SO<sub>2</sub> signal. If H<sub>2</sub>S is, indeed, reforming with water then the concentration of SO<sub>2</sub> should increase as the H<sub>2</sub> concentration increases. In fact, the SO<sub>2</sub> trend (not shown) for both the dry and humid experiments as a function of temperature is largely the same and shows no obvious trend except for a slight tapering reduction as the temperature increases. The signals at m/z = 48 and 64 were compared to see if the partial oxidation of sulfur was perhaps contributing in some way but the trend for both fragments was identical. While it remains possible that H<sub>2</sub> and SO<sub>2</sub> might combine in the capillary to reform H<sub>2</sub>O and H<sub>2</sub>S, the indications from the experiments suggest that the generation of additional H<sub>2</sub> is not associated with SO<sub>2</sub> formation. As a result H<sub>2</sub> generation via Equation 2 is an unlikely route to explain the virtually complete reduction of copper at 750 °C under humid conditions.

The thermal cracking reaction described by Equation 1 is not facile and a residence time of even 2 seconds is insufficient to approach equilibrium at temperatures below 1000 °C<sup>26</sup>. Using a flow rate of 500 ml/min, our serpentine reactor allowed even shorter residence times; about 1.5 seconds at 200 °C and dropping to about 650 ms at 850 °C. The short contact time afforded by our reactor implies that the thermal cracking reaction described by Equation 1 is certainly far from equilibrium. Accepting that H<sub>2</sub> is the only reactant in our system capable of

reducing copper oxide to elemental copper - coupled with the observation SO<sub>2</sub> is not apparently a product of reaction - it remains that Equation 1 is likely the sole source of the H<sub>2</sub> in the system. Though speculative, and only partially supported by the data, it appears that the presence of moisture may promote the thermal cracking reaction by providing a diluting effect on the products in much the same way that it does during an ethane cracking reaction<sup>27</sup>.

#### **4-7. Conclusions**

The presence of water vapor in an inert gas stream containing 500 ppm H<sub>2</sub>S promotes the reduction of copper on the surface of Cu-ETS-2. The influence of moisture is most clearly seen in the breakthrough experiments carried out at temperatures above 750 °C where the presence of moisture virtually eliminates the H<sub>2</sub>S capacity for the adsorbent and the XRD for the reacted sample shows the presence of elemental copper on the surface. Though the mechanism remains somewhat ambiguous, the H<sub>2</sub> responsible for reducing the copper appears to come, not from the direct reaction of H<sub>2</sub>S and H<sub>2</sub>O, but through an apparent enhancement in the degree of thermal cracking of the H<sub>2</sub>S.

#### **4-8- Acknowledgements**

Financial support from the Initiative and Networking Fund of the Helmholtz Association (HGF) through the Helmholtz-Alberta Initiative is kindly acknowledged.

#### 4-9 References

- (1) Stirling, D., *The sulfur problem: cleaning up industrial feedstocks*. Royal Society of Chemistry: 2000.
- (2) Boon, J.; van Dijk, E.; Pirgon-Galin, Ö.; Haije, W.; van den Brink, R., Water–gas shift kinetics over FeCr-based catalyst: effect of hydrogen sulphide. *Catal. Lett.* **2009**, 131, (3-4), 406-412.
- (3) Cal, M.; Strickler, B.; Lizzio, A., High temperature hydrogen sulfide adsorption on activated carbon: I. Effects of gas composition and metal addition. *Carbon* **2000**, 38, (13), 1757-1765.
- (4) Hass, R. H.; Hansford, R. C.; Hennig, H., Catalytic incineration of hydrogen sulfide from gas streams. In Google Patents: 1978.
- (5) Ko, T.-H.; Chu, H.; Chung, L.-K., The sorption of hydrogen sulfide from hot syngas by metal oxides over supports. *Chemosphere* **2005**, 58, (4), 467-474.
- (6) Yumura, M.; Furimsky, E., Comparison of calcium oxide, zinc oxide, and iron (III) oxide hydrogen sulfide adsorbents at high temperatures. *Ind. Eng. Chem. Proc. D. D.* **1985**, 24, (4), 1165-1168.
- (7) Abbasian, J. *Development of novel copper-based sorbents for hot-gas cleanup*; Institute of Gas Technology, Chicago, IL (United States): 1991.
- (8) Tamhankar, S.; Garimella, S.; Wen, C., Kinetic study on the reactions involved in hot gas desulfurization using a regenerable iron oxide sorbent—III. Reactions of the sulfided sorbent with steam and steam-air mixtures. *Chem. Eng. Sci.* **1985**, 40, (6), 1019-1025.
- (9) Rosso, I.; Galletti, C.; Bizzi, M.; Saracco, G.; Specchia, V., Zinc oxide sorbents for the removal of hydrogen sulfide from syngas. *Ind. Eng. Chem. Res.* **2003**, 42, (8), 1688-1697.
- (10) Lew, S.; Jothimurugesan, K.; Flytzani-Stephanopoulos, M., High-temperature hydrogen sulfide removal from fuel gases by regenerable zinc oxide-titanium dioxide sorbents. *Ind. Eng. Chem. Res.* **1989**, 28, (5), 535-541.
- (11) Patrick, V.; Gavalas, G. R.; Flytzani-Stephanopoulos, M.; Jothimurugesan, K., High-temperature sulfidation-regeneration of copper (II) oxide-alumina sorbents. *Ind. Eng. Chem. Res.* **1989**, 28, (7), 931-940.

- (12) Slimane, R. B.; Abbasian, J., Copper-based sorbents for coal gas desulfurization at moderate temperatures. *Ind. Eng. Chem. Res.* **2000**, 39, (5), 1338-1344.
- (13) Kyotani, T.; Kawashima, H.; Tomita, A.; Palmer, A.; Furimsky, E., Removal of H<sub>2</sub>S from hot gas in the presence of Cu-containing sorbents. *Fuel* **1989**, 68, (1), 74-79.
- (14) Yasyerli, S.; Dogu, G.; Ar, I.; Dogu, T., Activities of copper oxide and Cu-V and Cu-Mo mixed oxides for H<sub>2</sub>S removal in the presence and absence of hydrogen and predictions of a deactivation model. *Ind. Eng. Chem. Res.* **2001**, 40, (23), 5206-5214.
- (15) Sick, G.; Schwerdtfeger, K., Hot desulfurization of coal gas with copper. *Metall. Trans. B* **1987**, 18, (3), 603-609.
- (16) Flytzani-Stephanopoulos, M.; Gavalas, G. R.; Tamhankar, S. S.; Center, U. S. D. o. E. M. E. T.; Laboratory, J. P., *Novel Sorbents for High Temperature Regenerative H<sub>2</sub>S Removal*. United States Department of Energy: 1984.
- (17) Li, Z.; Flytzani-Stephanopoulos, M., Cu-Cr-O and Cu-Ce-O regenerable oxide sorbents for hot gas desulfurization. *Ind. Eng. Chem. Res.* **1997**, 36, (1), 187-196.
- (18) Reddy, G. K.; Smirniotis, P. G., Chapter 1 - Introduction About WGS Reaction. In *Water Gas Shift Reaction*, Smirniotis, G. K. R. G., Ed. Elsevier: Amsterdam, 2015; pp 1-20.
- (19) Huang, C.-C.; Chen, C.-H.; Chu, S.-M., Effect of moisture on H<sub>2</sub>S adsorption by copper impregnated activated carbon. *J. Hazard. Mater.* **2006**, 136, (3), 866-873.
- (20) Yazdanbakhsh, F.; Bläsing, M.; Sawada, J. A.; Rezaei, S.; Müller, M.; Baumann, S.; Kuznicki, S. M., Copper exchanged nanotitanate for high temperature H<sub>2</sub>S adsorption. *Ind. Eng. Chem. Res.* **2014**, 53, (29), 11734-11739.
- (21) Kuznicki, S. M., Large-pored crystalline titanium molecular sieve zeolites. In Google Patents: 1989.
- (22) Tanchuk, B.; Sawada, J. A.; Kuznicki, S. M., Amine - functionalization of the nanotitanate ETS - 2. *AIChE J.* **2013**, 59, (12), 4727-4734.

- (23) Prakash, A., On the effects of syngas composition and water-gas-shift reaction rate on FT synthesis over iron based catalyst in a slurry reactor. *Chem. Eng. Commun.* **1994**, 128, (1), 143-158.
- (24) Yazdanbakhsh, F. A., M.; Sawada, J.A.; Kuznicki, Cu–Cr–O Functionalized ETS-2 Nanoparticles for Hot Gas Desulfurization. *J. Nanosci. Nanotechnol.* 15.
- (25) Alonso, L.; Palacios, J. M.; García, E.; Moliner, R., Characterization of Mn and Cu oxides as regenerable sorbents for hot coal gas desulfurization. *Fuel Proc. Tech.* **2000**, 62, (1), 31-44.
- (26) Karan, K.; Mehrotra, A. K.; Behie, L. A., On reaction kinetics for the thermal decomposition of hydrogen sulfide. *AIChE J.* **1999**, 45, (2), 383-389.
- (27) Ranjan, P.; Kannan, P.; Al Shoaibi, A.; Srinivasakannan, C., Modeling of Ethane Thermal Cracking Kinetics in a Pyrocracker. *Chem. Eng. Tech.* **2012**, 35, (6), 1093-1097.

## Chapter 5

# Cu-ETS-2 Regeneration

## 5-1 Introduction

In the previous chapters the reaction between Cu-ETS2 and H<sub>2</sub>S was discussed in detail. In summary, CuO is consumed during adsorption to produce Cu<sub>2</sub>S. This step can function as a stand alone unit, however due to economic reasons it is preferred to avoid disposing of consumed adsorbent and replacing it with fresh materials.

A regeneration process is complementary to the adsorption process and can oxidize Cu<sub>2</sub>S back to CuO. During this process SO<sub>2</sub> is generated, which can also be further oxidized to SO<sub>3</sub>. The generated SO<sub>3</sub> can in turn be used to produce sulfuric acid<sup>1</sup>.

The objective of the experiments presented in this chapter is to investigate the ability of Cu-ETS2 to be regenerated and present the reactions that can occur during the oxidation of copper sulfide. The result presented in this chapter together with the detailed understanding of copper oxide sulfidation presented in the previous chapters can be used to enable an optimal design of an adsorption/regeneration process for H<sub>2</sub>S separation.

The concept of copper sulfide oxidation has been widely investigated due to its use in refining naturally occurring copper sulfides. It has been found that during oxidation, CuS is first converted into Cu<sub>2</sub>S and generates elemental (gaseous) sulfur<sup>2</sup>. The formed Cu<sub>2</sub>S is then oxidized further into Cu<sub>2</sub>O and eventually into CuO. At temperatures above 663 °C CuO was the only observed final product; at temperatures below 663 °C copper sulfate was also found.

Lewis et al.<sup>3</sup> studied the oxidation of Cu<sub>2</sub>S (powder with a particle size between 0.149 -0.074 mm) in both air and in pure oxygen at temperatures between 250 and 700 °C. The main objective of the study was to determine the amount of water soluble components formed. They found the optimum temperature for the formation of water soluble copper components (CuSO<sub>4</sub>) to be 450 °C, when using air or oxygen as the reaction gas. When using pure oxygen as oxidizing agent only 8% of the Cu<sub>2</sub>S was converted into water soluble copper components.

In a study conducted by Ganguly and Mukherjee<sup>4</sup>, it was found that once CuS is subject to oxidation, the first step in the overall reaction is the decomposition of CuS to Cu<sub>2</sub>S and elemental sulfur. The formed elemental sulfur immediately reacts with oxygen to form SO<sub>2</sub>.

Asaki et al.<sup>5</sup> studied the oxidation of a pellet of Cu<sub>2</sub>S at atmospheric pressure, under various temperatures and oxygen concentrations. The reaction temperature was varied between 750 and 850 °C. The oxygen concentration was varied between 5 and 20 vol%. They used pellets with an approximate diameter of 6 mm. The oxidation of Cu<sub>2</sub>S appeared to be a two stage process. First Cu<sub>2</sub>S was oxidized to Cu<sub>2</sub>O, which was then oxidized further to CuO. The results were supported by the intersection of a partly oxidized pellet. This pellet showed a layered structure with the core being unreacted Cu<sub>2</sub>S, the inner layer being Cu<sub>2</sub>O, and the outer layer consisting of CuO. Under the experimental conditions the rate of the reaction was determined by the gas phase mass transfer resistance. As the reaction proceeded, diffusion through the product layer was assumed to become rate determining. At a temperature of 850 °C the pellets were partially melted due to the exothermic reaction. The time needed for complete conversion of a single pellet of Cu<sub>2</sub>S to CuO was estimated to be 3 hours.

Shah and Khalafallah<sup>6</sup> studied the oxidation of covellite, CuS, in detail to determine the sequence of reactions and intermediate phases during its roasting. They studied the reaction under different conditions using DTA (differential thermal analysis), TGA, and XRD of the reaction products. They reported that tenorite, CuO, and dolerophenite, CuO.CuSO<sub>4</sub>, form prior to the formation of the copper sulfate phase and that they are physically located below the CuSO<sub>4</sub> layer. Their proposed sequence was<sup>7</sup>:



### 5-1-1 Thermodynamics

Figure 5-1 shows the phase diagram of Cu-S-O system as a function of oxygen and sulfur dioxide partial pressures at 727 °C plotted using the thermodynamic data given by Brian<sup>8</sup>.

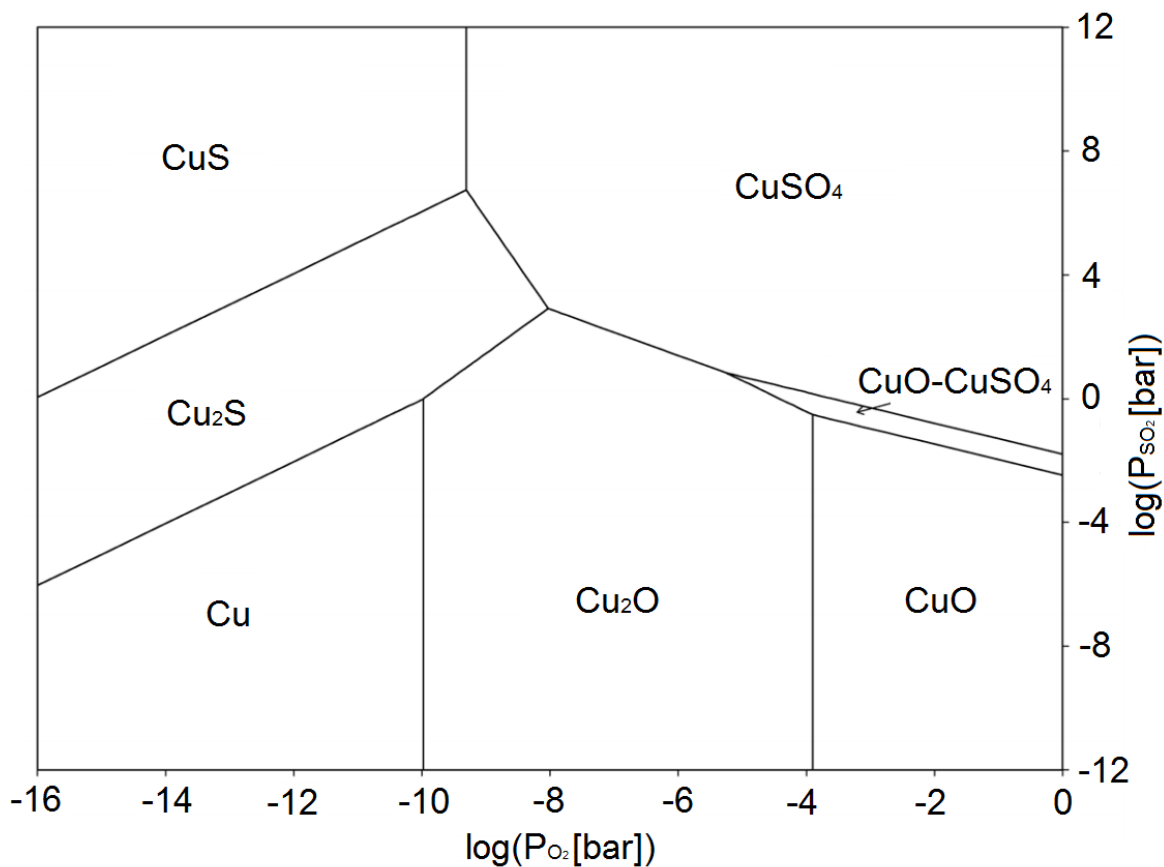


Figure 5-1- Phase diagram of Cu-S-O system at 727°C

As Figure 5-1 indicates, CuO is the most stable component when a copper-sulfur component is brought in contact at 727°C with partial pressure of O<sub>2</sub> being more than 10<sup>-4</sup> and a partial pressure of SO<sub>2</sub> less than 10<sup>-2</sup>. As Figure 5-1 shows higher partial pressures of oxygen and lower partial pressures of SO<sub>2</sub> favor formation of CuO.

Considering the aim of this study to be the first investigation on the ability of Cu-ETS-2 to be regenerated, oxygen was used as the oxidizing agent for our experiments instead of air, which is commonly used in industries. Having negligible amount of SO<sub>2</sub> in the feed also ensures formation of CuO after the regeneration process and enables us to have a better understanding of the regeneration behavior of Cu-ETS-2.

### **5-2 Materials preparation:**

ETS2 was prepared according to the same procedure described in chapters 1- 4 and later ion exchanged with copper nitrate solution. During ion exchange, the weight proportion of ETS-2 to copper salt to water was 1:2:100. The mixture was kept at 80°C and stirred for 1 day. Copper exchanged ETS-2 was later filtered and washed extensively with deionized water and dried in a vacuum oven at 60°C overnight. Prior to adsorption experiments, the adsorbent was activated by heating at 500°C under static air flow in a furnace for two hours.

### **5-3 Characterization**

#### **Powder X-ray Diffraction (XRD) Analysis**

The crystalline structures of the adsorbents were examined by XRD measurements using a Rigaku Geigerflex model 2173 diffractometer equipped with a cobalt ( $\lambda = 1.79021 \text{ \AA}$ ) rotating anode source and a graphite monochromator for filtering the K $\beta$  wavelengths.

#### **Mass spectrometry**

The gas species present in the exhaust stream of the reactor were sampled using a Pfeiffer Omnistar GSD 320 with QMA 200 residual gas analyzer. Different gas fragments were tracked using a one second sampling time to monitor the relative concentrations of H<sub>2</sub>S and SO<sub>2</sub> in the exhaust stream.

#### **Scanning Electron Microscope (SEM):**

Zeiss Ultra 55 device (Carl Zeiss NTS GmbH, Oberkochen, Germany) scanning electron microscopy (SEM) has been used to study the microstructure of the adsorbents.

#### 5-4 Experimental setup

The experiments were performed in the same setup used in the previous experiments and described in previous chapters. For every run, 0.5 g of adsorbent was packed in the center of an 8 mm (ID) quartz tube between two plugs of quartz wool.

The setup was equipped with an oxygen stream and a three way valve to switch between a He-H<sub>2</sub>S stream for adsorption and O<sub>2</sub> for oxidation cycles. Figure 5-2 shows a schematic of the reactor system used in the experiments.

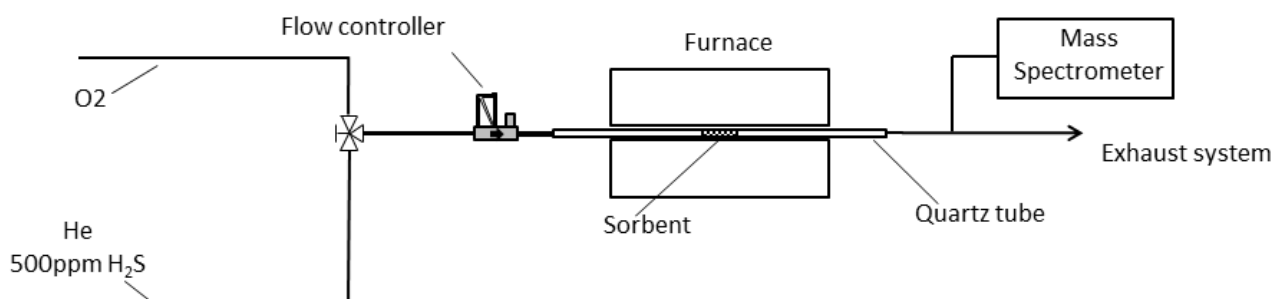


Figure 5-2- Schematic diagram of the experimental setup

#### 5-5 Results and discussion

The adsorbent was tested for several adsorption and regeneration cycles at 350, 550, 750 and 950°C.

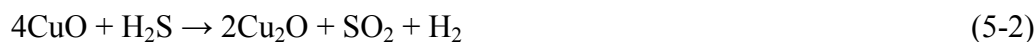
A typical adsorption breakthrough curve for adsorption experiment is presented in Figure 5-3. The inlet concentration of 470 ppmv H<sub>2</sub>S is effectively removed by the adsorbent as the concentration of H<sub>2</sub>S in the outlet is maintained below the detection limit of the instrument. As time passes, the H<sub>2</sub>S concentration rises above the baseline and the curve inflects as H<sub>2</sub>S “breaks though”. The concentration rises

rapidly after breakthrough as a result of the adsorbent becoming saturated and having fewer sites which can react with H<sub>2</sub>S.

As the figure shows, the adsorbent shows almost the same breakthrough time for different adsorption cycles. During adsorption CuO reacts with H<sub>2</sub>S to form Cu<sub>2</sub>S and SO<sub>2</sub> as per reaction 1<sup>9</sup>.



Reaction (1) is the overall reaction of four sub reactions (2-6) (7):



Hydrogen generated in reaction (1) can further react with CuO to reduce it to Cu<sub>2</sub>O. Cu<sub>2</sub>O later react with H<sub>2</sub>S to form Cu<sub>2</sub>S:



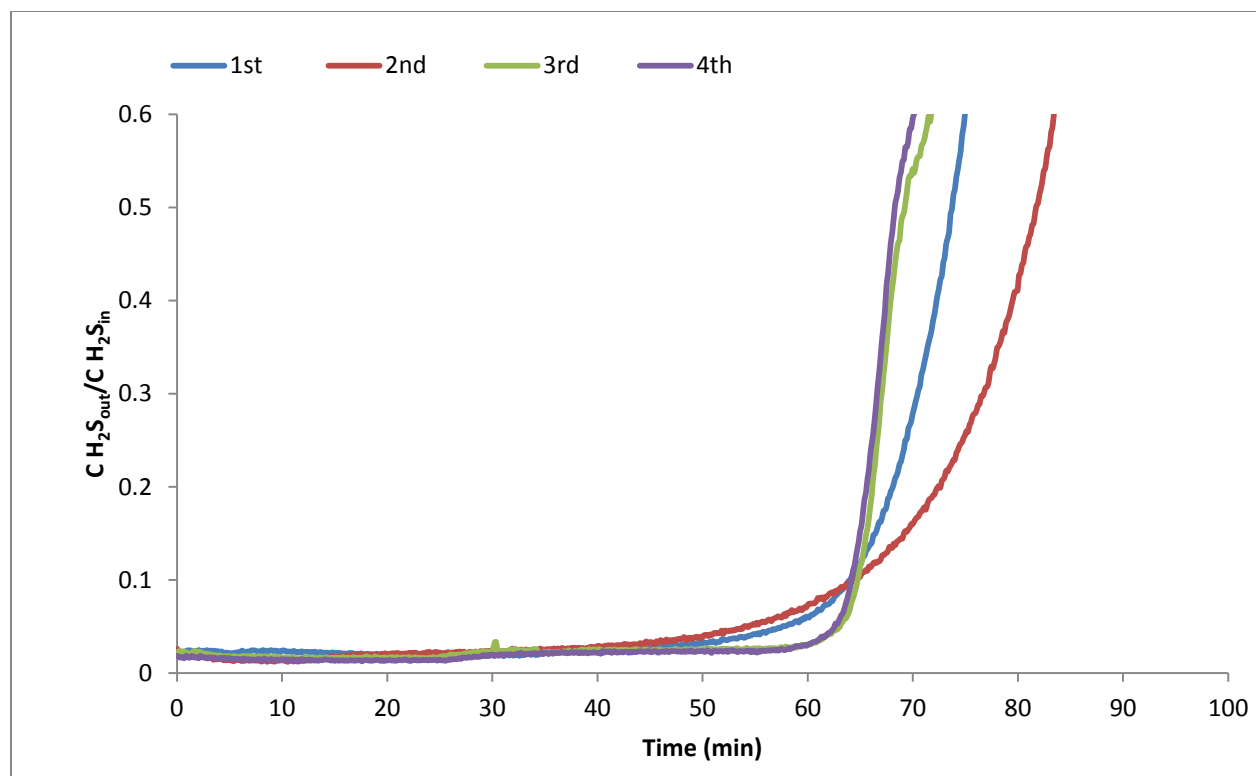


Figure 5-3 – Typical adsorption breakthrough curves for multiple adsorption cycles on Cu-ETS-2. (the presented data are for experiments at 550 °C)

Figure 5-4 shows the breakthrough times for adsorption experiments at different temperatures and different adsorption cycles. It is worth mentioning that breakthrough time has been chosen to be the time in which H<sub>2</sub>S concentration in the exit reaches 10% of the amount in the feed stream.

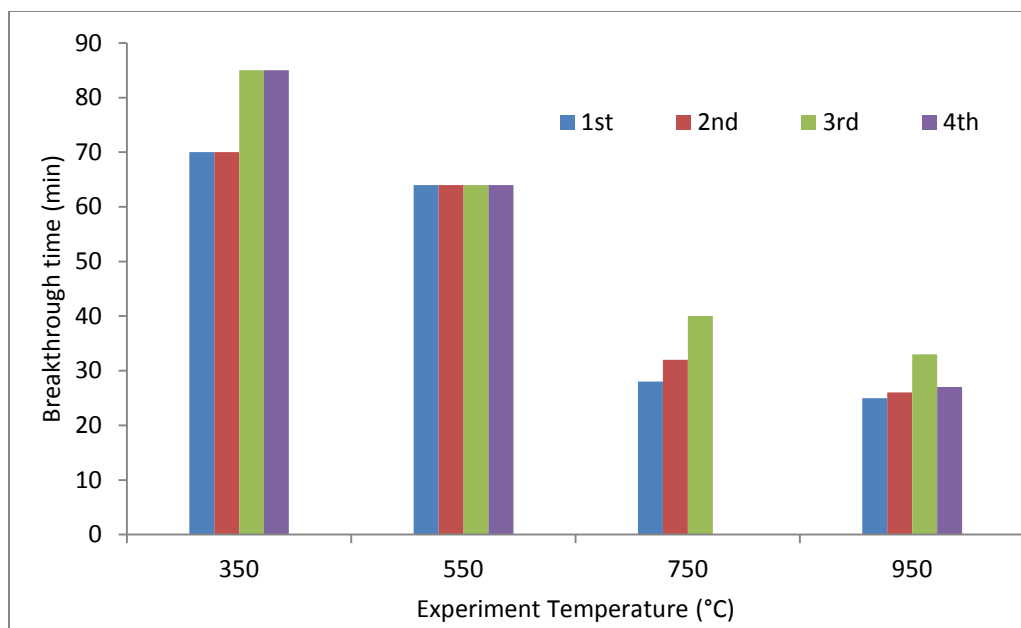


Figure 5-4 - Breakthrough times (in minutes) for different adsorption cycles at different temperatures

As Figure 5-4 shows, average adsorption breakthrough times are in agreement with the results for the previous experiments presented in chapter 1 with the reduction of breakthrough time to almost a half after 750°C. In this section and unlike chapter 1, the results are presented in breakthrough time instead of adsorption capacity because we developed a better understanding on the adsorption capacity and H<sub>2</sub>S stability at higher temperatures compared to chapter 1. For 350, 550 and 950°C experiments, the adsorbent underwent 4 adsorption and 3 regeneration processes. Terminating the experiments with an adsorption cycle enabled us to investigate the morphology and surface chemistry of the adsorbent after desulfurization. At 750°C, the experiments were terminated by an oxidation (regeneration) step in order to investigate the adsorbent after consumption by H<sub>2</sub>S.

During oxidation (regeneration) process, copper sulfide reacts with oxygen to form copper oxide and sulfur dioxide. The reaction happens in two steps. Oxidation of copper sulfide to Cu<sub>2</sub>O and then further oxidation of Cu<sub>2</sub>O to CuO:

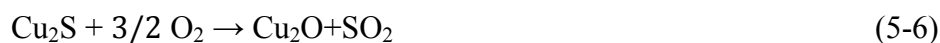
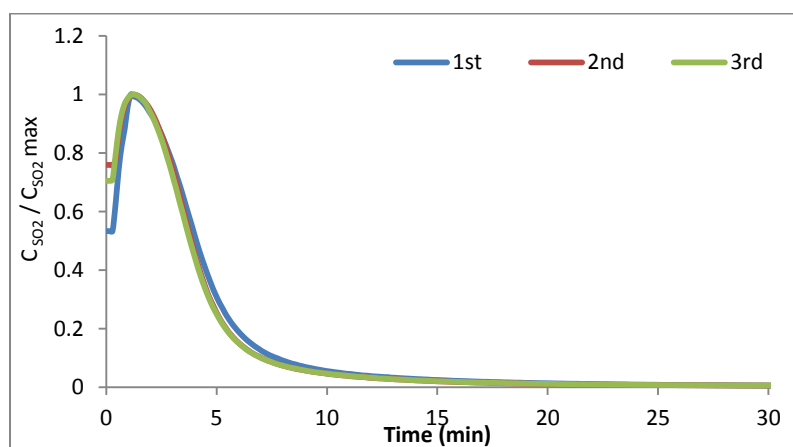
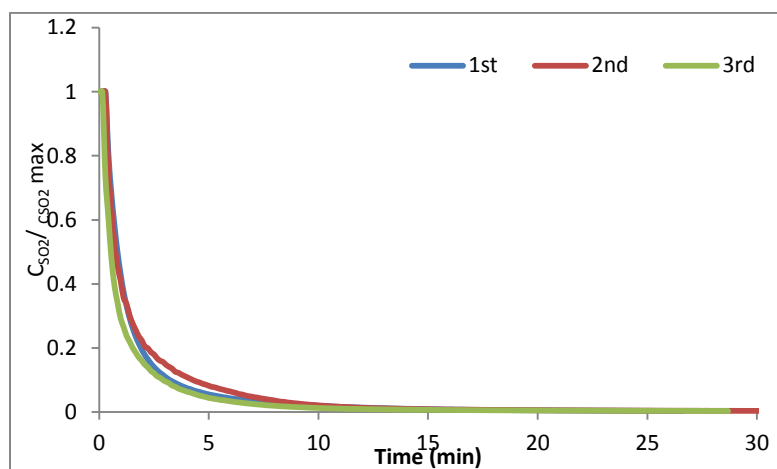




Figure 5-5 shows a typical  $\text{SO}_2$  concentration change versus time during the oxidation process at different oxidation cycles. As the figure shows, a considerable amount of  $\text{SO}_2$  is generated at the very early stages of the oxidation process, indicating a fast reaction rate. Having considerable higher superficial feed gas velocity in the tube at higher temperatures, results in a different  $\text{SO}_2$  profile for low and high temperature experiments. Figures 5-5-A and 5-5-B show  $\text{SO}_2$  concentration changes at 350 and 950°C respectively. As Figure 5-5-A show,  $\text{SO}_2$  concentration increases as the oxidation reaction proceeds and after a few minutes, plateaus before decaying to almost zero at 350°C while at 950°C, the maximum is observed almost instantaneously in the beginning of the process followed by a decay to zero.



(A)



(B)

Figure 5-5 – Change in  $\text{SO}_2$  concentration in the exit at (A) 350 and (B) 950 °C

As reported in the literature (3), other products can also be formed during the oxidation process such as  $\text{CuO}\cdot\text{CuSO}_4$ . It is formed through the reaction of  $\text{SO}_2$  produced by reaction (6) with  $\text{Cu}_2\text{O}$  and oxygen:



Since  $\text{CuO}\cdot\text{CuSO}_4$  is stable between 450 and 600 °C (10), it is expected to be present on the adsorbent for oxidation processes of 350 and 550°C resulting in lower adsorption capacities for the 2<sup>nd</sup>, 3<sup>rd</sup> and 4<sup>th</sup> cycles. However as Figure 5-4 shows, adsorption breakthrough times are almost constant for all four cycles and no decline is observed.

In order to understand the reason behind a rather constant adsorption breakthrough time, XRD analysis was performed on the samples. The results revealed an interesting phase change in the adsorbent. As reported in chapter 1, the  $\text{TiO}_2$  in ETS-2 is in the form of anatase. However once it is heated above 700°C, it transforms into rutile. The results of XRD analysis for the sample regenerated at 350°C is presented in Figure 5-6. As the figure shows, the only detectable phase on the sample other than  $\text{Cu}_2\text{S}$  is  $\text{TiO}_2$  in the form of rutile.

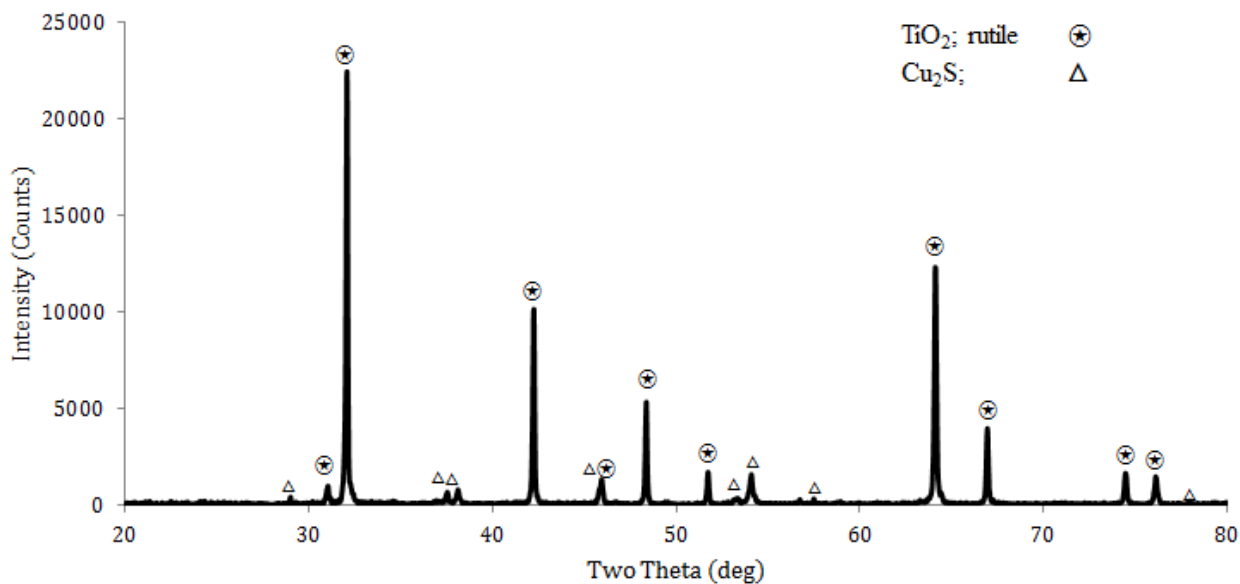


Figure 5-6 – XRD analysis of the adsorbent after 4 adsorption and 3 oxidation cycles at 350°C

The presence of rutile indicates that the heat of the exothermic oxidation reactions (reactions 6 and 7) are so high than the adsorbent heats up to at least 700°C.

Massive heat generation during the oxidation process and exceeding temperatures above 700°C was discovered to be the reason behind having no CuO.CuSO<sub>4</sub> at the end of the oxidation process and as a result formation of fresh adsorbent at the end of each oxidation cycle.

### 5-5-1 Thermodynamic simulation

To investigate the adiabatic reaction temperature and also possible phases that can formed during regeneration, FactSage<sup>®</sup> thermodynamics software was used to model the process. The same amount of sorbent, gas concentration and temperature range used in the experiments was used as inputs for the simulation. The software uses an incremental Gibbs free energy minimization algorithm to calculate the stability of solid and gas species in the presence of a constant flow of a specified gas stream. The results of each step are then used to calculate the next stage until equilibrium in the solid composition is obtained. Figure 5-7 shows the change in the solid phases (in mol) during oxidation process versus the amount of oxygen (in mmol).

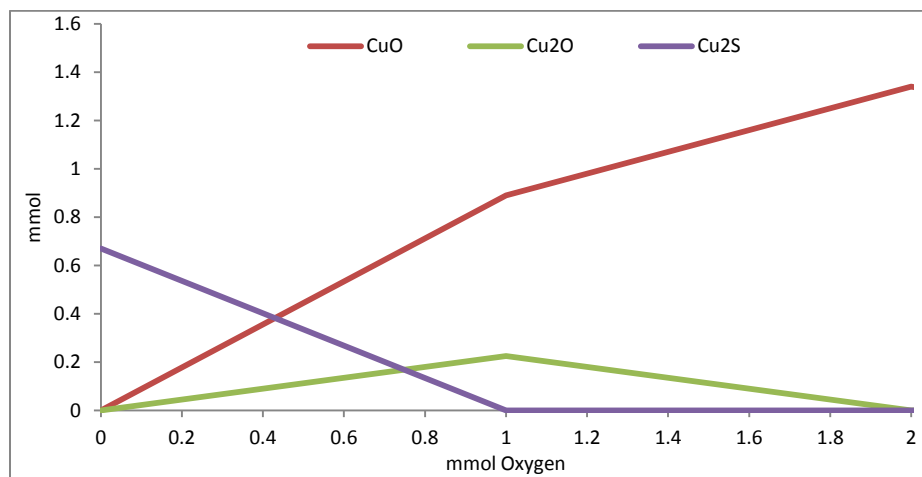


Figure 5- 7 – change in solid phases versus the amount of oxygen entering the system for oxidation process at 350°C

As the figure shows, once oxygen is in contact with Cu<sub>2</sub>S, it oxidizes and forms Cu<sub>2</sub>O as per reaction 6. Cu<sub>2</sub>O further reacts with oxygen and forms CuO as per

reactoion 7. Once enough oxygen is fed into the system,  $\text{Cu}_2\text{S}$  totally converts into  $\text{Cu}_2\text{O}$  and eventually  $\text{CuO}$  and the only active solid phase found on the adsorbent is  $\text{CuO}$ .

The same analysis was also performed on the adsorbent at  $950^\circ\text{C}$  and the results for solid and gas phases are shown in Figures 5-8 and 5-9.

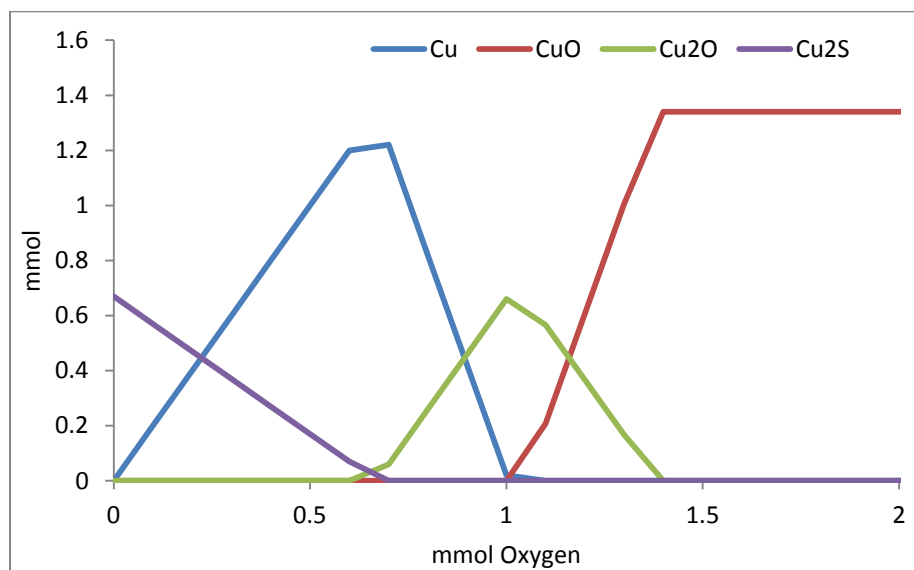


Figure 5-8 - change in solid phases versus the amount of oxygen entering the system for oxidation process at  $950^\circ\text{C}$

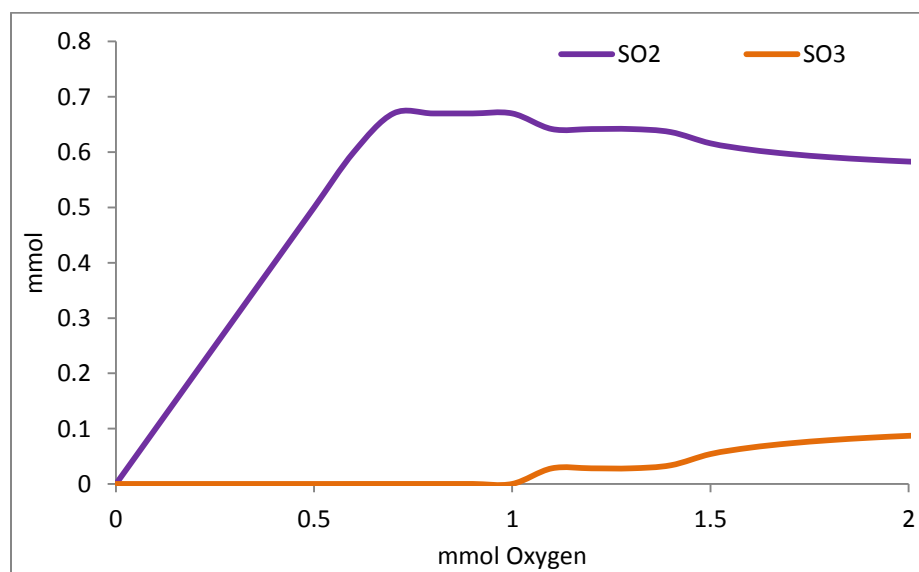


Figure 5-9 - change in gas phases versus the amount of oxygen entering the system for oxidation process at  $950^\circ\text{C}$

Interestingly at 950°C, thermodynamic simulations indicate that  $\text{Cu}_2\text{S}$  reduces to elemental copper at the early stages of oxidation and later oxidizes to  $\text{Cu}_2\text{O}$  and eventually  $\text{CuO}$  in the presence of oxygen. The reason behind initial formation of elemental copper is believed to be the massive heat generated through the early stages of the oxidation reaction at 950°C. Also, according to Figure 5-9 and as reported in the literature<sup>1</sup>, the  $\text{SO}_2$  generated by reaction (6) partially oxidizes and forms  $\text{SO}_3$ .

### 5-5-2 Adiabatic reaction temperature

The result of the simulation on adiabatic reaction temperature for oxidation at 350°C is presented in Figure 5-10. As the figure shows, the temperature of the system can increase up to 1100°C (assuming adiabatic process) in the early stages of oxidation and cools down to the furnace temperature over time.

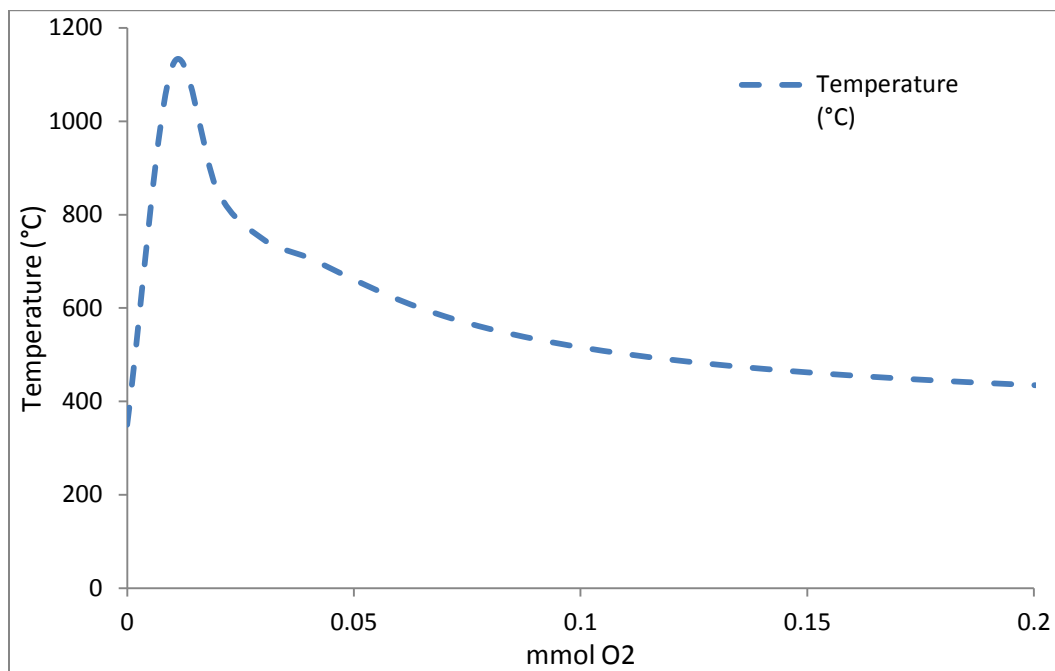


Figure 5-10 – Temperature profile in  $\text{Cu}_2\text{S} - \text{O}_2$  system versus the amount of oxygen fed into the system for Cu-ETS-2 oxidation at 350°C assuming an adiabatic system

Due to the high temperature of the system,  $\text{CuO}\cdot\text{CuSO}_4$  that could possibly form during oxidation at constant temperature of  $450\text{ }^\circ\text{C}$  decomposes and forms  $\text{CuO}$  and  $\text{SO}_3$ :



At the highest experiment temperature of  $950^\circ\text{C}$ , an enormous amount of heat can be generated by reactions 6 and 7. Adiabatic simulation of the process predicts the temperature can reach temperatures as high as  $2200^\circ\text{C}$ . However, due to the flow of the gas over the adsorbent and higher rates of heat transfer at elevated temperatures, the system will probably not see such high temperatures and stays below  $\text{TiO}_2$ 's melting point of  $1843^\circ\text{C}$ . However, SEM analysis suggests that elemental copper formed at the early stages of oxidation (Figure 5-8) has possibly been in liquid state during oxidation.

### 5-5-3 SEM/ EDX analysis

SEM analysis:

In order to investigate the effect of heat of the oxidation reaction and to understand the surface chemistry of the adsorbent SEM/ EDX analysis was also performed on the adsorbent. As mentioned in section 5-5 at  $350$ ,  $550$  and  $950^\circ\text{C}$  the process was terminated with an adsorbent cycle and at  $750^\circ\text{C}$ , the final process was chosen to be an oxidation process in order to enable us to study the properties of the adsorbent after the adsorption and the oxidation process.

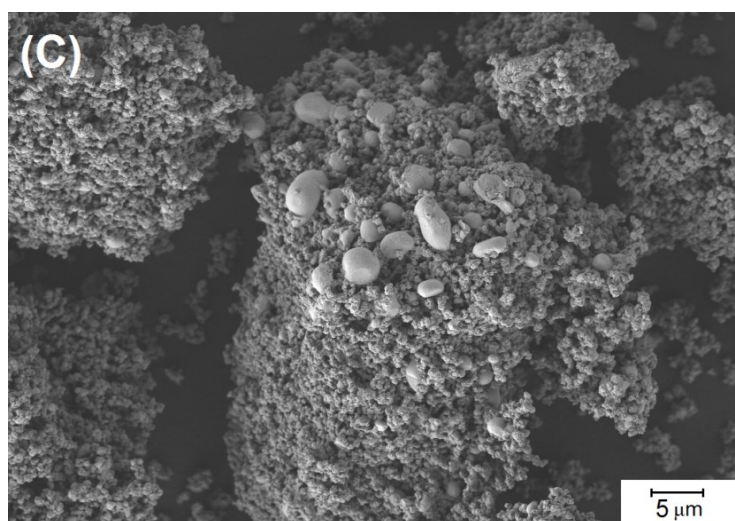
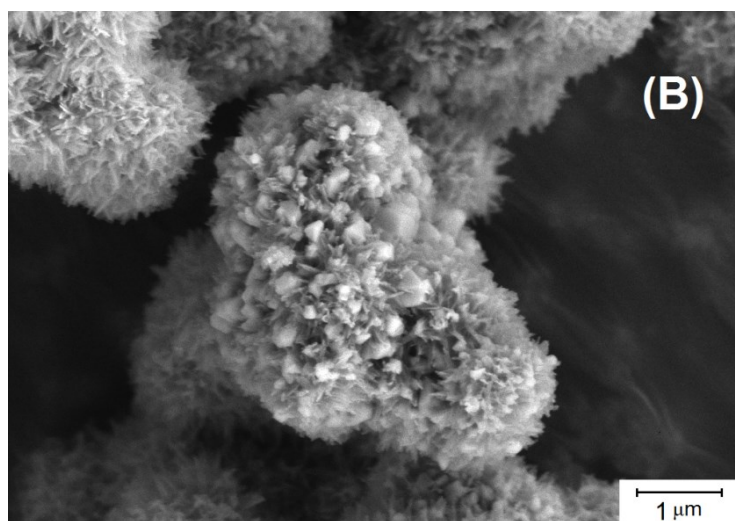
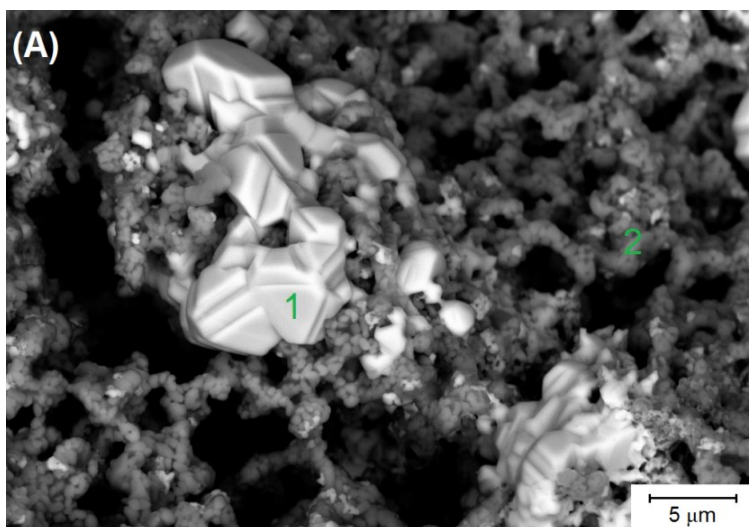


Figure 5-11- Scanning electron micrographs of Cu-ETS-2 after: (A) Adsorption and previously regeneration at 350°C, (B) Only 1 adsorption at 350°C and (C) Only 1 adsorption at 950°C

Figure 5-11 (A) shows the SEM micrographs of the adsorbent after 4 cycles of adsorption and 3 cycles of oxidation. Figures 5-11(B) and (C) are from an earlier study described in chapter 1. As the images show, copper sulfide crystals are formed on the surface of the adsorbent. Comparing Figure 5-11(A) with 5-11(B) and (C) confirms that the adsorbent has undergone intense heat during the oxidation process. Without undergoing an oxidation process, ETS-2 is almost intact at 350°C and keeps its needle like structure. However, once it is heated up to 950°C as shown in Figure 5-11(C), ETS-2 particles sinter and change morphology.

Although the adsorbent in Figure 5-11(B) has been kept in a furnace at constant 350°C, the morphology of ETS-2 is very close to an adsorbent undergoing temperatures like 950°C (Figure 5-11(C)). The SEM image together with adiabatic heat of reaction simulations presented in section 5-6-1 confirms that during oxidation an enormous amount of heat is generated resulting in an immense temperature rise.

SEM images of the adsorbent at 950°C experiment are also interesting. As Figure 5-12 shows, a new morphology is seen in this sample.

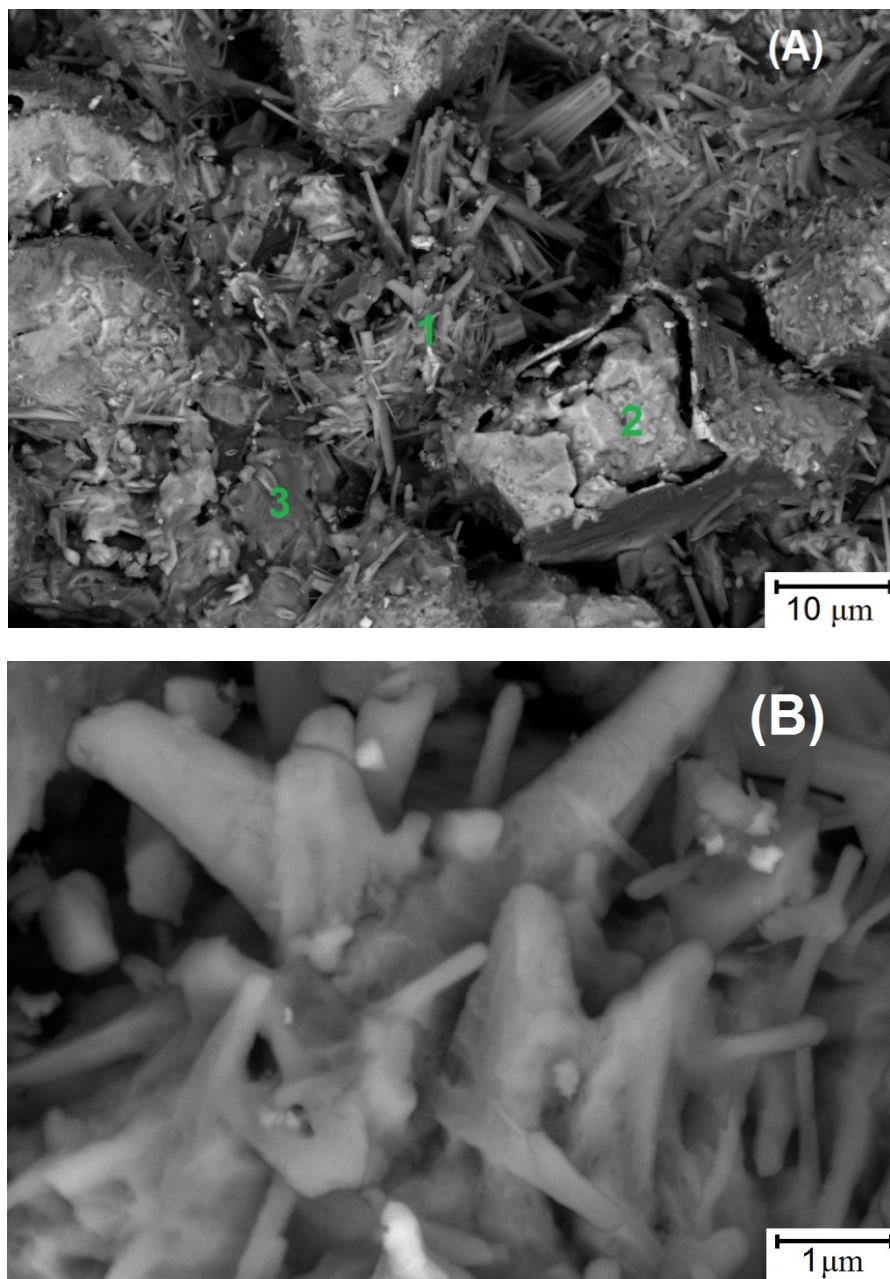


Figure 5-12 – Scanning electron micrographs of Cu-ETS-2 after adsorption and previous oxidation at 950°C

Big, needle like particles seen in Figure 5-12 are most probably formed due to recrystallization of  $\text{TiO}_2$  particles present in ETS-2 at very high temperatures because ETS-2 particles are on the average 100nm in length; however, these particles are almost 5 μm each. The exact nature of the needle like phases are not

clear to us; however, we had previously seen formation of such phases in Cu-Cr-ETS-2 (chapter 2) experiments at 1100°C.

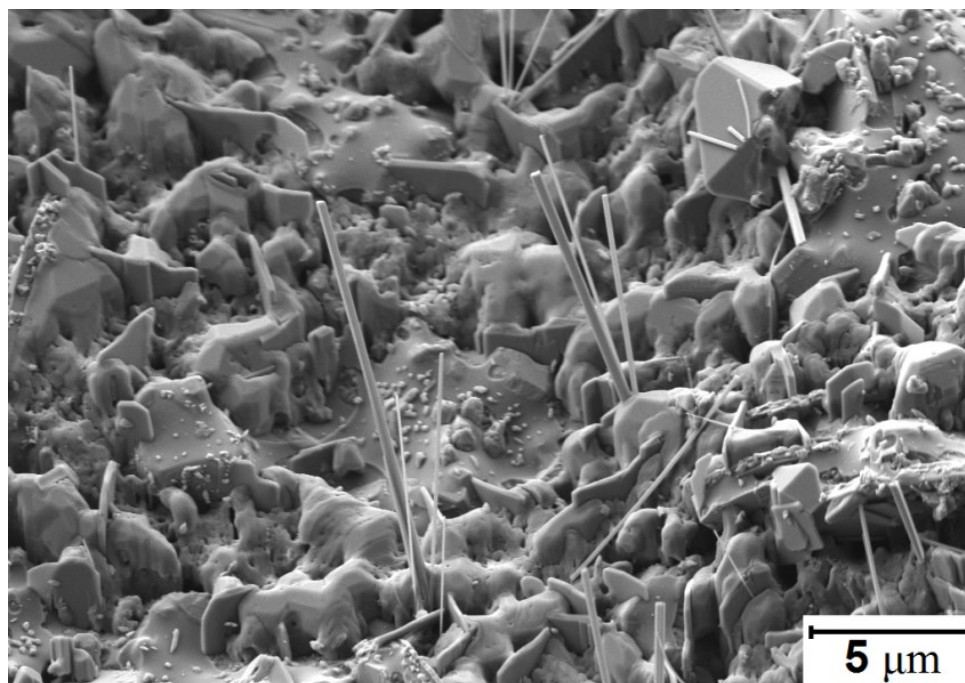


Figure 5-13 – Needle like phases observed in a previous study after adsorption of H<sub>2</sub>S on Cu-Cr-ETS-2 at 1100°C

#### EDX analysis

In order to further investigate the nature of the phases formed on the adsorbent at different temperatures, energy-dispersive X-ray spectroscopy was performed on the samples.

Different regions in Figures 5-11-A and 5-12-A are marked with numbers. Tables 5-1 and 5-2 show the composition of the phases mentioned in both images.

Table 5-1 – EDX analysis results for the selected points on Figure 5-11-A. (All data are in atomic%)

Point 1				
Cu	Ti	Si	S	O
60.32	4.44	0.67	29.20	5.37
Point 2				
Cu	Ti	Si	S	O
0.69	20.19	5.17	0.44	73.51

Table 5-2 – EDX analysis results for the selected points on Figure 5-12-A. (All data are in atomic%)

Point 1				
Cu	Ti	Si	S	O
20.27	0.68	0.26	16.58	62.22
Point 2				
Cu	Ti	Si	S	O
67.72	1.28	1.79	10.72	17.07
Point 3				
Cu	Ti	Si	S	O
2.81	46.07	2.26	4.13	44.74

As the data show, in Figure 5-11-A, the brighter phase (point 1) is copper sulfide (with atomic ratio of Cu:S being 2) and the darker phase being ETS-2. However in Figure 5-12-A, there are three major phases. Phase 1 being the needle like phase mostly containing copper, oxygen and sulfur. Phase 2 mostly consists of the reduced elemental copper formed during adsorption in the presence of hydrogen and phase 3 is the sintered ETS-2 particles with a little copper sulfide formed on the surface.

As mentioned earlier, the needle like structures formed on Cu-ETS-2 after adsorption and regeneration at 950°C had previously been observed during Cu-Cr-ETS-2 experiments at 1100°C. The nature of the needle like phase seems to be the same in both experiments as they present almost the same EDX pattern. We believe that at very high temperatures, TiO<sub>2</sub> and CuO might form a copper titanate. Figures 5-14 and 5-15 show an SEM image of the needle line structure in Cu-Cr-ETS-2 experiments together with the EDX pattern showing a qualitative elemental composition of the selected phase. As Figure 5-15 shows, similar to the composition of the needle like structure in Figure 5-12, the needle like phase formed at Cu-Cr-ETS-2 experiments mostly consists of Cu, O and S.

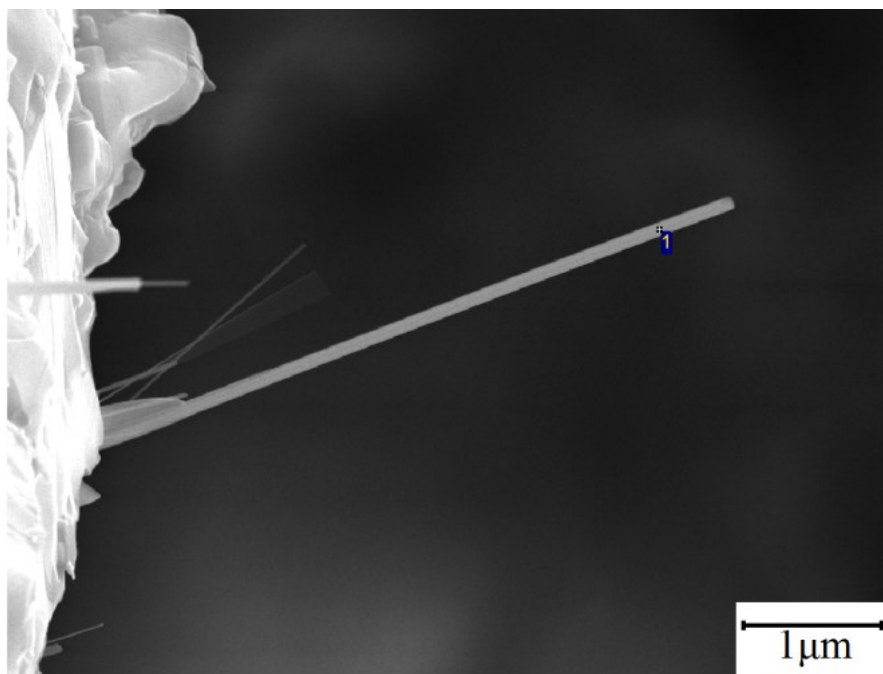


Figure 5-14 – Needle like structures formed at Cu-Cr-ETS-2 experiments at 1100°C

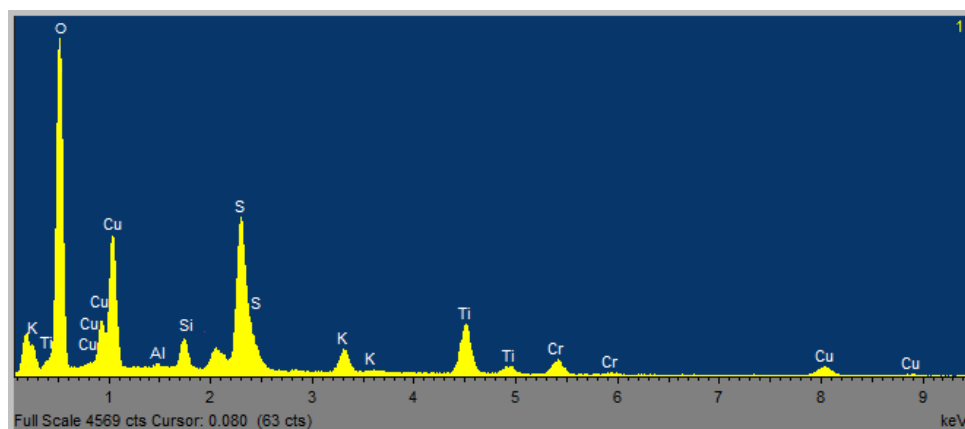


Figure 5-15 – EDX analysis for Cu-Cr-ETS2 at 1100°C

#### 5-5-4 H<sub>2</sub>S Thermal Dissociation and Adsorption Capacity

##### H<sub>2</sub>S thermal dissociation

In chapters 1 and 2 we discussed the effect of thermal dissociation of H<sub>2</sub>S on generation of hydrogen and consequently reduction of CuO to Cu<sub>2</sub>O and Cu. However, adsorption capacity results that are presented in chapters 1 and 2 are based on the presence of 500ppm H<sub>2</sub>S in the feed gas. In order to measure the exact

adsorption capacity by taking  $\text{H}_2\text{S}$  thermal dissociation into account, an experiment was done to see the actual concentration of  $\text{H}_2\text{S}$  at every temperature. Figure 5-16 shows the mass spectrometer results for change in  $\text{H}_2\text{S}$  concentration and  $\text{H}_2$  ion current at different temperatures starting from 150 to 950°C. It is worth mentioning that we were able to calculate the concentration of  $\text{H}_2\text{S}$  due to having a certified 470 ppmv gas tank purchased from Praxair. However we were not able to quantify the exact amount of  $\text{H}_2$  due to lack of a certified gas reference. As a result, the data for  $\text{H}_2$  are presented in terms of ion current in Figure 5-16.

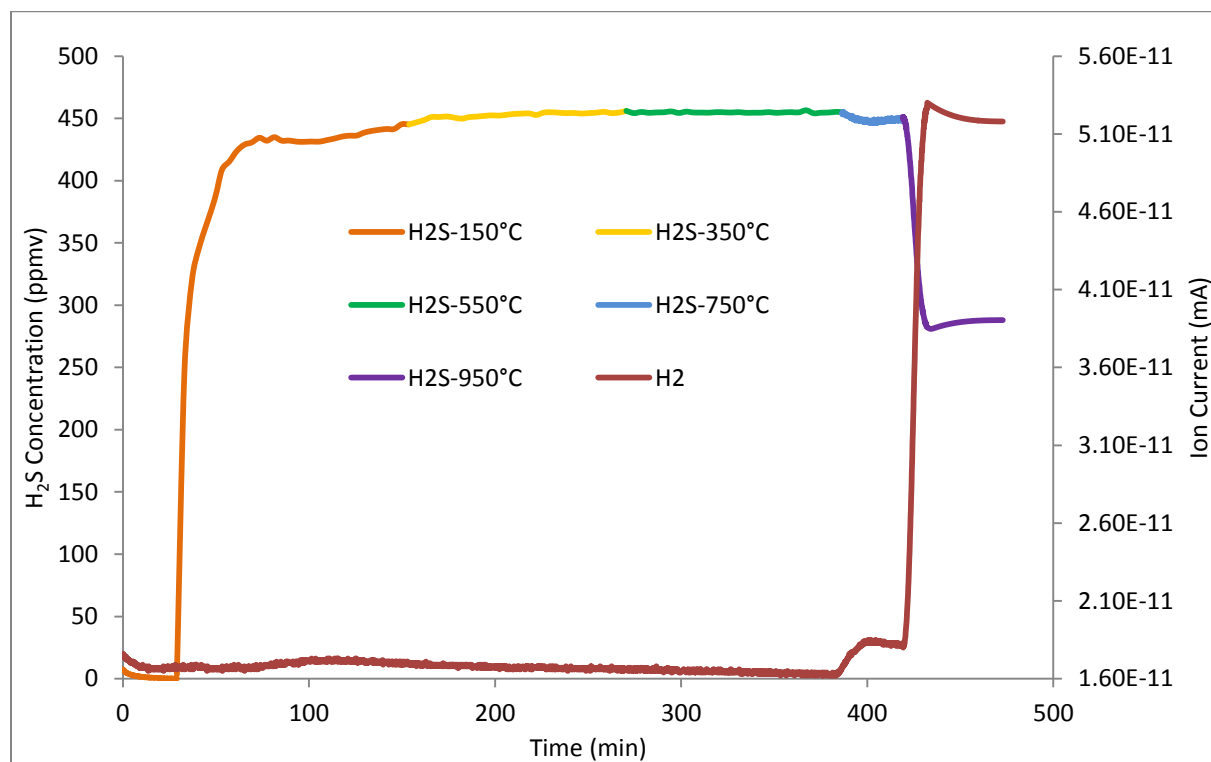


Figure 5-16 – the change in  $\text{H}_2\text{S}$  concentration and  $\text{H}_2$  ion current at different temperatures

The amount of  $\text{H}_2\text{S}$  concentration at different temperatures is presented in Figure 5-17. As the figure shows,  $\text{H}_2\text{S}$  concentration drops down from 470 to 288ppm at 950°C.

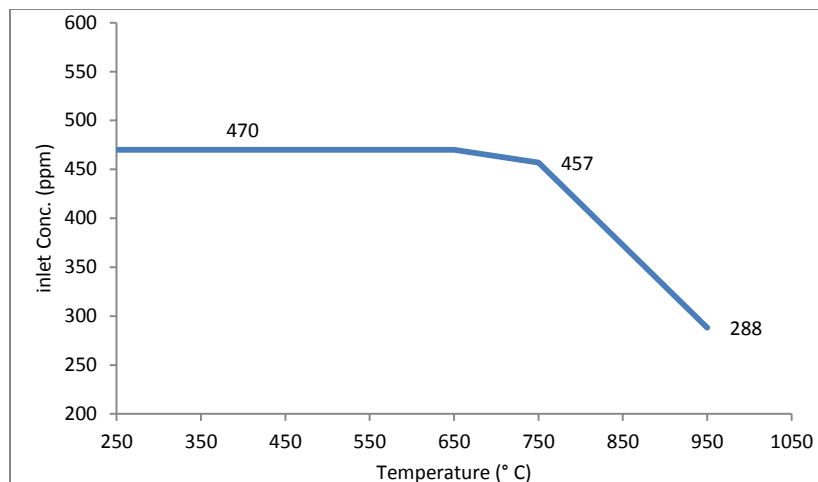


Figure 5-17 – Change in H<sub>2</sub>S inlet concentration at different temperatures due to thermal dissociation

Based on the experimental data presented in Figure 5-17, and based on the same procedure for adsorption capacity calculation, the capacity of Cu-ETS-2 at different temperatures and adsorption cycles was calculated. The results are presented in Figure 5- 18.

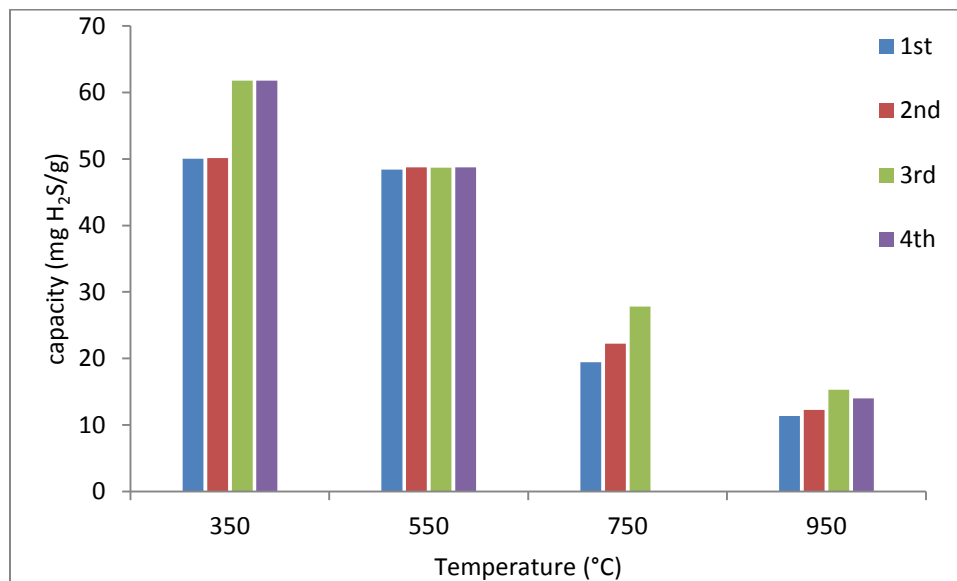


Figure 5-18- Adsorption capacity of Cu-ETS-2 in mg H<sub>2</sub>S/g adsorbent at different temperatures and adsorption cycles

## 5-6 Conclusions

A series of experiments were performed to investigate the regenerability of sulfided Cu-ETS-2. Experiments were carried out to collect data for four adsorption/regeneration cycles at a series of temperatures. For each experiment the adsorption and regeneration temperature were the same. The results indicated that the adsorbent is completely regenerable. This result was unexpected for the lower adsorption temperatures as the sulfate formed at lower temperature ( $\text{CuO}\cdot\text{CuSO}_4$ ) cannot be easily removed due to its thermal stability. However due to the immense heat generated through oxidation of copper sulfides,  $\text{CuO}\cdot\text{CuSO}_4$  also decomposes and forms CuO at furnace temperatures as low as  $350^\circ\text{C}$ , making Cu-ETS-2 a fully regenerable  $\text{H}_2\text{S}$  adsorbent.

**5-7 References:**

- (1) T. Arnold , J. chem. Phys. 101, 7399 (1994),doi: 10.1063
- (2) E.A. Peretti, Disc. Faraday Soc. 4 (1948) 174–179
- (3) J.R. Lewis, J.H. Hamilton, J.C. Nixon, C.L. Graversen, TMS–AIME 182 (1949) 177–185
- (4) N.D. Ganguly, S.K. Mukherjee, Chem. Eng. Sci. 22 (1967) 1091–1105
- (5) Z. Asaki, A. Ueguchi, T. Tanabe, Y. Kondo, Oxidation of Cu<sub>2</sub>S pellet, Trans. Jpn.Instit. Met. 27 (1986) 361–371.
- (6) S.E. Khalafalla, I.D. Shah, Metallurgical Transactions, 1 (1970) 2151-2156
- (7) H.Y. Sohn, M.E. Wadsworth, Rate Processes of extractive metallurgy, Springer, New York, 1979
- (8) I. Barin, Thermochemical Data of Pure Substances, VCH, Weinheim, 1993
- (9) S. Yasyerli, G. Dogu, I. Ar, T. Dogu, *Ind. Eng. Chem. Res.* 40 (2001) 5206–5214
- (10) J. Madarasz, P. Bombicz, M. Okuya, S. Kaneko, *Solid State Ionics*, 141-142 (2001) 439-446

## Chapter 6

# Conclusion and Future Work

## 6-1 Conclusions

The results in chapter 2 indicated that Cu-ETS-2 has a high adsorption capacity for H<sub>2</sub>S in non-reducing environments and is capable of removing H<sub>2</sub>S to levels below our detection limit (ca. 0.1 ppm) at temperatures ranging from 250 up to 950°C. The results, however, indicated that the adsorption capacity is sensitive to the presence of hydrogen in the system. Even small amounts of hydrogen in the system can reduce CuO to Cu<sub>2</sub>O and elemental copper, resulting in lower adsorption capacity. The H<sub>2</sub> present in the otherwise inert gas was determined to be due to the thermal dissociation of H<sub>2</sub>S into H<sub>2</sub> and S<sub>2</sub> at temperatures above 750°C. This judgement was based on the presence of elemental sulfur at the cold exhaust of the reactor tube.

In order to combat the problem associated with copper reduction, chromium oxide was combined with copper oxide to stabilize the oxidation state of copper. A previously reported Cu-Cr-O adsorbent was prepared according to the literature and its capacity for H<sub>2</sub>S adsorption was measured. As reported in the literature, Cu-Cr-O performs best at a narrow temperature range of 450 to 850°C with the highest adsorption capacity being 35 milligram sulfur per gram of adsorbent. The results for the bimetallic copper-chromium oxide prepared for this work showed no reduction in adsorption capacity at temperatures as high as 950°C.

The presence of chromium has the same benefit for bimetallic, Cu-Cr-ETS-2 adsorbents. Adsorption experiments indicated that once copper and chromium oxides are functionalized on ETS-2, the adsorbent develops a rather uniform adsorption capacity of ~55 milligram sulfur per gram of adsorbent at a wider temperature range of 350 to 950°C. Adsorption results for Cu-Cr-O and Cr-Cr-ETS-2 shows that ETS-2 functions as a great support for the active adsorbent and results in considerable improvement in adsorption capacity.

This study was the first to advance an understanding of the effect of water vapor on the adsorption characteristics of copper-based H<sub>2</sub>S adsorbents. Our results indicate that 10 vol% water has little influence on the H<sub>2</sub>S capacity of Cu-ETS-2 at

temperatures 350 °C and below. At temperatures around 550°C, under 10% humidity, Cu-ETS-2 is capable of removing H<sub>2</sub>S to concentrations below detection limit for a considerable amount of time (breakthrough time found to be almost 70% of dry gas experiments). The negative effect of water on the H<sub>2</sub>S adsorption capacity continued at higher temperature until, at 750 °C, virtually all of the copper on the adsorbent was reduced to non-adsorbing metal (verified by XRD). It was found that the presence of water vapor promotes the thermal dissociation of H<sub>2</sub>S which increases the amount of H<sub>2</sub> in the feed stream. The additional H<sub>2</sub> promotes metal reduction and explains the observations made in the study. This study established that the presence of water vapor in a syngas stream does not create a special problem because the amount of H<sub>2</sub> generated by the thermal dissociation of H<sub>2</sub>S will be negligible compared to the H<sub>2</sub> present in a typical syngas stream.

One of the desired features of an adsorbent is the ability to regenerate it multiple times. A series of experiments were performed to investigate the regenerability of sulfided Cu-ETS-2. Experiments were carried out to collect data for four adsorption/regeneration cycles at a series of temperatures. For each experiment the adsorption and regeneration temperature were the same. The results indicated that the adsorbent is completely regenerable. This result was unexpected for the lower adsorption temperatures because thermodynamics suggests that the sulfate formed at lower temperature cannot be easily removed. It was determined that, due to the use of pure O<sub>2</sub> as the regenerating gas, the heat of reaction during regeneration resulted in a massive increase in temperature. The adsorbent, therefore, experienced temperatures much higher than the adsorption temperature and perhaps as high at 1800°C. The heat generated during oxidation thus allowed complete regeneration of the adsorbent. The ability to maintain the same adsorption capacity even after experiencing such high temperatures shows one of the best benefits of ETS-2 as a support for adsorbent materials used in high temperature applications.

---

## 6-2 Recommendations for Future Work

Knowing that water simply promoted  $H_2$  generation via  $H_2S$  dissociation, the next logical step would be to gain an understanding of the effect of other species in syngas such as carbon monoxide. It is recommended for the future researchers to investigate the effect of  $H_2:CO$  ratio on adsorption capacity of Cu-ETS-2 and Cu-Cr-ETS-2. Ideally, any composition that stabilizes CuO against reduction should be able to limit the effects of negative effects of water and other reducing gases on the capacity of the adsorbent.

Once the effect of independent operating parameters (temperature, pressure, gas composition) has been established on Cu-ETS-2 and Cu-Cr-ETS-2, the adsorbents should be tested under actual gasification conditions. Establishing that the adsorbent works under conditions that reflect the total process complexity is the final proof that the adsorbent should be ready for pilot trials.

Rare earth metal oxides such as cerium oxide have also been reported in the literature to have good  $H_2S$  adsorption capacity. It is also interesting to compare the adsorption results for Cu-ETS-2 and Ce-ETS-2 under the same operating conditions. Such alternate compositions may have higher adsorption capacity or may be more resistant to reduction.

Understanding the influence of the exotherm on the regeneration of Cu-ETS-2 requires further investigation. Using air (a lower partial pressure of  $O_2$ ) should be investigated. The lower temperature limit to completely regenerate sulfide Cu-ETS-2 (or Cu-Cr-ETS-2) in air should also be determined. Lower temperatures and ambient gas mixtures would improve the economics of implementing the adsorbent.

## Complete List of References

**Chapter 1:**

- (1) Health and Safety Fact Sheet, Hydrogen Sulfide. [http://cupe.ca/health-and-safety/Hydrogen\\_Sulfide](http://cupe.ca/health-and-safety/Hydrogen_Sulfide) (Accessed November 1, 2011)
- (2) Patnaik, P., "A Comprehensive Guide to the Hazardous Properties of Chemical Substances," 2nd ed., John Wiley, New York (1999), pp. 505-536.
- (3) Stirling, D. Sulfur Problem - Cleaning up Industrial Feedstocks, 2000.
- (4) U.S. DOE Topical Report # 21, Clean Coal Technology: Coproduction of Power, Fuels, and Chemicals, p., September 2001.
- (5) Chauk SS, Agnihotri R, Jadhav RA, Misro SK, Fan L-S: Kinetics of high-pressure removal of hydrogen sulfide using calcium oxide powder. *AIChE Journal* 2000;46:1157.
- (6) <http://energy.gov/fe/how-coal-gasification-power-plants-work>
- (7) Hee Kwon J, Tae Jin L, Si Ok R, Jae Chang K: A study of Zn - Ti-based H<sub>2</sub>S removal sorbents promoted with cobalt oxides. *Industrial and Engineering Chemistry Research* 2001;40:3547.
- (8) R. Kam, J. Scott, R. Amal, C. Selomulya, Pyrophoricity and stability of copper and platinum based water-gas shift catalysts during oxidative shut-down/start-up operation, *Chem Eng Sci*, 65 (24) (2010), pp. 6461-6470
- (9) N.A. Koryabkina, A.A. Phatak, W.F. Ruettinger, R.J. Farrauto, F.H. Ribeiro, *J. Catal.* 217 (2003) 233.
- (10) Ko T-H, Chu H, Chung L-K: The sorption of hydrogen sulfide from hot syngas by metal oxides over supports. *Chemosphere* 2005;58:467.
- (11) Prakash, A., On the effects of syngas composition and water-gas-shift reaction rate on FT synthesis over iron based catalyst in a slurry reactor. *Chem. Eng. Commun.* **1994**, 128, (1), 143-158.

(12) Bachu, S., and W. D. Gunter, "Overview of Acid-Gas Injection Operations in Western Canada", Proceedings of 7th International Conference on Green House Gas Control Technologies (2005).

(13) Wang, H., D. Fang, and K.T. Chuang, "A Sulfur Removal and Disposal Process through H<sub>2</sub>S Adsorption and Regeneration: Ammonia Leaching Regeneration," Process Safety and Environment Protection, 8, 296-302 (2008).

(14) Wang, L. K., "Advanced Air and Noise Pollution Control," Humana Press, New York (2004), pp. 367-420.

(15) Sublette, K. L., and N. D. Sylvester, "Oxidation of Hydrogen Sulfide: Desulfurization of Natural Gas," Biotechnology and Bioengineering, 29, 595- 600 (1987).

(18) Sardesai, P., "Exploring the Gas Anaerobic Bioremoval of H<sub>2</sub>S for Coal Gasification Fuel Cell Feed Streams," Fuel Processing Technology, 87, 319-324 (2006).

(17) Jensen AB, Webb C: Treatment of H<sub>2</sub>S-containing gases: a review of microbiological alternatives. Enzyme and Microbial Technology 1995;17:2.

(18) Wang, H., D. Fang, and K.T. Chuang, "A Sulfur Removal and Disposal Process through H<sub>2</sub>S Adsorption and Regeneration: Ammonia Leaching Regeneration," Process Safety and Environment Protection, 8, 296-302 (2008).

(19) Eow JS: Recovery of sulfur from sour acid gas: A review of the technology. Environmental Progress 2002, 21:143.

(20) Westmoreland, P. R.; Harrison, D. P. Evaluation of candidate solids for high-temperature desulfurization of low-Btu gases. Environ. Sci. Technol. 1976, 10, 659.

(21) Crynes, B. L., "Chemical Reactions as a Means of Separation: Sulfur Removal," Marcel Dekker, New York (1977), pp. 212-223.

- (22) Miura, K., "Simultaneous Removal of COS and H<sub>2</sub>S from Coke and Oven Gas at Low Temperature by Use of an Iron Oxide," *Industrial and Engineering Chemistry Research*, 31, 415-419 (1992).
- (23) Xue, M., R. Chitrakar, K. Sakane, and K. Ooi, "Screening of Adsorbents for Removal of H<sub>2</sub>S at Room Temperature," *Green Chemistry*, 5, 529-534 (2003).
- (24) Li Z, Flytzani-Stephanopoulos M: Cu-Cr-O and Cu-Ce-O Regenerable Oxide Sorbents for Hot Gas Desulfurization. *Industrial & Engineering Chemistry Research* 1997;36:187-196.
- (25) Li K-T, Chi Z-H: Selective oxidation of hydrogen sulfide on rare earth orthovanadates and magnesium vanadates. *Applied Catalysis A: General* 2001;206:197.
- (26) Flytzani-Stephanopoulos M, Sakbodin M, Wang Z: Regenerative adsorption and removal of H<sub>2</sub>S from hot fuel gas streams by rare earth oxides. *Science* 2006;312:1508.
- (27) Ayala, R. E.; Marsh, D. W. Characterization and Long-Range Reactivity of Zinc Ferrite in High-Temperature Desulfurization Processes. *Industrial and Engineering Chemistry Research* 1991, 30, 55-60.
- (28) Abbasian, J.; Hill, A. H.; Wangerow, J. R.; Flytzani-Stephanopoulos, M.; Bo, L.; Patel, C.; Chang, D. Development of novel copper-based sorbents for hot-gas cleanup. Final technical report, September 1, 1991-August 31, 1992
- (29) Lew, S.; Sarofim, A. F.; Flytzani-Stephanopoulos, M. Sulfidation of zinc titanate and zinc oxide solids. *Ind Eng Chem Res* 1992, 31, 1890-1899.
- (30) Ko, T.; Chu, H.; Chaung, L. The sorption of hydrogen sulfide from hot syngas by metal oxides over supports. *Chemosphere* 2005, 58, 467-474.
- (31) Gasper-Galvin, L.; Atimtay, A. T.; Gupta, R. P. Zeolite-supported metal oxide sorbents for hot-gas desulfurization. *Ind Eng Chem Res* 1998, 37, 4157-4166.

- (32) Kyotani, T.; Kawashima, H.; Tomita, A.; Palmer, A.; Furimsky, E. Removal of H<sub>2</sub>S from Hot Gas in the Presence of Cu-Containing Sorbents. *Fuel* 1989, 68, 74-80.
- (33) Bagreev A, Bandosz TJ: A role of sodium hydroxide in the process of hydrogen sulfide adsorption/oxidation on caustic-impregnated activated carbons. *Industrial and Engineering Chemistry Research* 2002;41:672
- (34) Bagreev A, Adib F, Bandosz TJ: pH of activated carbon surface as an indication of its suitability for H<sub>2</sub>S removal from moist air streams. *Carbon* 2001;39:1897.
- (35) Turk A, Sakalis E, Rago O, Karamitsos H. Activated carbon systems for removal of light gases. *Ann NY Acad Sci* 1992;661:221-7.
- (36) A, Mahmood K, Mozaffari J. Activated carbon for air purification in New York City's sewage treatment plants. *Water Sci Techn* 1993;27:121-6.
- (37) Bandosz TJ: Effect of pore structure and surface chemistry of virgin activated carbons on removal of hydrogen sulfide. *Carbon* 1999;37:483.
- (38) Davini P: Flue gas desulphurization by activated carbon fibers obtained from polyacrylonitrile by-product. *Carbon* 2003;41:277.
- (39) Li, Huixing, Selective catalytic oxidation of hydrogen sulfide from syngas, M.Sc theis, university of Pittsburg, June 2008
- (40) <http://www.bza.org/zeolites.html>
- (41) Mer'kov, A.N.; Bussen, I.V.; Goiko, E.A.; Kul'chitskaya, E.A.; Men'shikov, Yu.P.; Nedorezova, A.P. Raite and zorite-new minerals from the Lovozero Tundra. *Zapiski Vsesoyuznogo Mineralogicheskogo Obshchestva*, 1973, 102, 54-62 (in Russian).
- (42) Kuznicki, S. M. *Large-Pored Crystalline Titanium Molecular Sieve Zeolites*; Patent US 4,853,202, 1989

(43) Anderson, M.W.; Terasaki, O. Structure of the microporous titanosilicate ETS-10, *Nature*, 367, 347-351, 1994

## Chapter 2

(1) Gupta, R. P.; Turk, B. S.; Portzer, J. W.; Cicero, B. C. Desulfurization of Syngas in a Transport Reactor. *Environ. Prog.* **2001**, 20, 187.

(2) Bartholomew, C. H.; Agrawal, P. K.; Katzer, J. R. Sulfur Poisoning of Metals. *Adv. Catal.* **1982**, 31, 135-242.

(3) Stirling, D.; Clark, J. H.; Braithwaite, M. J. *Sulfur Problem - Cleaning up Industrial Feedstocks*; The Royal Chemical Society: Cambridge, 2000.

(4) Bläsing, M., Müller, M. Release of Alkali Metal, Sulphur, and Chlorine Species from High Temperature Gasification of High- And Low-Rank Coals. *Fuel Process. Technol.* **2013**, 106, 289.

(5) Koryabkina, N. A.; Phatak, A. A.; Ruettinger, W. F.; Farrauto, R. J.; Ribeiro, F. H. Determination of Kinetic Parameters for the Water-Gas Shift Reaction on Copper Catalysts under Realistic Conditions for Fuel Cell Applications. *J. Catal.* **2003**, 217, 233.

(6) Jensen, A. B.; Webb, C. Treatment of H<sub>2</sub>S-Containing Gases: A Review of Microbiological Alternatives. *Enzyme Microb. Technol.* **1995**, 17, 2.

(7) Klein, J.; Henning, K. D. Catalytic Oxidation of Hydrogen Sulfide on Activated Carbons. *Fuel* **1984**, 63, 1064.

(8) Elseviers, W. F.; Verelst, H. Transition Metal Oxides for Hot Gas Desulphurization. *Fuel* **1999**, 78, 601.

(9) Melo, D. M. A.; De Souza, J. R.; Melo, M. A. F.; Martinelli, A. E.; Cachima, G. H. B.; Cunha, J. D. Evaluation of the Zinox and Zeolite Materials as Adsorbents to Remove H<sub>2</sub>S from Natural Gas. *Colloids Surf., A*: **2006**, 272, 32.

- (10) Ko T. H.; Chu, H.; Chaung, L. K. The Sorption of Hydrogen Sulfide from Hot Syngas by Metal Oxides over Supports. *Chemosphere* **2005**, *58*, 467.
- (11) Müller, M. Integration of Hot Gas Cleaning at Temperatures above the Ash Melting Point in IGCC. *Fuel* **2013**, *108*, 37.
- (12) Westmoreland, P. R.; Harrison, D. P. Evaluation of Candidate Solids for High-Temperature Desulfurization of Low-Btu Gases. *Environ. Sci. Technol.* **1976**, *10*, 659.
- (13) Crynes, B. L. *Chemical Reactions as a Means of Separation: Sulfur Removal*; Marcel Dekker: New York, 1977.
- (14) Gollmer, H. A. in *Chemistry of Coal Utilization*; Lowry, H.H., Eds.; John Wiley & Sons: New York, 1945; pp947-1007.
- (15) Swisher, J. H.; Swerdtfeger, K.; Review of Metals and Binary Oxides as Sorbents for Removing Sulfur from Coal-Derived Gases. *JMEPEG* **1992**, *1*, 399.
- (16) Kyotani, T.; Kawashima, H.; Tomita, A. High Temperature Desulfurization with Copper-Containing Sorbents. *Environ. Sci. Technol.* **1989**, *23* (2), 218-223.
- (17) Patrick, V.; Gavalas, G. R. Structure and Reduction of Mixed Copper-Aluminum Oxide. *J. Am. Ceram. Soc.* **1990**, *73* (2), 358-369
- (18) Stemmler, M.; Tamburro, A.; Müller, M. Laboratory Investigations on Chemical Hot Gas Cleaning of Inorganic Trace Elements for the “UNIQUE” Process. *Fuel* **2013**, *108*, 31.
- (19) Ayala, R. E.; Marsh, D. W. Characterization and Long-Range Reactivity of Zinc Ferrite in High-Temperature Desulfurization Processes. *Ind. Eng. Chem. Res.* **1991**, *30*, 55.
- (20) Abbasian, J.; Hill, A. H.; Wangerow, J. R.; Flytzani-Stephanopoulos, M.; Bo, L.; Patel, C.; Chang, D. Development of Novel Copper-Based Sorbents for Hot-Gas Cleanup. *IGT-Final technical report to CRSC; IGT project No. 40330*, **1992**.

- (21) Li, Z.; Flytzani-Stephanopoulos, M. Cu-Cr-O and Cu-Ce-O Regenerable Oxide Sorbents for Hot Gas Desulfurization. *Ind. Eng. Chem. Res.* **1997**, *36*, 187.
- (22) Gasper-Galvin, L.; Atimtay, A. T.; Gupta, R. P. Zeolite-Supported Metal Oxide Sorbents for Hot-Gas Desulfurization. *Ind. Eng. Chem. Res.* **1998**, *37*, 4157.
- (23) Kuznicki, S. M. *Large-Pored Crystalline Titanium Molecular Sieve Zeolites*; Patent US 4,853,202, 1989.
- (24) Rezaei, S.; Tavana, A.; Sawada, J.; Junaid, A.; Kuznicki, S. M. Novel Copper-Exchanged Titanosilicate Adsorbent for Low Temperature H<sub>2</sub>S Removal. *Ind. Eng. Chem. Res.* **2012**, *51*, 12430.
- (25) Yogamalar, R.; Srinivasan, R.; Vinu, A.; Ariga, K. X-ray Peak Broadening analysis in ZnO Nanoparticles. *Solid state Commun.* **2009**, *149*, 1919–1923.
- (26) Donnay, G.; Donnay, J. D. H.; Kullerud, G. Crystal Structure of Digenite, Cu<sub>9</sub>S<sub>5</sub>. *Am. Mineral.* **1958**, *43*, 228-242.
- (27) Fukuda, K.; Dokiya, M.; Kameyana, T.; Kotera, Y. Catalytic Decomposition of Hydrogen Sulfide. *Ind. Eng. Chem. Res.* **1978**, *17*, 243-248.
- (28) Barin, I.; Knacke, O. *Thermochemical Properties of Inorganic Substances*; Springer-Verlag: Berlin, 1973.
- (29) Patrick, V.; Gavalas, G. R.; Flytzani-Stephanopoulos, M.; Jothimurugesan, K. High Temperature Sulfidation-Regeneration of CuO-Al<sub>2</sub>O<sub>3</sub> Sorbents. *Ind. Eng. Chem. Res.* **1989**, *28*, 931-940.

### Chapter 3:

- (1) M. Müller, *Fuel* 108, 37 (2013)
- (2) L. Fenouil, G. Towler and S. Lynn, *Ind. Eng. Chem. Res.* 33(2), 265 (1994)
- (3) N. A. Khan, H. Zubair and H. J. Sung, *Adv. Porous Mater.* 1(1), 91 (2013)

- (4) M. Müller, D. Pavone, M. Rieger and R. Abraham, 4th International Conference on Clean Coal Technologies, Dresden, Germany, May (2009)
- (5) J. W. Portzer, J. R. Albritton, C. C. Allen, R. P. Gupta. *Fuel process. Technol.* 85(6), 621 (2004)
- (6) D. Stirling, J. H. Clark and M. J. Braithwaite, *Sulfur Problem - Cleaning up Industrial Feedstock*, The Royal Chemical Society, Cambridge, (2000)
- (7) M. Bläsing and M. Müller, *Fuel Process. Technol.* 106, 289 (2013)
- (8) D. S. Newsome, *Catal. Rev.* 21(2), 275 (1980)
- (9) C. Rhodes, G. J. Hutchings and A. M. Ward, *Catal. Today* 23(1), 43 (1995)
- (10) M. Stemmler and M. Müller, *Biomass. Bioenerg.* 35, S105 (2011)
- (11) P. Hou, D. Meeker and H. Wise, *J. Catal.* 80(2), 280 (1983)
- (12) G. Ma, Y. Hou, X. Han, and Z. Huang. *Energy Environm. Focus.* 3(1), 74 (2014)
- (13) M. P. Cal, B. W. Strickler and A. A. Lizzio, *Carbon* 38(13), 1757 (2000)
- (14) R. C. Hansford, R. H. Hass and H. Hennig, U.S. Patent No. 4,088,743. 9 May (1978)
- (15) T. Ko, H. Chu and L. Chuang, *Chemosphere.* 58, 467 (2005)
- (16) J. J. Park, C. G. Park, S. Y. Jung, S. C. Lee, D. Ragupathy and J. C. Kim, *Nanoelectron. Optoelectron.* 6(3), 306 (2011)
- (17) J.J. Park, S.Y. Jung, C.Y. Ryu, C.G. Park, J.N. Kim, and J.C. Kim. *J. Nanoelectron. Optoelectron.* 5(2), 222 (2010)
- (18) Y. Motoo and E. Furimsky, *Ind. Eng. Chem. Process. Des. Dev.* 24(4), 1165 (1985)
- (19) Y. Zeng, S. Zhang, F. R. Groves, and D. P. Harrison. *Chem. Eng. Sci.* 54(15),

3007 (1999)

(20) S. K. Gangwal, in *Proceedings of the 3rd International Symposium and Exhibition: High-Temperature Gas Cleaning*, University of Karlsruhe, Karlsruhe, Germany (1996), p. 489.

(21) J. S. Yong, S. C. Lee and J. C. Kim. *J. Nanoelectron. Optoelectron.* 7(5), 536 (2012)

(22) L. Zhijiang and M. Flytzani-Stephanopoulos, *Ind. Eng. Chem. Res.* 36(1), 187 (1997)

(23) M. Flytzani-Stephanopoulos, G. R. Gavalas, S. S. Tamhankar and P. K. Sharma, Final Report to DOE, DOE/MC/ 20417-1898, (1985)

(24) G. Sick and K. Schwerdtfeger, *Metall. Trans. B.* 18(3), 603 (1987)

(25) T. Kyotani, H. Kawashima, A. Tomita, A. Palmer and E. Furimsky, *Fuel.* 68(1), 74 (1989)

(26) M. Flytzani-Stephanopoulos, G. R. Gavalas, and S. S. Tamhankar, U.S. Patent No. 4,729,889 (1988)

(27) P. Valerle and G. Gavalas, *J. Am. Ceram. Soc.* 73(2). 358 (1990)

(28) A. T. Atimtay and D. P. Harrison, eds. *Desulfurization of hot coal gas*. No. 42. Springer, (1998)

(29) J. Abbasian, A. H. Hill, J. R. Wangerow, M. Flytzani-Stephanopoulos, L. Bo, C. Patel and D. Chang, IGT-Final Technical Report to CRSC; IGT Project No. 40330, (1992)

(30) S. M. Kuznicki, Patent US4853202, (1989)

(31) S. Rezaei, A. Tavana, J. A. Sawada, L. Wu, A.S. Junaid and S. M. Kuznicki, *Ind. Eng. Chem. Res.* 51(38), 12430 (2010)

- (32) M. Shi, C.C. Lin, L. Wu, C. Holt, D. Mitlin and S. M. Kuznicki. *J. Nanosci. Nanotechnol.* 10(12), 8448 (2010)
- (33) B. Tanchuk, J. A. Sawada and S. M. Kuznicki, *AIChE J.* 59(12), 4727 (2013)
- (34) A. Tavana, *Characterization of Copper Supported on Titanosilicates for Room Temperature H<sub>2</sub>S Adsorption*. MSc thesis, University of Alberta, Edmonton (2012)
- (35) Q. Geng, X. Zhao, X. Gao, S. Yang and G. Liu, *J. Sol-Gel. Sci. Techn.* 61(1), 281 (2012)
- (36) W. Li and H. Cheng, *J. Cent. South Univ. T.* 14, 291 (2007)
- (37) A. M. Kawamoto, L. C. Pardini and L.C. Rezende. *Aerosp. Sci. Technol.* 8, 591 (2004)
- (38) K. Fukuda, M. Dokiya, T. Kameyana, Y. Kotera, *Ind. Eng. Chem. Res.* 17, 243 (1978)
- (39) S. Yasyerli, G. Dogu and I. Ar, *Ind. Eng. Chem. Res.* 40(23), 5206 (2001)

#### Chapter 4:

- (1) Stirling, D., *The sulfur problem: cleaning up industrial feedstocks*. Royal Society of Chemistry: 2000.
- (2) Boon, J.; van Dijk, E.; Pirgon-Galin, Ö.; Haije, W.; van den Brink, R., Water-gas shift kinetics over FeCr-based catalyst: effect of hydrogen sulphide. *Catal. Lett.* **2009**, 131, (3-4), 406-412.
- (3) Cal, M.; Strickler, B.; Lizzio, A., High temperature hydrogen sulfide adsorption on activated carbon: I. Effects of gas composition and metal addition. *Carbon* **2000**, 38, (13), 1757-1765.

- (4) Hass, R. H.; Hansford, R. C.; Hennig, H., Catalytic incineration of hydrogen sulfide from gas streams. In Google Patents: 1978.
- (5) Ko, T.-H.; Chu, H.; Chaung, L.-K., The sorption of hydrogen sulfide from hot syngas by metal oxides over supports. *Chemosphere* **2005**, 58, (4), 467-474.
- (6) Yumura, M.; Furimsky, E., Comparison of calcium oxide, zinc oxide, and iron (III) oxide hydrogen sulfide adsorbents at high temperatures. *Ind. Eng. Chem. Proc. D. D.* **1985**, 24, (4), 1165-1168.
- (7) Abbasian, J. *Development of novel copper-based sorbents for hot-gas cleanup*; Institute of Gas Technology, Chicago, IL (United States): 1991.
- (8) Tamhankar, S.; Garimella, S.; Wen, C., Kinetic study on the reactions involved in hot gas desulfurization using a regenerable iron oxide sorbent—III. Reactions of the sulfided sorbent with steam and steam-air mixtures. *Chem. Eng. Sci.* **1985**, 40, (6), 1019-1025.
- (9) Rosso, I.; Galletti, C.; Bizzi, M.; Saracco, G.; Specchia, V., Zinc oxide sorbents for the removal of hydrogen sulfide from syngas. *Ind. Eng. Chem. Res.* **2003**, 42, (8), 1688-1697.
- (10) Lew, S.; Jothimurugesan, K.; Flytzani-Stephanopoulos, M., High-temperature hydrogen sulfide removal from fuel gases by regenerable zinc oxide-titanium dioxide sorbents. *Ind. Eng. Chem. Res.* **1989**, 28, (5), 535-541.
- (11) Patrick, V.; Gavalas, G. R.; Flytzani-Stephanopoulos, M.; Jothimurugesan, K., High-temperature sulfidation-regeneration of copper (II) oxide-alumina sorbents. *Ind. Eng. Chem. Res.* **1989**, 28, (7), 931-940.
- (12) Slimane, R. B.; Abbasian, J., Copper-based sorbents for coal gas desulfurization at moderate temperatures. *Ind. Eng. Chem. Res.* **2000**, 39, (5), 1338-1344.

- (13) Kyotani, T.; Kawashima, H.; Tomita, A.; Palmer, A.; Furimsky, E., Removal of H<sub>2</sub>S from hot gas in the presence of Cu-containing sorbents. *Fuel* **1989**, 68, (1), 74-79.
- (14) Yasyerli, S.; Dogu, G.; Ar, I.; Dogu, T., Activities of copper oxide and Cu-V and Cu-Mo mixed oxides for H<sub>2</sub>S removal in the presence and absence of hydrogen and predictions of a deactivation model. *Ind. Eng. Chem. Res.* **2001**, 40, (23), 5206-5214.
- (15) Sick, G.; Schwerdtfeger, K., Hot desulfurization of coal gas with copper. *Metall. Trans. B* **1987**, 18, (3), 603-609.
- (16) Flytzani-Stephanopoulos, M.; Gavalas, G. R.; Tamhankar, S. S.; Center, U. S. D. o. E. M. E. T.; Laboratory, J. P., *Novel Sorbents for High Temperature Regenerative H<sub>2</sub>S Removal*. United States Department of Energy: 1984.
- (17) Li, Z.; Flytzani-Stephanopoulos, M., Cu-Cr-O and Cu-Ce-O regenerable oxide sorbents for hot gas desulfurization. *Ind. Eng. Chem. Res.* **1997**, 36, (1), 187-196.
- (18) Reddy, G. K.; Smirniotis, P. G., Chapter 1 - Introduction About WGS Reaction. In *Water Gas Shift Reaction*, Smirniotis, G. K. R. G., Ed. Elsevier: Amsterdam, 2015; pp 1-20.
- (19) Huang, C.-C.; Chen, C.-H.; Chu, S.-M., Effect of moisture on H<sub>2</sub>S adsorption by copper impregnated activated carbon. *J. Hazard. Mater.* **2006**, 136, (3), 866-873.
- (20) Yazdanbakhsh, F.; Bläsing, M.; Sawada, J. A.; Rezaei, S.; Müller, M.; Baumann, S.; Kuznicki, S. M., Copper exchanged nanotitanate for high temperature H<sub>2</sub>S adsorption. *Ind. Eng. Chem. Res.* **2014**, 53, (29), 11734-11739.
- (21) Kuznicki, S. M., Large-pored crystalline titanium molecular sieve zeolites. In Google Patents: 1989.

- (22) Tanchuk, B.; Sawada, J. A.; Kuznicki, S. M., Amine - functionalization of the nanotitanate ETS - 2. *AIChE J.* **2013**, 59, (12), 4727-4734.
- (23) Prakash, A., On the effects of syngas composition and water-gas-shift reaction rate on FT synthesis over iron based catalyst in a slurry reactor. *Chem. Eng. Commun.* **1994**, 128, (1), 143-158.
- (24) Yazdanbakhsh, F. A., M.; Sawada, J.A.; Kuznicki, Cu–Cr–O Functionalized ETS-2 Nanoparticles for Hot Gas Desulfurization. *J. Nanosci. Nanotechnol.* 15.
- (25) Alonso, L.; Palacios, J. M.; García, E.; Moliner, R., Characterization of Mn and Cu oxides as regenerable sorbents for hot coal gas desulfurization. *Fuel Proc. Tech.* **2000**, 62, (1), 31-44.
- (26) Karan, K.; Mehrotra, A. K.; Behie, L. A., On reaction kinetics for the thermal decomposition of hydrogen sulfide. *AIChE J.* **1999**, 45, (2), 383-389.
- (27) Ranjan, P.; Kannan, P.; Al Shoaibi, A.; Srinivasakannan, C., Modeling of Ethane Thermal Cracking Kinetics in a Pyrocracker. *Chem. Eng. Tech.* **2012**, 35, (6), 1093-1097.

### Chapter 5:

- (1) T. Arnold , *J. chem. Phys.* 101, 7399 (1994),doi: 10.1063
- (2) E.A. Peretti, *Disc. Faraday Soc.* 4 (1948) 174–179
- (3) J.R. Lewis, J.H. Hamilton, J.C. Nixon, C.L. Graversen, *TMS–AIME* 182 (1949) 177–185
- (4) N.D. Ganguly, S.K. Mukherjee, *Chem. Eng. Sci.* 22 (1967) 1091–1105
- (5) Z. Asaki, A. Ueguchi, T. Tanabe, Y. Kondo, Oxidation of Cu<sub>2</sub>S pellet, *Trans. Jpn.Instit. Met.* 27 (1986) 361–371.
- (6) S.E. Khalafalla, I.D. Shah, *Metallurgical Transactions*, 1 (1970) 2151-2156

- (7) H.Y. Sohn, M.E. Wadsworth, *Rate Processes of extractive metallurgy*, Springer, New York, 1979
- (8) I. Barin, *Thermochemical Data of Pure Substances*, VCH, Weinheim, 1993
- (9) S. Yasyerli, G. Dogu, I. Ar, T. Dogu, *Ind. Eng. Chem. Res.* 40 (2001) 5206–5214
- (10) J. Madarasz, P. Bombicz, M. Okuya, S. Kaneko, *Solid State Ionics*, 141-142 (2001) 439-446